Federal Aviation Administration

Safety Study Report for Dependent Converging Instrument Approaches (DCIAs) with Converging Runway Display Aid (CRDA)

Flight Systems Laboratory
DOT-FAA-AFS-450-42

September 2010

Flight Systems Laboratory
6500 S. MacArthur Blvd.
Systems Training Building Annex, RM 217
Oklahoma City, Oklahoma 73169
Phone: (405) 954-8191

OK-11-0219

NOTICE

This document is disseminated under the sponsorship of the U.S. Department of Transportation in the interest of information exchange. The United States Government assumes no liability for the contents or use thereof.

The United States Government does not endorse products or manufacturers. Trade or manufacturers' names appear herein solely because they are considered essential to the objective of this report.

DOT-FAA-AFS-450-42

Flight Systems Laboratory
Flight Technologies and Procedures Division
Flight Standards Service

Safety Study Report for Dependent Converging Instrument Approaches (DCIAs) with Converging Runway Display Aid (CRDA)

Reviewed by:

September 24, 2010

Stephen W. Barnes **Date**
Manager, Flight Systems Laboratory

Released by:

G L Powell for 9/24/10

Leslie H. Smith **Date**
Manager, Flight Technologies and Procedures Division

September 2010

Technical Report

Safety Study Report for Dependent Converging Instrument Approaches (DCIAs) with Converging Runway Display Aid (CRDA)

DOT-FAA-AFS-450-42 **September 2010**

Technical Report Documentation Page

1. Report No.	2. Government Accession No.	3. Recipient's Catalog No.
DOT-FAA-AFS-450-42		

4. Title and Subtitle	5. Report Date
Safety Study Report for Dependent Converging Instrument Approaches (DCIAs) with Converging Runway Display Aid (CRDA)	September 2010
6. Author(s)	**7. Performing Organization Code**
Gerry McCartor, AFS-450 Shahar Ladecky, ATSI	
8. Performing Organization Name and Address	**9. Type of Report and Period Covered**
Federal Aviation Administration Flight Systems Laboratory, AFS-450 6500 S. MacArthur Blvd. STB Annex, RM 217 Oklahoma City, OK 73169	Technical Report

10. Sponsoring Agency Name and Address

Federal Aviation Administration
Flight Systems Laboratory, AFS-450
6500 S. MacArthur Blvd., STB Annex, RM 217
Oklahoma City, OK 73169
Phone: (405) 954-8191

11. Supplementary Notes

12. Abstract

To increase airport capacity during periods of Instrument Meteorological Conditions for airports with converging runways, the Federal Aviation Administration (FAA) developed Dependent Converging Instrument Approach (DCIA) operations. A DCIA operation uses alternating (staggered) approaches to the two converging runways. The governing document for DCIA operations is FAA Order 7110.110A. A DCIA operation developed in accordance with this order permits lower Decision Heights (DHs) on the associated instrument approaches while also protecting for possible simultaneous missed approaches. An integral part of a DCIA operation is the use of the Converging Runway Display Aid (CRDA) by Air Traffic Control (ATC). The CRDA presents “ghost” targets on ATC displays of aircraft on approach to the other converging runway to provide adequate spacing for the DCIA operation.

Concurrent with the development and publication of FAA Order 7110.110A, safety aspects of DCIA with CRDA operations were analyzed. However, a comprehensive safety study that considers risks from both possibilities of collision and wake vortex encounters, has heretofore not been completed. This report presents the results of a safety study performed on DCIA with CRDA operations as described in FAA Order 7110.110A. The study was performed by the FAA Flight Systems Laboratory (AFS-450) and Air Traffic Simulation, Inc. (ATSI) and focused on the risks of potential collision or encountering wake vortices during DCIA operations with CRDA while executing a missed approach.

13. Key Words	14. Distribution Statement
Dependent Converging Instrument Approach (DCIA), Converging Runway Display Aid (CRDA), Wake vortex	Controlled by AFS-450
15. Security Classification of This Report	**16. Security Classification of This Page**
Unclassified	Unclassified

Executive Summary

To increase airport capacity during periods of Instrument Meteorological Conditions for airports with converging runways, the Federal Aviation Administration (FAA) developed Dependent Converging Instrument Approach (DCIA) operations. A DCIA operation uses alternating (staggered) approaches to the two converging runways to support two arrival streams, thus increasing airport capacity. The governing document for DCIA operations is FAA Order 7110.110A, *Dependent Converging Instrument Approaches (DCIA) with Converging Runway Display Aid (CRDA)*, [1]. A DCIA operation developed in accordance with [1] permits lower Decision Heights (DHs) on the associated instrument approaches while also protecting aircraft during possible simultaneous missed approaches. An integral part of a DCIA operation is the use of the CRDA by Air Traffic Control (ATC).

The FAA Flight Systems Laboratory (AFS-450) performed a safety study on DCIA with CRDA operations focused on the risks of collision or encountering wake vortices. .Of 108 cases evaluated, three did not meet the selected target level of safety (TLS). The three cases were in the highest DH range considered of 501 to 700 feet. Two other cases that did not exceed the TLS showed an elevated risk. A more in-depth analysis of the higher risk cases concluded that the 110° to 120° runway convergence angle sector presented the greatest risk.

Three possible mitigation strategies for these cases and runway convergence angle sectors are: (1) to further extend the required stagger distances defined in Order 7110.110A, (2) to avoid DCIA operations for the high risk cases in the 110° to 120° runway convergence angle sector or (3) to develop turning missed approach procedures for one or both aircraft. Decision Heights in this range normally allow the pilot to start an immediate turn during the missed approach. The higher DHs also allow more time for ATC to identify a potential conflict and take corrective action.

All 108 cases resulted in wake vortex encounters as defined in this study. Due to the geometry of the operation, the encounters were generally of very short duration. There is no established definition of a “hazardous” wake vortex encounter, so it is currently not possible to draw any conclusions as to the risks associated with the wake encounters. The FAA is currently performing studies and developing tools to identify hazardous wake encounters. Previous studies have examined low angle intercepts, i.e. the encountering aircraft is following the generating aircraft. Future studies are planned to evaluate the effects of flying through a wake or a pair of wake vortices at higher angles of encounter. When a definition of a hazardous encounter is established, each real-world implementation of a DCIA operation should be evaluated for wake turbulence hazards.

TABLE OF CONTENTS

1.0	Introduction	1
1.1	Purpose and Structure of the Report	1
1.2	Background	1
2.0	Description of the Model	2
2.1	Typical DCIA with CRDA Operation	2
2.2	Domain of the Model—FAA Order 7110.110A Cases	3
2.3	Airspace Simulation and Analysis Tool (ASAT)	4
2.3.1	ASAT Modifications—Geodetic Scenario	5
2.3.2	ASAT Modifications—Operational Scenario	5
2.3.3	ASAT Modifications—Wake Vortex Evaluation	6
2.3.3.1	Aircraft Vortex Spacing System (AVOSS) Prediction Algorithm	6
2.3.3.2	Wake Vortex Simulation Description	8
2.3.3.3	Wake Vortex Encounter Criteria	9
2.4	Wake Turbulence Aircraft Classes	9
2.5	ASAT Monte Carlo Simulation Runs	9
2.5.1	Simulation Parameters	9
2.5.2	Collision Risk Criteria Violation Related Simulation Runs	10
2.5.3	Wake Vortex Encounter Related Simulation Runs	11
3.0	Summary of Data Analysis	12
3.1	Evaluation of TCV	13
3.1.1	Target Level of Safety	13
3.1.2	Probability of Dual Missed Approaches During DCIA Operations	13
3.1.3	FAA Order 7110.110A Cases with TCVs	14
3.1.4	In-Depth Analysis of Highest Risk FAA Order 7110.110A Cases	15
3.2	Evaluation of Wake Encounters	15
4.0	Results and Conclusions	16
4.1	Collision Risk Criteria Violations	16
4.2	Wake Vortex Encounters	17
	Appendix A: Additional Parameter Descriptions	18
	Appendix B: Statistical Analysis of ASAT Output	20
	Appendix C: Statistical Analysis of Higher Risk DCIA Cases	65
	References	79

LIST OF ILLUSTRATIONS

Tables

Table 1	Summary of FAA Order 7110.110A Cases	3
Table 2	FAA Order 7110.110A Cases with Probability of TCV Exceeding TLS	14
Table 3	Other FAA Order 7110.110A Cases of Interest	14
Table 4	DCIA Cases of Interest with Highest Risk Runway Convergence Angles Identified	15

Figures

Figure 1	Typical DCIA with CRDA Operation	3
Figure 2	DCIA with CRDA Operational Model	6
Figure 3	APA Output Implementation in ASAT	7
Figure 4	Wake Vortex Evaluation “Tiles”	8
Figure 5	Typical ASAT Depiction of TCV Related Simulation Runs	11
Figure 6	Typical ASAT Depiction of Wake Vortex Related Simulation Runs	12
Figure 7	Probability of Encounter by Intensity	16

Safety Study Report for Dependent Converging Instrument Approaches (DCIA) with Converging Runway Display Aid (CRDA)

1.0 Introduction

This report presents the results of a safety study performed on Dependent Converging Instrument Approaches (DCIAs) with a Converging Runway Display Aid (CRDA). The study was performed by the Federal Aviation Administration (FAA) Flight Systems Laboratory (AFS-450) and Air Traffic Simulation, Inc. (ATSI). This section of the report describes the purpose of the study and structure of this document and provides background information about the development of DCIA operations.

1.1 Purpose of the Study and Structure of the Report

This study focused on the risk of collision or encountering wake vortices during DCIA operations with CRDA while executing a missed approach. This report describes the model used to simulate the DCIA operations and the modifications to the simulation in Section 2. Section 3 provides a summary of the data from the simulation. Conclusions and recommendations based upon the study are given in Section 4.

1.2 Background

To increase airport capacity during periods of Instrument Meteorological Conditions for airports with converging intersecting and nonintersecting runways, the FAA developed DCIA operations. A DCIA operation uses alternating (staggered) approaches to the two converging runways to support two arrival streams, thus increasing airport capacity. The governing document for DCIA operations is FAA Order 7110.110A, *Dependent Converging Instrument Approaches (DCIA) with Converging Runway Display Aid (CRDA)*, [1]. A DCIA operation developed in accordance with [1] permits lower Decision Heights (DHs) on the associated instrument approaches while also addressing possible simultaneous missed approaches.

Concurrent with the development and publication of [1], various aspects of DCIA with CRDA operations were analyzed. However, a comprehensive safety study that considers risks from both potential collision and wake vortex encounters has heretofore not been completed.

2.0 Description of the Model

This section of the report describes the models and tools used in the study. This study examined a series of scenarios involving different combinations of DHs, runways converging angles, aircraft speeds, and distances from the thresholds to runway intersections. To compute the risk of a TCV, the study modified the Airspace Simulation and Analysis Tool (ASAT) and to examine possible wake vortex encounters, ASAT was modified further to include the Aircraft Vortex Spacing System (AVOSS) Prediction Algorithm (APA) (see reference "An Aircraft Vortex Spacing System (AVOSS) for Dynamical Wake Vortex Spacing Criteria." [2] for details).

2.1 Typical DCIA with CRDA Operation

An integral part of a DCIA operation is the use of the CRDA by Air Traffic Control (ATC). The CRDA presents "ghost" targets on ATC displays of aircraft on approach to the other converging runway to provide adequate spacing for the DCIA operation.

Figure 1 shows a typical DCIA with CRDA operation. Aircraft are approaching to land on converging Runways A and B. In this case, the runways also intersect one another, although DCIA operations can also include converging nonintersecting runways. Figure 1 also shows the common point. The common point is the point where runways intersect as they do in Figure 1, or it is the point where the extended centerlines of nonintersecting runways intersect. The common point is used by the CRDA software to project the ghost target.

As Figure 1 shows, the ghost target is projected in the landing stream for Runway A at the same distance (X1) as the actual aircraft landing on Runway B. This projection of the ghost target by the CRDA aids ATC in establishing the proper longitudinal separation distance to the next real aircraft approaching to land on Runway A. The longitudinal separation is referred to as the stagger.

Dual missed approaches represent a safety concern because the in-trail aircraft (on Runway A in the figure) may be faster than the leading aircraft. If the stagger is not adequate, the in-trail aircraft may catch up with the leading aircraft by the intersection area.

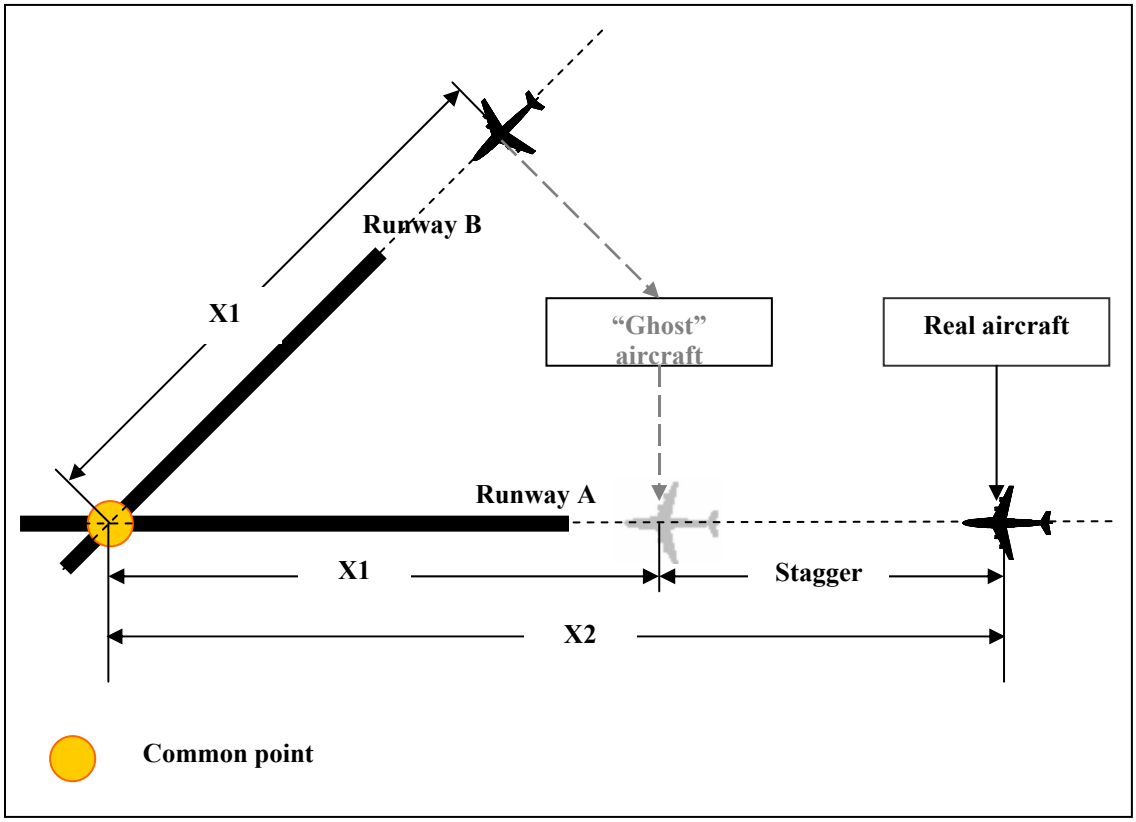

Figure 1: Typical DCIA with CRDA Operation

2.2 Domain of the Model—FAA Order 7110.110A Cases

The software model developed for this study covered all cases listed in FAA Order 7110.110A. The cases are contained in three sets of tables for three DH ranges. Each set of tables established the stagger distances behind Heavy and non-Heavy aircraft for combinations of runway lengths and aircraft speeds allowed for a given range of DH values. FAA Order 7110.110A cases are summarized in Table 1. A total of 108 cases are contained in the order.

Table 1: Summary of FAA Order 7110.110A Cases

DH (ft)	Distance Range From Threshold to Intersection (ft)	Runways Converging Angle (°)	Number of Cases
Up to 250 (DH250)	2,600 to 19,700	45 to 120	44
251 to 500 (DH500)	2,100 to 17,000	45 to 120	29
501 to 700 (DH700)	1,600 to 16,000	45 to 120	35
Total			108

2.3 Airspace Simulation and Analysis Tool (ASAT)

The primary analysis tool for this safety evaluation was ASAT. ASAT is a multifaceted, highly adaptable computer-based tool for aviation-related simulations and safety evaluations. ASAT consists of high-fidelity models and in some cases, empirical data representing the following major components of a typical real-world operational aviation scenario:

- At the heart of the system are flight dynamics models enhanced and tailored by empirical data collected in flight simulators and flight tests. Aircraft avionics are modeled based on the requirements of a particular scenario. ASAT can model a broad range of advanced navigation systems such as a Flight Management System, Global Positioning System, and Required Navigation Performance as well as other navigation systems, such as the Instrument Landing System, Microwave Landing System, and Distance Measuring Equipment.

- ASAT has access to a wide range of environmental models including temperature, atmospheric pressure, and both lateral and vertical wind profiles. The aerodynamic flight models described above respond to the ASAT-generated atmosphere in the same manner as actual aircraft.

- ASAT also uses official FAA databases providing the precise geographic locations of airports, runways, navaids, routes, fixes, waypoints, and other facilities, such as radar site locations. In addition, ASAT incorporates the FAA's obstacle and terrain database for obstacle clearance studies.

- The impact of air traffic equipment on scenarios is based on computer models of radar systems using manufacturer and government specifications. If necessary, ASAT also incorporates human factors variables, such as a Probability Density Function (PDF) of controller response times.

- ASAT uses PDFs derived from real-time tests to determine the responses of controllers and pilots involved in the modeled operation.

Once the scenario(s) of interest is defined and the previously mentioned components have been statistically characterized, ASAT can perform thousands of runs in a Monte Carlo simulation. ASAT can also statistically analyze the results of the Monte Carlo simulation.

ASAT was modified for purposes of this study to effectively model the DCIA scenario shown in Figure 2. The following sections describe the major modifications that were made to ASAT.

2.3.1 ASAT Modifications—Geodetic Scenario

The geodetic scenario was comprised of two runways of given lengths and converging angle at sea level elevation. The runways' lengths and converging angles were randomly selected for each run to replicate the cases in FAA Order 7110.110A. All computations used a WGS-84 earth model.

2.3.2 ASAT Modifications—Operational Scenario

As shown in Figure 2, the operational scenario consisted of two aircraft approaching a pair of converging runways. Both aircraft were initialized prior to the Missed Approach Point (MAP). Once at the MAP, each aircraft executed a missed approach procedure consisting of a climb while maintaining a nominal ground track that coincided with the approach ground track.

Aircraft speeds and DHs were set according to the various cases in FAA Order 7110.110A. The speeds of both aircraft were maintained throughout the duration of each simulation run. The ASAT simulation model accounted for the ground track deviations that occur during the missed approach procedure. These deviations were assumed to be normally distributed with a mean value of 0º and a standard deviation (σ) of 5º and bounded between ±15º. Therefore, a wider area of potential conflict existed as shown by the overlapping yellow areas associated with each runway as shown in Figure 2.

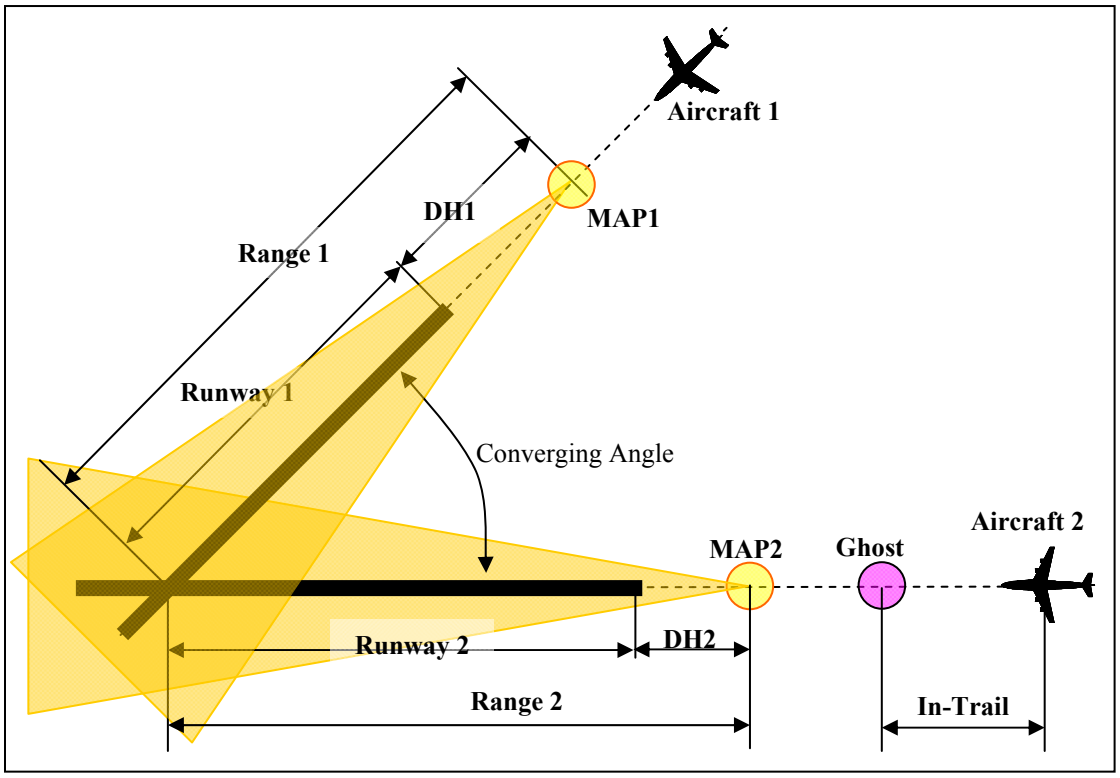

Figure 2: DCIA with CRDA Operational Model

2.3.3 ASAT Modifications—Wake Vortex Evaluation

For this study, the wake vortex evaluation consisted of modifying ASAT with a wake prediction algorithm, correlating the positions of aircraft and wake vortices, and establishing specific parameters for defining a wake vortex encounter.

2.3.3.1 Aircraft Vortex Spacing System (AVOSS) Prediction Algorithm

For this study, the National Aeronautics and Space Administration's (NASA) Aircraft Vortex Spacing System (AVOSS) Prediction Algorithm (APA) Version 3.2 was integrated into ASAT[1].

The APA accepted as input meteorological data and aircraft data. After accepting the meteorological and aircraft data, the APA computed a transport and decay time for a wake. The decay time expressed the decrease in wake strength versus time. The analysis in this report used the APA transport and decay times coupled with the ASAT Monte

[1] Refer to [2] for a more complete description of AVOSS and its prediction algorithm.

Carlo simulation capability to determine if aircraft on numerous and varied simulated DCIA missed approaches encountered a wake.

The APA handled both wakes out-of-ground effect and wakes in-ground effect (i.e., close to the ground). Wakes out-of-ground effect descended from the point at which they were generated and were transported horizontally by any crosswinds. Wakes in-ground effect could no longer descend and could even bounce back into the air upon contact with the ground.

The level of atmospheric turbulence present in the immediate vicinity of the wake directly influenced the speed of the wake decay. The measure of atmospheric turbulence is called the Eddy Dissipation Rate (EDR). Typical values for EDR range from 1×10^{-2} m^2/sec^3 to 1×10^{-6} m^2/sec^3. An EDR in the middle of the typical range, i.e., 1×10^{-3} m^2/sec^3, was used for this study.

The APA output within ASAT was modified to make vortices respond to wind as if it was coming from different directions so that vortices from the same aircraft were transported in opposite directions, as shown in Figure 3. As a result, ASAT checked for wake encounters in a wider area in half as many simulation runs.

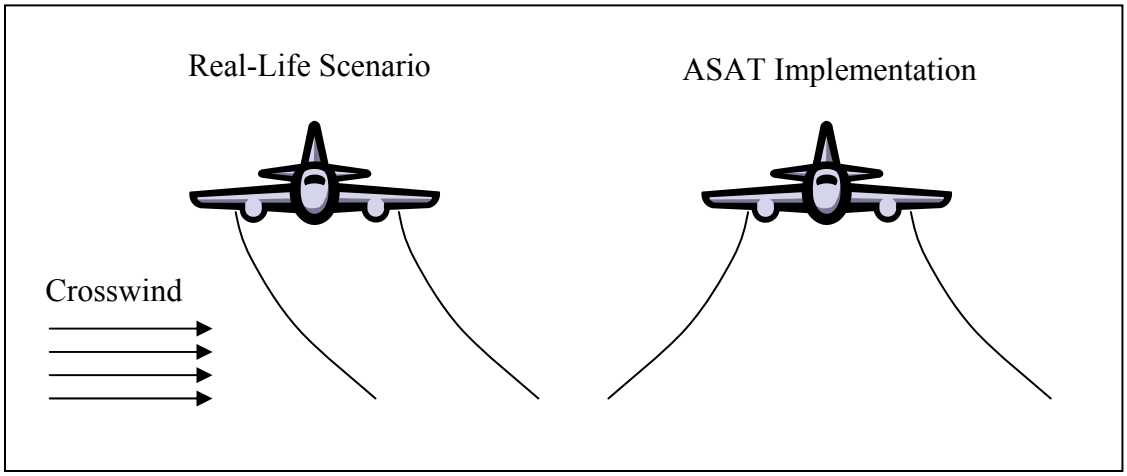

Figure 3: APA Output Implementation in ASAT

2.3.3.2 Wake Vortex Simulation Description

Every second of the simulation, ASAT generated an APA "tile" as shown in Figure 4. Each "tile" contained a pair of vortices generated by the APA using a set of given initial conditions at the point the tile was created. Thereafter, both vortices of the wake were simulated for 240 seconds (4 minutes). At the end of the run, the positions of the aircraft and the wake vortices were time-correlated to evaluate whether a wake encounter occurred. Note that in the illustrative Figure 4, the wakes from both wings are responding to the same wind vector whereas in the simulation the vortices would travel outward from both wings as explained in the previous section.

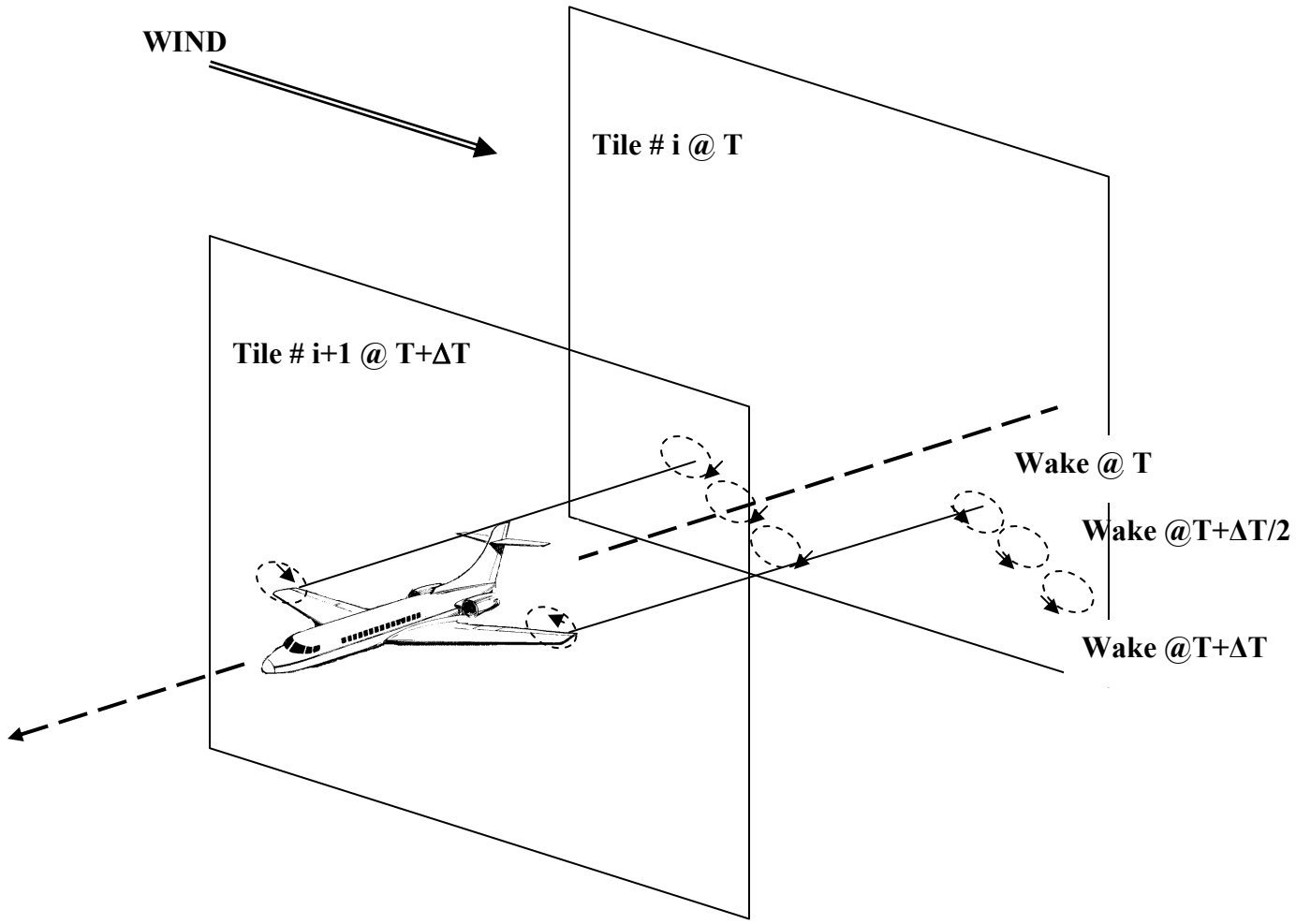

Figure 4: Wake Vortex Evaluation "Tiles"

2.3.3.3 Wake Vortex Encounter Criteria

There is no "official" definition of what qualifies as a wake encounter. Since the strength of a wake is dependent on many factors (mass, wingspan, and speed of the generating aircraft, wind, temperature, age of vortex, etc.) and the significance of an encounter to the trailing aircraft is dependent on additional factors (mass, size, speed, encounter geometry), this is a very complex issue. For the purposes of this study, an aircraft was considered to have encountered a wake vortex if a wake with strength exceeding 70 m^2/sec came within a distance of 200 feet of the aircraft's center of mass. The 70 m^2/sec value was selected as a lower limit to facilitate the evaluation. It represented a relatively weak wake strength that would not normally constitute a hazard to an aircraft but was significant and within the strength region where the wake model was quite stable. The 200 foot separation distance was selected based on the size of wakes and typical wingspan values so that if the wake was within 200 feet of the aircraft's center of mass, the vortex would likely be impacting some part of the airframe.

2.4 Wake Turbulence Aircraft Classes

For wake separation purposes, *Air Traffic Control* [3] classifies aircraft as Heavy, Large, or Small based on the following criteria:

- Heavy - Aircraft capable of takeoff weights of more than 255,000 pounds whether or not they are operating at this weight during a particular phase of flight.

- Large - Aircraft of more than 41,000 pounds, maximum certificated takeoff weight, up to 255,000 pounds. (While technically a Large aircraft, the B757 has its own set of wake turbulence separation minima which closely resembles that of a Heavy aircraft.)

- Small - Aircraft of 41,000 pounds or less maximum certificated takeoff weight.

Only Heavy and Large aircraft were considered as potential sources of wake in the simulation. Because wake vortex encounters were based only on the strength of the wake, the weight class of the encountering aircraft was not considered.

2.5 ASAT Monte Carlo Simulation Runs

Simulation runs were conducted for the following purposes: (1) to determine the probability of a TCV between DCIA aircraft during dual missed approaches and (2) to determine if either aircraft encountered a wake vortex during dual missed approaches.

2.5.1 Simulation Parameters

ASAT simulations used the following critical parameters:

- Decision Height - Uniform probability distribution bounded between one of the three ranges listed in Table 1.

- Distance from threshold to intersection - Specific combinations of lengths as per the cases listed in FAA Order 7110.110A.

- Aircraft speed - Except where otherwise required by *Dependent Converging Instrument Approaches (DCIA) with Converging Runway Display Aid (CRDA)* [1], the speed range was uniformly distributed between 80 knots true airspeed (KTAS) and 160 KTAS.

- Converging angle - Uniform probability distribution bounded between 45º and 120º.

In addition, ASAT used the following variations in critical parameters to account for deviations from a nominal scenario:

- Variation in speed - Uniform probability distribution bounded between ±5.0 KTAS around the mean values.

- Variation in position - Uniform probability distribution of ±0.25 nautical miles (NM) between "ghost" and trailing aircraft to account for radar-displayed position error.

Additional aircraft performance parameters relevant to this study can be found in Appendix A, Section 1.

2.5.2 Collison Risk Criteria Violation Related Simulation Runs

Each of the 108 cases described in [1] was initially evaluated using a set of 10,000 ASAT Monte Carlo simulation runs. During the initial stage of the study, ASAT performed a total of 1.08 million (1.08×10^6) simulation runs.

During the course of each simulation run, ASAT computed the slant distance between the centers of gravity of both aircraft as they executed missed approaches. At the end of each run, the shortest slant range distance between aircraft, the Closest Point of Approach (CPA), was recorded. At the end of each set of 10,000 Monte Carlo simulation runs, a

histogram of the CPA values was generated and stored. CPA values less than 500 feet were considered to be Test Criteria Violations (TCV)[2].

Figure 5 shows an ASAT screen capture depicting a set of 300 simulation runs associated with case number 18 in Table 1-A of [1]. Figure 5 also shows the flight track variation of the aircraft on missed approach.

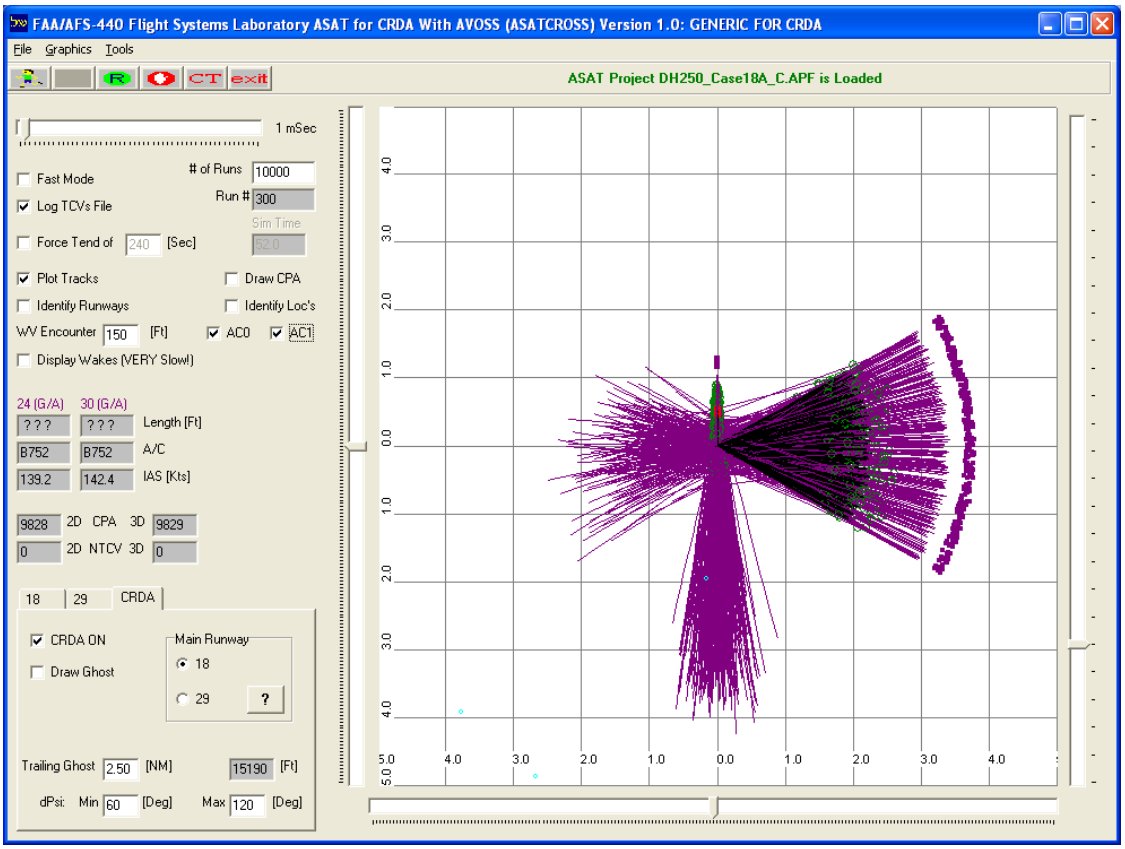

Figure 5: Typical ASAT Depiction of TCV Related Simulation Runs

2.5.3 Wake Vortex Encounter Related Simulation Runs

The purpose of the wake vortex analysis was to determine if one aircraft encountered the wake of the other aircraft during simultaneous missed approaches.

Using NASA's APA Version 3.2 model, ASAT generated a pair of vortices each second of a simulation run. Due to the complex nature of the wake vortex generation and encounter detection algorithms, ASAT executed the wake vortex related simulation runs

[2] For this as well as other similar studies, CPAs of less than 500 feet, while not technically mid-air collisions, are considered unacceptable and therefore, violations of the test criteria.

significantly slower than the runs only related to separation based TCVs. To perform all necessary ASAT Monte Carlo simulation runs in a timely manner, the wake generation and encounter detection algorithms were performed only on every tenth run. Thus, for all 108 cases, 1,000 runs included the wake vortex encounter evaluation resulting in a total of 108,000 runs with wake vortex generation and encounter detection algorithms active. A small number of cases did not experience encounters in the first 1,000 runs, but follow-up testing of those cases did show encounters.

Figure 6 depicts an ASAT screen capture of a single simulation run depicting two flight trajectories, APA wake vortex "tiles" and a wake vortex encounter. While the 1,000 runs would normally be an unacceptably small sample size, the simulation was only checking for wake encounters and, in all cases, one or more encounters were detected.

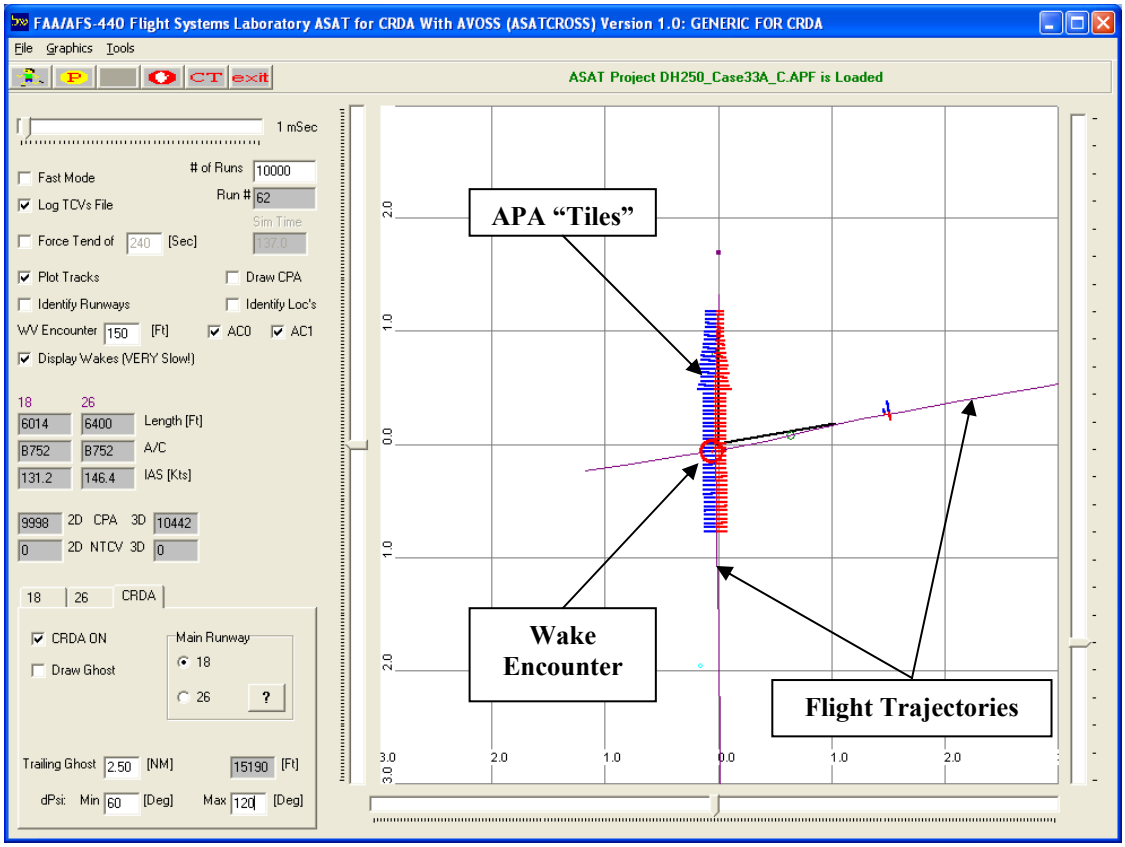

Figure 6: Typical ASAT Depiction of Wake Vortex Related Simulation Runs

3.0 Summary of Data Analysis

The output of the simulation runs was analyzed to determine the risks of both unsafe separation (as defined by the TCV) and wake turbulence encounters during DCIA with CRDA operations in 108 cases. The study collected data on the risk of the runway convergence angles and DHs.

3.1 Evaluation of Risk of TCV

To evaluate the risk of TCV during the simulated DCIA operations, first the benchmark for the maximum allowable risk was established. The probability of a TCV was computed based on the separation analysis and the probability of simultaneous missed approaches.

3.1.1 Target Level of Safety

The Target Level of Safety (TLS) is the maximum acceptable risk associated with an operation. For the purposes of this analysis, a collision risk of 1.0×10^{-9} per operation will be considered an acceptable level of risk. This value is our interpretation of the intent of the Air Traffic Organization Safety Management System Manual's limit on the occurrence of catastrophic events.

3.1.2 Probability of Dual Missed Approaches during DCIA Operations

Appendix B shows the results of the statistical analysis used to determine the probability of DCIA aircraft on missed approaches coming within 500 feet of each other for each of the cases in Table 1. The raw values in Appendix B were multiplied by the probability of a dual missed approach to determine the overall probability of a TCV that was then compared to the TLS.

A recent evaluation of missed approach rates based on several international data collection programs was documented in [4]. That report suggested a generic rate of 2×10^{-3} or 2 missed approaches for every 1000 approaches. Assuming independence, this rate would put the probability of dual missed approaches at 4×10^{-6}. However, for many reasons such as common inclement weather conditions, failure of a shared air traffic control facility, or a disabled aircraft at or near the converging intersection of the runways, dual missed approaches during DCIA operations may not be independent events but may have a common source. Therefore, for purposes of this study, a more conservative value of 4×10^{-5} was assigned to the probability of dual missed approaches.

3.1.3 FAA Order 7110.110A Cases with TCVs

Appendix B contains the results of the statistical analysis used to determine the probability of DCIA aircraft on missed approaches coming within 500 feet of each other for each of the cases in Table 1. The results of that analysis were multiplied by 4×10^{-5}, the assumed probability of a dual missed approach, to obtain the TCV probabilities shown in Table 2. Of the 108 DCIA cases examined, three cases resulted in a probability of a TCV that did not meet the TLS discussed in paragraph 3.1.1. These cases are shown in Table 2.

Table 2: FAA Order 7110.110A Cases with Probability of TCV Exceeding TLS

Case	DH (ft)	Shorter Distance from Threshold to Intersection (ft)	Longer Distance from Threshold to Intersection (ft)	Probability of TCV	Number of TCVs per Billion Runs
DH700 case 07	501 to 700	up to 1,600	6,101 to 7,900	1.78×10^{-9}	1.78
DH700 case 08	501 to 700	up to 1,600	7,901 to 9,900	2.43×10^{-9}	2.43
DH700 case 29	501 to 700	4,101 to 5,000	11,301 to 15,300	4.08×10^{-9}	4.08

While not exceeding the TLS, the two cases shown in Table 3 had TCV probabilities just under the TLS threshold and are high when compared to the other cases.

Table 3: Other FAA Order 7110.110A Cases of Interest

Case	DH (ft)	Shorter Distance from Threshold to Intersection (ft)	Longer Distance from Threshold to Intersection (ft)	Probability of TCV	Number of TCVs per Billion Runs
DH500 case 08	251 to 500	up to 2,100	8,901 to 11,200	7.6×10^{-10}	0.76
DH700 case 06	501 to 700	up to 1,600	4,801 to 6,100	7.8×10^{-10}	0.78

3.1.4 In-Depth Analysis of High Risk FAA Order 7110.110A Cases

The five cases identified in Section 3.1.3 as having a higher probability of TCV were examined in greater depth to determine which runway convergence angle combinations present the greatest risk. One hundred thousand additional ASAT runs were made for each of the five cases of interest. A complete description of the statistical analysis used to evaluate the ASAT runs is contained in Appendix C. The results of this extended analysis are shown in Table 4.

Table 4: DCIA Cases of Interest with Highest Risk Runway Convergence Angles Identified

Case	DH (ft)	Runway Convergence Angles (°)	Probability of TCV	TCVs per Billion
DH500 case 08	251 to 500	110 to 120	1.88×10^{-8}	18.8
DH700 case 06	501 to 700	110 to 120	3.64×10^{-8}	36.4
DH700 case 07	501 to 700	110 to 120	4.88×10^{-8}	48.8
DH700 case 08	501 to 700	110 to 120	4.72×10^{-8}	47.2
DH700 case 29	501 to 700	110 to 120	1.12×10^{-8}	11.2

Note that the cases with the highest risk of a TCV in Table 4 are the cases with runway convergence angles of 110° to 120°. The probability of a TCV in the 110° to 120° runway convergence angle range (shown in Table 4) was greater than the probability of a TCV for the entire range of runway convergence angles as reported in Table 2 and Table 3. This is because the original 10,000 ASAT runs per case were uniformly distributed over the entire runway convergence angle range; however, the risk is not uniformly distributed across the same range. Therefore, the additional 100,000 ASAT runs concentrated on the range of runway convergence angles that demonstrated a higher probability for a TCV.

3.2 Evaluation of Wake Encounters

Using the wake vortex encounter criteria described in Section 2.3.3.3, encounters were observed in all 108 cases. Figure 7 shows the probabilities of encountering a wake of a particular intensity for the cases broken down by DH. The text overlay gives the overall probability of an encounter of any wake intensity greater than 70 m^2/sec. The data shows that, as the DH increases, the probability of a wake encounter decreases but the likelihood that the wake encounter will be stronger increases. In general, the higher DH puts the aircraft farther away from the intersection point and allows more time for the normal dispersive effects (variations in heading and climb rates) to separate the aircraft (so that there are fewer encounters for a given number of dual go-arounds) but also allows more time for the trailing aircraft to catch up and thus experience a more significant encounter if one occurs. A point to consider is that the aircraft that are most susceptible to hazardous wake vortex encounters (smaller general aviation aircraft) are less likely to be gaining ground on a significant wake generator. As of the writing of this report, no definitive criteria for hazardous wake vortex encounters exist. Because the scope of this study addressed operations to runways with converging angles between 45º to 120º, the relative geometry suggests that any wake encounters will have a relatively short duration because the trailing aircraft will be flying across the vortex rather than along it. Historical studies have generally examined wake encounters by trailing aircraft but studies are underway that will include consideration of higher angle encounters such as converging runway operations could generate.

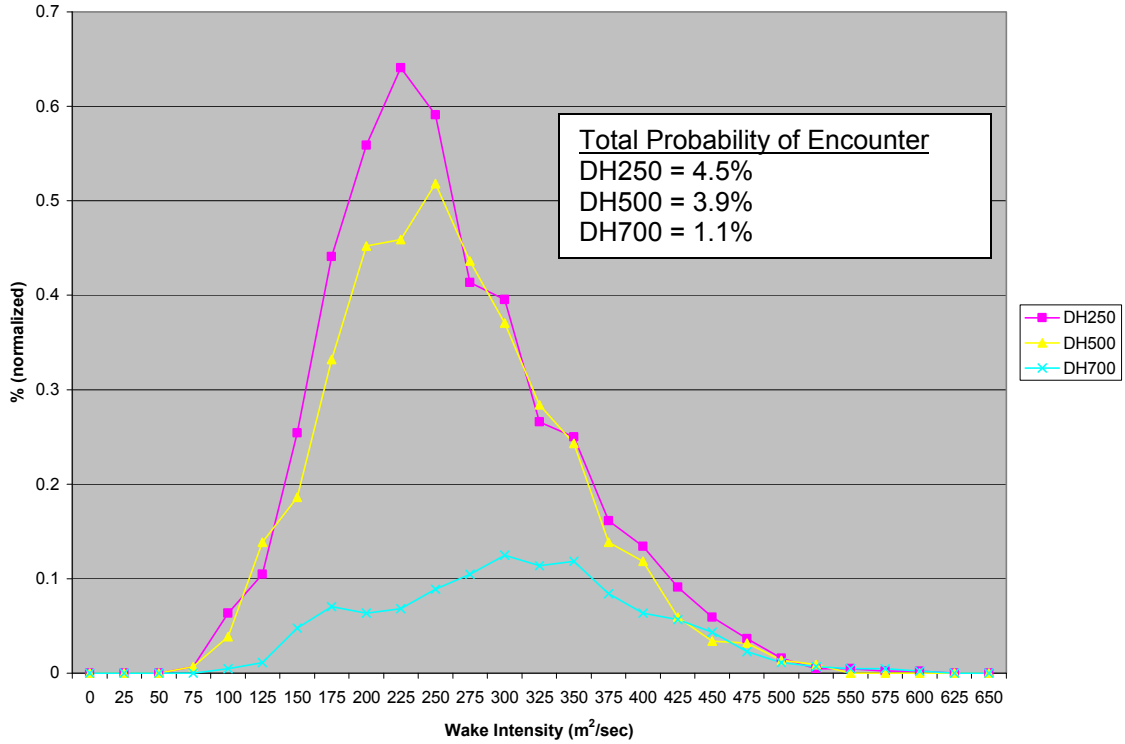

Figure 7. Probability of Encounter by Intensity

4.0 Results and Conclusions

4.1 Risk of TCV (Separation less than 500 feet)

As Table 2 shows, three of the 108 cases evaluated did not meet the TLS of 1×10^{-9} per approach. All three cases (DH700 case 07, DH700 case 08, and DH700 case 29) were in the highest DH range of 501 to 700 feet. While two other cases did not exceed the TLS, they showed an elevated risk of TCV when compared to the other DCIA cases. These cases were DH500 case 08 and DH700 case 06.

A more in-depth analysis of the higher risk DCIA cases concluded that the 110° to 120° runway convergence angle sector presented the greatest risk for loss of safe separation (less than 500 feet) during simultaneous missed approaches. Three possible mitigation strategies for these cases and runway convergence angle sectors are: (1) to further extend the required stagger distances defined in Order 7110.110, (2) to avoid DCIA operations for the high risk cases in the 110° to 120° runway convergence angle sector or (3) to develop turning missed approach procedures for one or both aircraft. Decision Heights in this range normally allow the pilot to start an immediate turn during the missed approach. The higher DHs also allow more time for ATC to identify a potential conflict and take corrective action.

Consideration should also be given to the low probability of an airport having these particular runway configurations and needing to perform simultaneous approach operations to them. For runway configurations with more than 90° of convergence, it would be unusual for wind conditions to support simultaneous operations.

4.2 Wake Vortex Encounters

All 108 cases resulted in wake vortex encounters as defined in this study. However, because a "hazardous" wake vortex encounter has not been defined, it is currently not possible to draw any conclusions from the 108 DCIA cases from a wake vortex standpoint. The DCIA allowed geometries also dictated that the duration of any encounter was brief. The aircraft encountering the wake was crossing the wake vortex rather than flying along it as might happen if the aircraft were both on approach to the same runway. To evaluate the safety of DCIA operations (as well as similar operations), a quantitative definition of a hazardous wake vortex encounter must be developed. The FAA is currently performing studies and developing tools to identify and define hazardous wake encounters. Studies are planned to evaluate the effects of flying through a wake or a pair of wake vortices, including at higher angles of encounter. When a definition of a hazardous encounter is established, each real-world implementation of a DCIA operation should be evaluated for wake turbulence hazards.

Appendix A: Additional Parameter Descriptions

Aircraft performance data used for flight trajectory generation

The following data items were used in the generation of flight trajectories:

- Airspeed - As per the values contained in Table 1-A, Table 1-B, and Table 1-C of *Dependent Converging Instrument Approaches (DCIA) with Converging Runway Display Aid (CRDA)* [1].

- Climb rate - Uniform probability distribution bounded between the values of 400 feet per minute (fpm) and 2,000 fpm. A distinct value was chosen for each aircraft for each run.

- Rate of change of climb rate - Aircraft reached their stabilized climb rate within a time range from 6 to 20 seconds. This rate translated to a uniform distribution of rate of change of climb rate between 30 fpm/sec and 100 fpm/sec. Again, a distinct value was chosen for each aircraft for each run.

The climb rate and rate of change of climb rate distributions were not intended to be representative of any particular fleet mix or airport environment. The ranges were selected to reflect reasonable performance values that could be seen in the NAS.

Aircraft characteristics used for wake vortex generation

NASA's Aircraft Vortex Spacing System (AVOSS) Prediction Algorithm (APA) required four inputs to calculate the initial condition for each of the two wake vortices:

- Weight
- True airspeed
- Air density
- Wing span

The following aircraft representative of a Heavy and a Large wake turbulence class were used in this study:

- **B757-200 (Heavy)**
    - Weight: 200,000 lb
    - True airspeed: 110–160 KTAS
    - Air density: 1.225 Kg/m^3
    - Wing span: 124.5 ft

- **MD88 (Large)**
    - Weight: 110,000 lb
    - True airspeed: 105–160 KTAS
    - Air density: 1.225 Kg/m^3
    - Wing span: 107.7 ft

In addition, where speeds lower than 105 knots were required, the following virtual aircraft was used to generate wake vortices:

- **Virtual Very Light Large (VVLL)**
    - Weight: 70,000 lb
    - True airspeed: 80–105 KTAS
    - Air density: 1.225 Kg/m^3
    - Wing span: 124.5 ft

Atmospheric characteristics

Once the initial conditions of the wake vortices were calculated, APA used the following three altitude-dependent parameters to determine the transport and decay of the vortices:

- Crosswind - A constant crosswind component of 1.0 m/sec (approximately 1.8 KTS) was used. For parallel runway studies, the crosswind component is very important as it determines how fast the vortex is transported to adjacent runways. In this study, the courses converged so the wake did not have to be transported. Time was less significant (since the trailing aircraft usually passed the intersection point very shortly after the generating aircraft) and a low wind speed was selected to maximize the vortex stability.

- Ambient temperature
    - Standard temperature (15 ºC) at ground level
    - Adiabatic lapse rate (-0.00976 ºC/meter)

- Eddy Dissipation Rate (EDR): Constant, 1×10^{-3} m^2/sec^3

(Typical EDR values range between 1×10^{-2} $m^2/sec^3$and 1×10^{-6} m^2/sec^3. The selected value of 1×10^{-3} caused the vortices to dissipate rather quickly but the time between leading and trailing aircraft passing through the intersection was fairly short. As stated earlier, with fairly conservative values, the simulation showed that all the cases resulted in encounters.)

Appendix B: Statistical Analysis of ASAT Output

This appendix contains the statistical analysis performed on the FAA Order 7110.110A cases. The results presented in this appendix were derived from the output generated by ASAT. Because all ASAT runs were conducted using a simultaneous dual missed approach scenario, the probabilities shown should be multiplied by the probability that simultaneous dual missed approaches may occur.

The purpose of this analysis was to determine the probability that a Closest Point of Approach (CPA) would be less than 500 feet. Data were generated and analyzed for 108 separate cases. For each case an attempt was made to find the best fit distribution that would match the ASAT Monte Carlo simulation results. Using the Kolmogorov-Smirnov and Anderson-Darling goodness of fit tests, it was determined that most of the data sets matched a Johnson S_B (bounded) distribution with appropriate parameters: ε (epsilon) (the minimum value of the function), λ (lambda), γ (gamma), and δ (delta). Using the approximating distribution and the empirical data, the probability that the CPA would be less than 500 feet was determined.

As an example, consider the case DH250_Case16A_C.

The best fit Johnson S_B distribution had the following parameters:

$\varepsilon = 176.57$
$\lambda = 15768.6$
$\gamma = 0.126628$
$\delta = 1.33898$

The Kolmogorov-Smirnov goodness of fit test gave a *p*-value of 0.292. The Anderson-Darling goodness of fit test gave a *p*-value of 0.282. At a threshold of 0.05, both tests indicated that the null hypothesis, i.e., the data set was from the indicated Johnson S_B distribution, should not be rejected.

The probability density function for this distribution was given by:

$$f(x) = \begin{cases} \dfrac{\delta}{\sqrt{2\pi}\, y(1-y)\lambda} \exp\left(-\tfrac{1}{2}\left(\gamma + \delta \ln\left(\dfrac{y}{1-y} \right) \right)^2 \right) & \text{if } (\varepsilon + \lambda) > x > \varepsilon, \\ 0 & \text{if } x \geq (\varepsilon + \lambda) \text{ or } x \leq \varepsilon. \end{cases}$$

where $y = \dfrac{x - \varepsilon}{\lambda}$.

Figure B1 shows the data histogram and the approximating Johnson S_B distribution. (Note that in the figures, S_B is written as SB.)

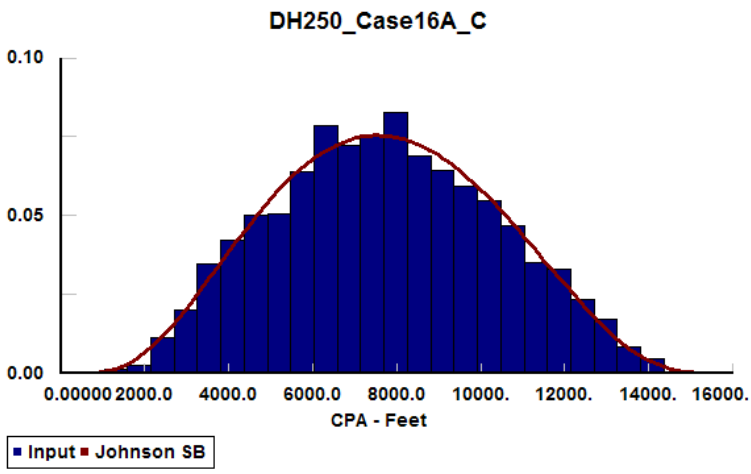

Figure B1: DH250_Case16A_C Histogram and Fitted Johnson S_B Distribution

If X is a random variable from this distribution, the probability that X is less than α is given by the following:

$$P(X < \alpha) = \int_{-\infty}^{\alpha} f(x)dx .$$

So for DH250_Case16A_C, where X denotes CPA:

$$P(CPA < 500) = \int_{-\infty}^{500} f(x)dx = 2.21 \times 10^{-7} .$$

In addition, the empirical probability that a CPA was less than 500 feet was calculated from the original data set. Of the 10,000 CPA values, one value was less than 500 feet, so the empirical probability is given by

$$P(CPA < 500) = \frac{1}{10000} = .0001 .$$

Each of the other 107 test cases was analyzed in a similar way.

For many of the cases, the minimum parameter value, ε, for the best fit Johnson S_B distribution was determined to be greater than 500 feet. Since this family of distributions was bounded below by the minimum parameter value, the probability calculated from the best fit distribution was identically zero for these cases.

Results

Table B1, Table B2, and Table B3 show the probabilities calculated for each case using the method described above.

Table B1: Probabilities for DH250 Cases

Case	P(CPA < 500) Best Fit Johnson S_B	P(CPA < 500) Empirical
01	0	0.0000
02	0	0.0000
03	0	0.0000
04	0	0.0000
05	0	0.0000
06	$1.18 \cdot \times 10^{-9}$	0.0000
07	0	0.0000
08	0	0.0000
09	0	0.0000
10	0	0.0000
11	0	0.0000
12	0	0.0000
13	0	0.0000
14	0	0.0000
15	0	0.0000
16	2.21×10^{-7}	0.0001
17	3.12×10^{-11}	0.0001
18	0	0.0000
19	0	0.0000
20	0	0.0000
21	0	0.0000
22	0	0.0000
23	0	0.0000
24	0	0.0000
25	0	0.0000
26	0	0.0000
27	0	0.0000
28	0	0.0000
29	0	0.0000
30	0	0.0000
31	0	0.0000
32	0	0.0000
33	0	0.0000
34	0	0.0000
35	0	0.0000
36	0	0.0000
37	0	0.0000
38	0	0.0000
39	0	0.0000
40	0	0.0000
41	0	0.0000
42	0	0.0000
43	0	0.0000
44	0	0.0000

Table B2: Probabilities for DH500 Cases

Case	P(CPA < 500) Best Fit Johnson S_B	P(CPA < 500) Empirical
01	0	0.0000
02	0	0.0000
03	0	0.0000
04	0	0.0000
05	0	0.0000
06	3.72×10^{-10}	0.0000
07	4.36×10^{-12}	0.0000
08	1.90×10^{-5}	0.0002
09	5.23×10^{-13}	0.0000
10	0	0.0000
11	0	0.0000
12	0	0.0000
13	0	0.0000
14	0	0.0000
15	1.04×10^{-12}	0.0001
16	4.86×10^{-8}	0.0000
17	0	0.0000
18	0	0.0000
19	0	0.0000
20	0	0.0000
21	0	0.0000
22	0	0.0000
23	0	0.0000
24	0	0.0000
25	0	0.0000
26	0	0.0000
27	0	0.0000
28	0	0.0000
29	0	0.0000

Table B3: Probabilities for DH700 Cases

Case	P(CPA < 500) Best Fit Johnson S_B	P(CPA<500) Empirical
01	0	0.0000
02	1.13×10^{-16}	0.0000
03	8.53×10^{-7}	0.0001
04	6.22×10^{-13}	0.0000
05	2.21×10^{-8}	0.0000
06	1.95×10^{-5}	0.0001
07	4.45×10^{-5}	0.0001
08	6.07×10^{-5}	0.0001
09	7.81×10^{-7}	0.0000
10	0	0.0000
11	0	0.0000
12	1.03×10^{-16}	0.0000
13	1.33×10^{-15}	0.0001
14	4.24×10^{-6}	0.0000
15	8.66×10^{-11}	0.0000
16	0	0.0000
17	0	0.0000
18	0	0.0000
19	2.77×10^{-9}	0.0000
20	0	0.0000
21	1.77×10^{-14}	0.0001
22	7.98×10^{-6}	0.0001
23	6.97×10^{-14}	0.0001
24	0	0.0000
25	0	0.0000
26	0	0.0000
27	2.01×10^{-10}	0.0000
28	1.57×10^{-8}	0.0000
29	1.02×10^{-4}	0.0001
30	0	0.0000
31	7.90×10^{-19}	0.0000
32	1.41×10^{-6}	0.0000
33	0	0.0000
34	2.39×10^{-16}	0.0000
35	0	0.0000

Table B4, Table B5, and Table B6 show the parameter values for the best fit Johnson S_B distribution for each case. The column labeled KS stands for Kolmogorov-Smirnov and the column labeled AD stands for Anderson-Darling. An asterisk (*) in one of these columns indicates that the best fit Johnson S_B distribution had a *p*-value less than 0.05 for the corresponding goodness of fit test, and according to this test it would be unlikely that the data came from the best fit distribution.

Table B4: Johnson S_B Parameter Values for DH250 Cases

Case	ε (epsilon)	λ (lambda)	γ (gamma)	δ (delta)	KS	AD
01	1,790.9	14,665.5	0.05920	1.07906		
02	1,561.7	15,069.7	0.03924	1.13994		
03	1,550.1	14,742.5	0.13792	1.18098		
04	2,590.8	13,547.2	0.12010	1.31421		*
05	4,147.6	11,481.9	0.21629	1.09738		*
06	330.0	15,609.2	0.17852	1.36379		*
07	931.7	13,954.3	0.28030	1.20895		
08	1,718.8	17,189.5	0.16833	1.25439		
09	1,148.7	17,963.5	0.14011	1.30813		
10	2,177.6	15,639.7	0.26184	1.12533		
11	1,690.8	20,097.7	0.15082	1.33192	*	*
12	1,429.5	15,458.6	0.04891	1.11896		
13	1,368.2	15,312.6	0.16869	1.16850		
14	1,221.0	15,520.7	0.16546	1.20429		
15	1,004.1	15,044.5	0.16098	1.20675		
16	176.6	15,768.6	0.12663	1.33898		
17	420.0	14,920.4	0.23560	1.29688		
18	1,865.4	16,702.9	0.30061	1.21579		
19	2,851.0	19,891.1	0.27732	1.24613		
20	712.4	16,555.6	0.16372	1.25396		
21	1,645.2	14,517.4	0.29176	1.31846	*	
22	1,360.3	15,290.3	0.16048	1.28675		
23	1,193.8	14,998.3	0.22537	1.31965	*	
24	1,772.5	13,060.2	0.24840	1.15456		
25	878.4	17,916.0	0.20515	1.29482		
26	2,707.3	19,627.2	0.22808	1.16202		
27	1,052.7	16,720.6	0.12241	1.27065		
28	2,679.0	18,288.4	-0.00116	1.13227		
29	4,244.0	17,469.0	0.19446	1.12435		
30	2,628.6	17,290.8	0.36837	1.25853		
31	1,808.2	18,819.1	0.35976	1.36212		
32	1,934.8	21,093.2	0.27644	1.22638		
33	3,239.3	18,531.7	0.18071	1.06825		
34	3,486.4	18,343.8	0.25826	1.23546		
35	1,819.1	18,915.8	0.15611	1.27643		
36	1,429.4	18,977.9	0.25510	1.34144		
37	1,922.1	18,777.9	0.37160	1.27817		
38	1,083.8	20,608.7	-0.04022	1.17234	*	*
39	1,628.3	20,102.3	0.09245	1.21251		
40	1,194.4	20,647.6	0.21360	1.36107		
41	6,814.5	14,184.7	-0.16168	0.90842		*
42	3,082.2	19,913.4	0.13566	1.21723		
43	3,155.6	19,334.9	0.22708	1.13285	*	*
44	2,895.4	17,894.8	-0.27533	0.95309	*	*

Table B5: Johnson S_B Parameter Values for DH500 Cases

Case	ε (epsilon)	λ (lambda)	γ (gamma)	δ (delta)	KS	AD
01	1,623.4	14,777.2	0.00583	1.11198		
02	1,107.5	15,700.9	-0.01407	1.24023		
03	1,199.9	15,230.3	0.09268	1.25916		
04	1,398.8	14,250.7	0.12574	1.20737		
05	888.4	14,521.8	0.15814	1.28441		
06	341.7	15,869.5	0.07423	1.35520		
07	425.0	15,267.4	0.17331	1.31789	*	
08	-201.7	15,552.5	0.10514	1.38408		
09	380.0	19,058.3	0.08802	1.42497	*	
10	1,131.4	21,686.2	0.05704	1.45619	*	*
11	1,147.6	15,919.8	0.04560	1.16544		
12	909.6	15,987.3	0.13355	1.25499		
13	1,224.5	15,599.9	0.18105	1.38802		
14	423.3	16,053.1	0.12747	1.50310		
15	370.0	15,652.2	0.20523	1.51265		
16	0.0	20,029.2	0.10382	1.48310		*
17	556.7	22,391.9	0.00027	1.45110	*	*
18	2,315.3	15,340.5	0.00934	1.32060		*
19	1,559.3	19,416.8	-0.00389	1.16336		
20	1,410.9	19,440.9	0.12884	1.21961		
21	1,195.4	18,914.8	0.12086	1.24367		
22	2,768.4	16,525.4	0.27141	1.17924	*	*
23	1,255.5	18,939.5	0.17508	1.41581	*	*
24	1,344.6	21,733.2	0.14548	1.32925		
25	1,523.4	20,312.9	0.08880	1.30398	*	
26	4,141.0	17,303.5	-0.10518	1.04142		
27	3,806.5	18,322.2	0.09179	1.10679		
28	978.0	21,690.1	-0.08519	1.40856		*
29	1,750.3	20,412.9	-0.07861	1.27818	*	*

Table B6: Johnson S_B Parameter Values for DH700 Cases

Case	ε (epsilon)	λ (lambda)	γ (gamma)	δ (delta)	KS	AD
01	1,013.8	15,236.5	-0.06934	1.16999	*	*
02	475.0	15,973.1	-0.13107	1.25046		
03	-10.0	16,655.7	-0.00573	1.38342		*
04	435.0	15,394.2	0.04134	1.30726		
05	255.0	15,093.1	0.03623	1.34239	*	
06	-399.3	16,669.5	-0.01306	1.43156		*
07	-506.5	16,383.1	0.02992	1.44839		
08	-436.6	15,599.8	0.02017	1.40443		
09	-136.5	19,108.1	-0.07046	1.40519		
10	1,773.1	21,287.3	0.20031	1.40000		
11	1,707.7	15,362.4	-0.12005	1.27930	*	*
12	450.0	16,610.6	-0.01909	1.41294		
13	400.0	17,727.8	0.33018	1.59236		
14	-374.7	16,378.5	-0.08853	1.51794		
15	355.0	14,766.6	0.03431	1.39105		*
16	550.0	21,200.5	0.49978	1.51763		*
17	869.9	21,262.6	-0.05117	1.36050		
18	820.0	18,656.4	0.43366	1.45914		*
19	246.1	16,896.3	0.10758	1.41957		
20	775.5	19,587.1	-0.00609	1.26112		
21	430.0	20,664.1	0.22819	1.37307		
22	-284.1	19,865.7	0.03163	1.36173		
23	410.0	22,301.5	-0.00289	1.34229		
24	773.7	20,394.2	-0.04184	1.19421		
25	1,389.3	19,699.5	0.01526	1.30364		
26	1,475.4	20,898.2	0.41224	1.45574		
27	211.7	20,339.9	0.10446	1.49864		
28	29.1	20,240.0	0.02046	1.48604		
29	-3,331.4	26,480.7	-0.03538	2.07072		
30	1,602.5	21,180.5	0.29009	1.32208		
31	364.7	23,411.4	0.01646	1.70957		
32	-1,481.2	26,753.6	-0.03064	1.84185		
33	584.5	22,354.9	-0.07553	1.54549		
34	-2,339.1	26,585.8	-0.01423	2.14709		
35	1,165.5	25,898.1	0.03607	1.78797		

For 11 of the 108 cases, both of the goodness of fit tests used indicated that the null hypothesis, i.e., the data set was from the indicated Johnson S_B distribution, should be rejected. In each of these cases, the data were sufficiently irregular that no member of the Johnson S_B family provided a good match. In addition, no other statistical distributions were found to provide a fit that would not be rejected on similar grounds.

Table B7 lists these 11 cases along with the CPA from the 10,000 simulation runs for that case. It can be seen that none of these had a CPA less than 1,000 feet. Therefore, the inability to find a statistically valid distribution was probably not an issue for these cases.

Table B7: Best Fit Probability Distributions Rejected by Both Goodness of Fit Tests

Case	CPA
DH250_Case11A_C	2,600
DH250_Case38A_C	1,490
DH250_Case43A_C	1,380
DH250_Case44A_C	2,480
DH500_Case10A_C	2,140
DH500_Case17A_C	1,350
DH500_Case22A_C	2,190
DH500_Case23A_C	1,930
DH500_Case29A_C	2,290
DH700_Case01A_C	1,330
DH700_Case11A_C	2,070

For an additional 18 cases, one, but not both, of the goodness of fit tests indicated that the null hypothesis should be rejected. Table B8 lists these 18 cases along with the CPA from the 10,000 simulation runs for that case.

Table B8: Best Fit Probability Distributions Rejected by One Goodness of Fit Test

Case	CPA
DH250_Case04A_C	3,000
DH250_Case05A_C	3,150
DH250_Case06A_C	660
DH250_Case21A_C	1,870
DH250_Case23A_C	1,570
DH250_Case41A_C	4,880
DH500_Case07A_C	850
DH500_Case09A_C	760
DH500_Case16A_C	780
DH500_Case18A_C	1,880
DH500_Case25A_C	1,900
DH500_Case28A_C	1,450
DH700_Case03A_C	400
DH700_Case05A_C	510
DH700_Case06A_C	60
DH700_Case15A_C	710
DH700_Case16A_C	550
DH700_Case18A_C	820

The following pages contain figures which correspond to the data histograms for each case along with the best fit Johnson S_B distribution. For each, the red curve is the graph of the Johnson S_B Probability Density Function with parameters as shown in Table B4, Table B5, and Table B6.

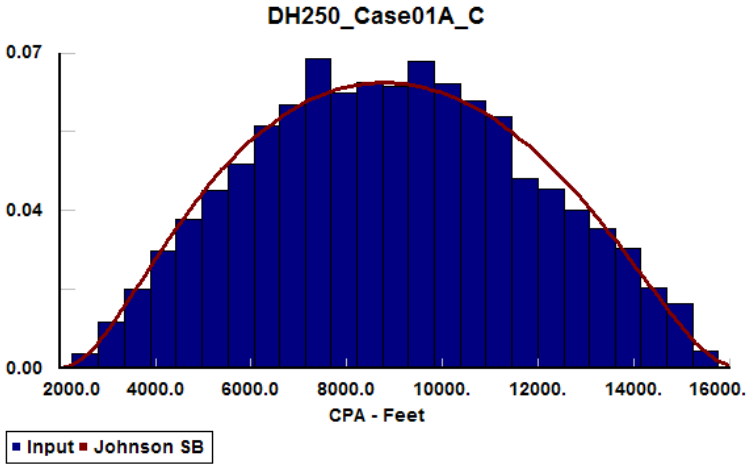
DH250_Case01A_C
0.07
0.04
0.00
2000.0
4000.0
6000.0
8000.0
10000.
12000.
14000.
16000.
CPA - Feet
Input
Johnson SB

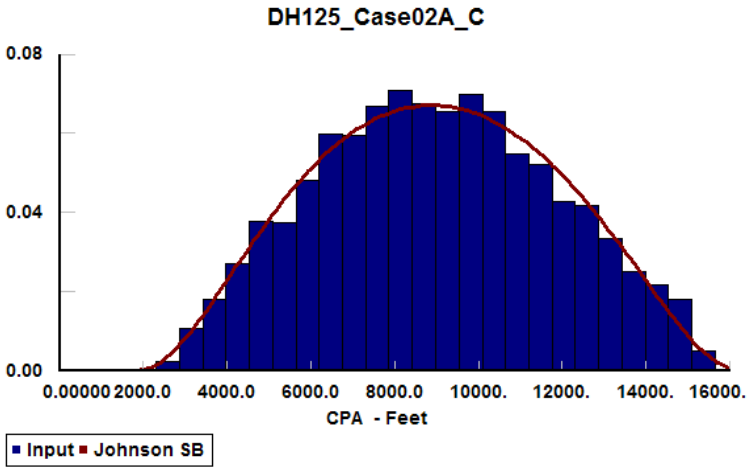
DH125_Case02A_C
0.08
0.04
0.00
0.00000
2000.0
4000.0
6000.0
8000.0
10000.
12000.
14000.
16000.
CPA - Feet
Input
Johnson SB

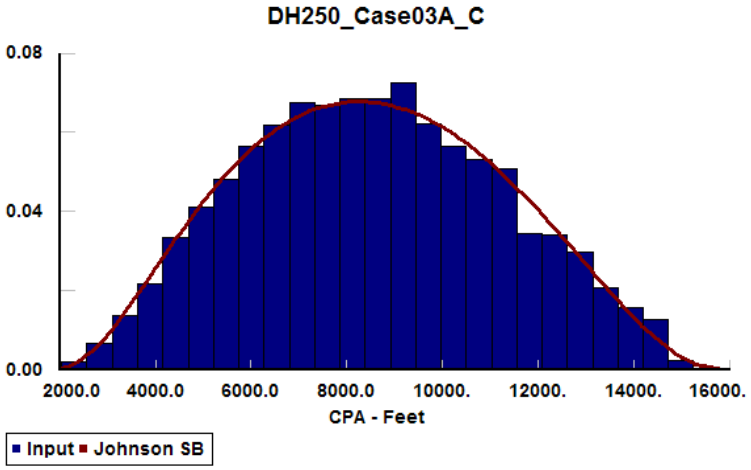
DH250_Case03A_C
0.08
0.04
0.00
2000.0
4000.0
6000.0
8000.0
10000.
12000.
14000.
16000.
CPA - Feet
Input
Johnson SB

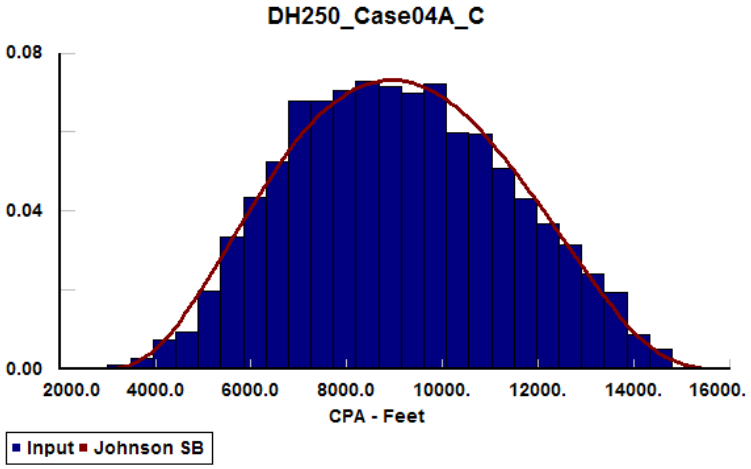
DH250_Case04A_C
0.08
0.04
0.00
2000.0
4000.0
6000.0
8000.0
10000.
12000.
14000.
16000.
CPA - Feet
Input
Johnson SB

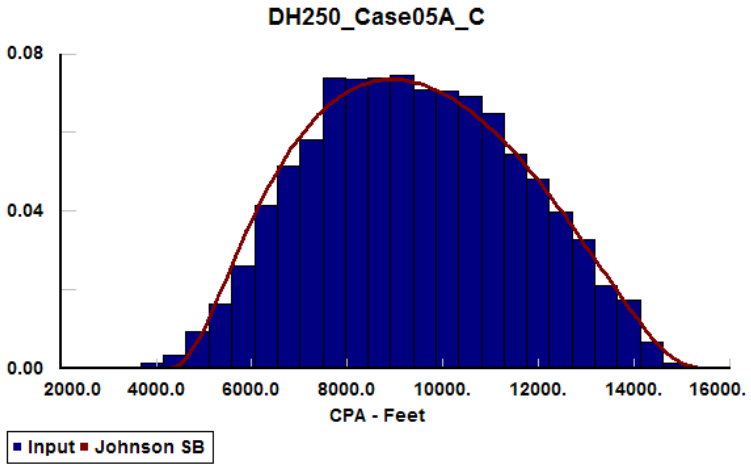
DH250_Case05A_C
0.08
0.04
0.00
2000.0
4000.0
6000.0
8000.0
10000.
12000.
14000.
16000.
CPA - Feet
Input
Johnson SB

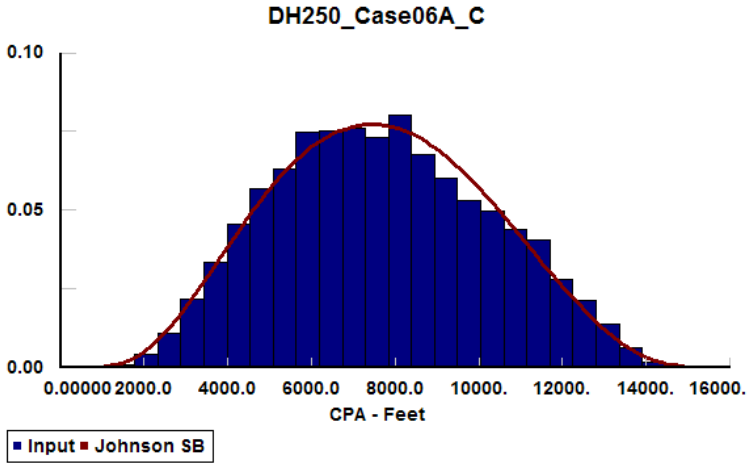
DH250_Case06A_C
0.10
0.05
0.00
0.00000
2000.0
4000.0
6000.0
8000.0
10000.
12000.
14000.
16000.
CPA - Feet
Input
Johnson SB

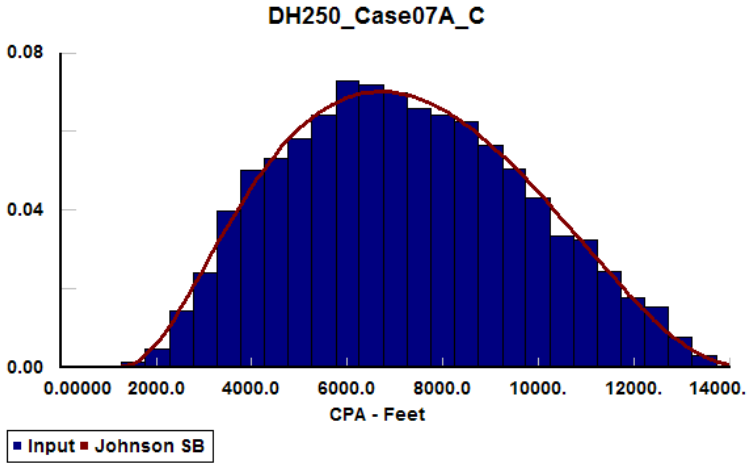
DH250_Case07A_C
0.08
0.04
0.00
0.00000
2000.0
4000.0
6000.0
8000.0
10000.
12000.
14000.
CPA - Feet
Input
Johnson SB

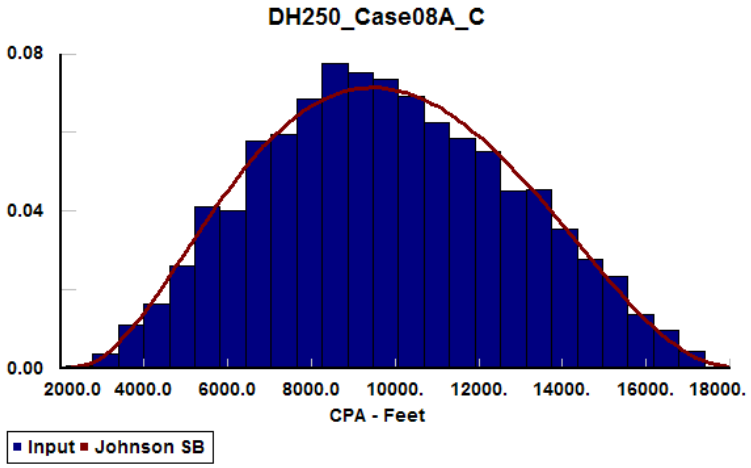
DH250_Case08A_C
0.08
0.04
0.00
2000.0
4000.0
6000.0
8000.0
10000.
12000.
14000.
16000.
18000.
CPA - Feet
Input
Johnson SB

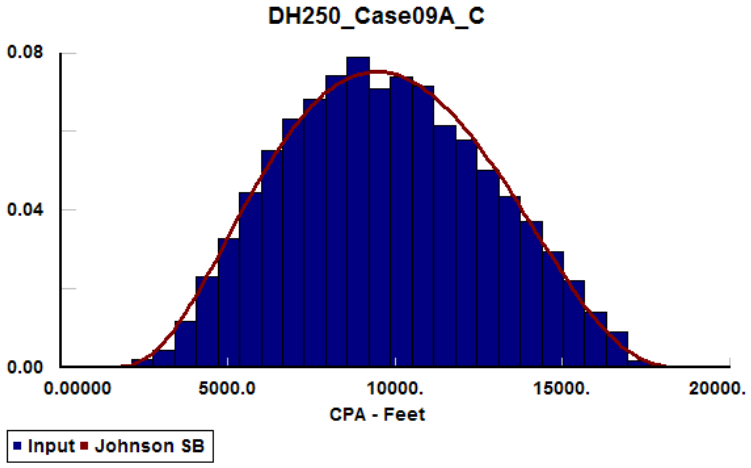
DH250_Case09A_C
0.08
0.04
0.00
0.00000
5000.0
10000.
15000.
20000.
CPA - Feet
Input
Johnson SB

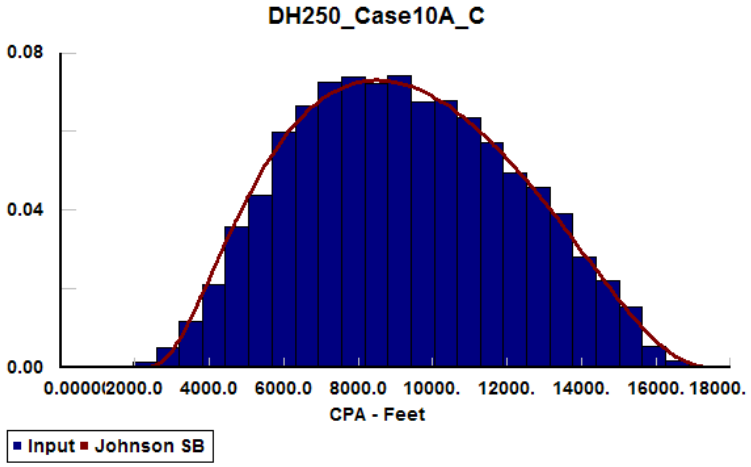
DH250_Case10A_C
0.08
0.04
0.00
0.00002000.0 4000.0 6000.0 8000.0 10000. 12000. 14000. 16000. 18000.
CPA - Feet
Input Johnson SB

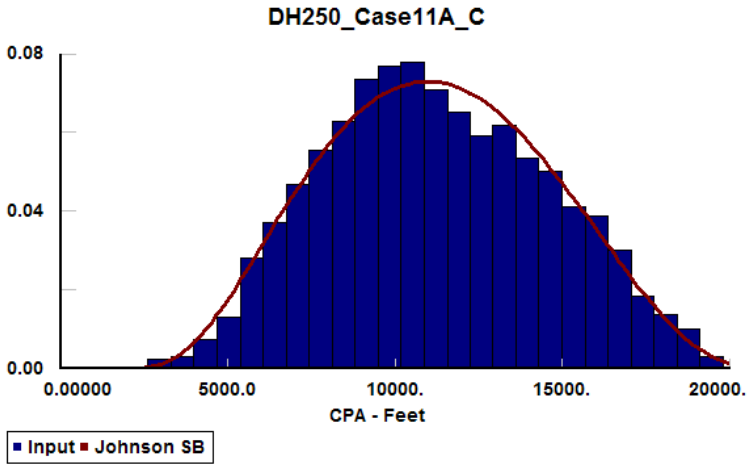
DH250_Case11A_C
0.08
0.04
0.00
0.00000 5000.0 10000. 15000. 20000.
CPA - Feet
Input Johnson SB

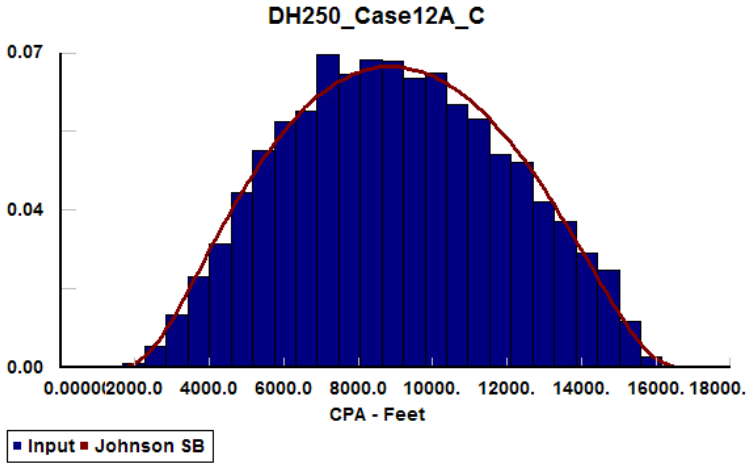
DH250_Case12A_C
0.07
0.04
0.00
0.00002000.0 4000.0 6000.0 8000.0 10000. 12000. 14000. 16000. 18000.
CPA - Feet
Input Johnson SB

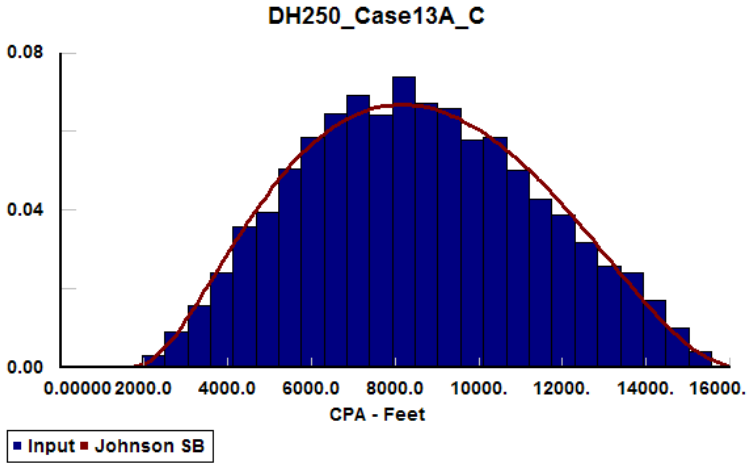
DH250_Case13A_C
0.08
0.04
0.00
0.00000 2000.0 4000.0 6000.0 8000.0 10000. 12000. 14000. 16000.
CPA - Feet
Input Johnson SB

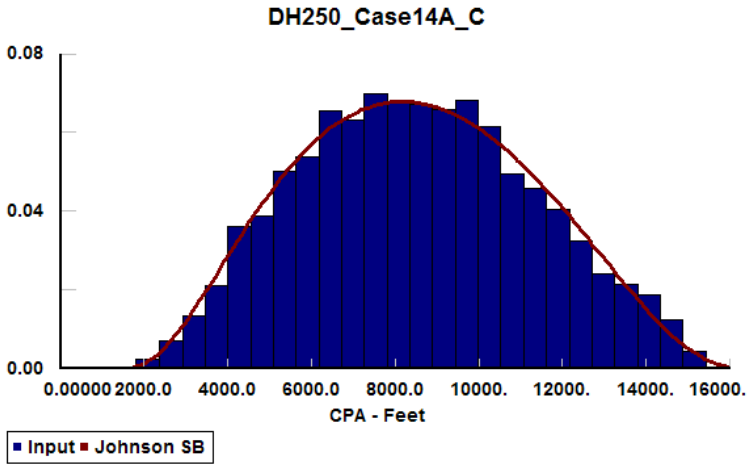
DH250_Case14A_C
0.08
0.04
0.00
0.00000 2000.0 4000.0 6000.0 8000.0 10000. 12000. 14000. 16000.
CPA - Feet
Input Johnson SB

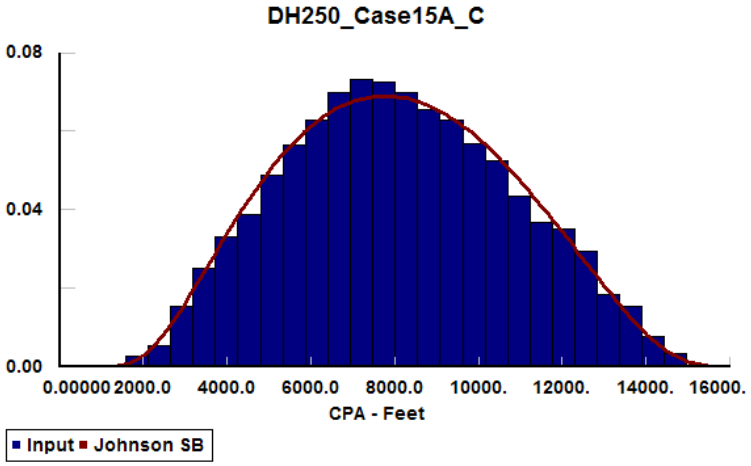
DH250_Case15A_C
0.08
0.04
0.00
0.00000 2000.0 4000.0 6000.0 8000.0 10000. 12000. 14000. 16000.
CPA - Feet
Input Johnson SB

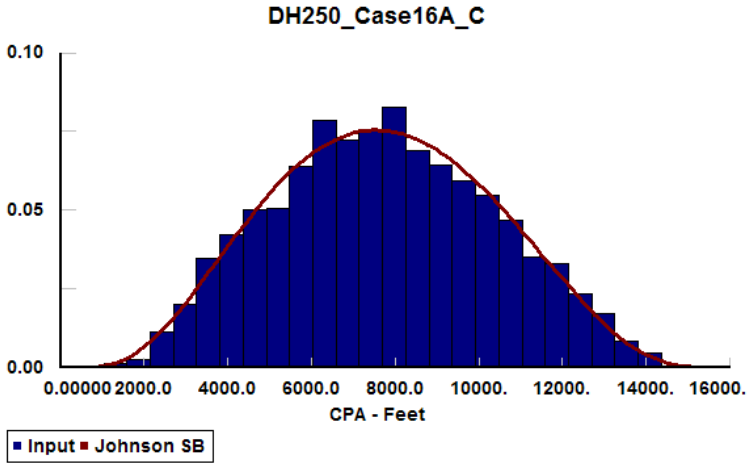
DH250_Case16A_C
0.10
0.05
0.00
0.00000 2000.0 4000.0 6000.0 8000.0 10000. 12000. 14000. 16000.
CPA - Feet
Input Johnson SB

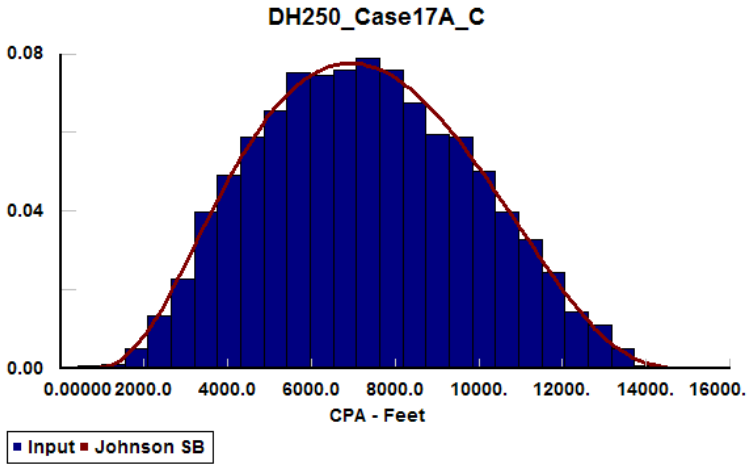
DH250_Case17A_C
0.08
0.04
0.00
0.00000 2000.0 4000.0 6000.0 8000.0 10000. 12000. 14000. 16000.
CPA - Feet
Input Johnson SB

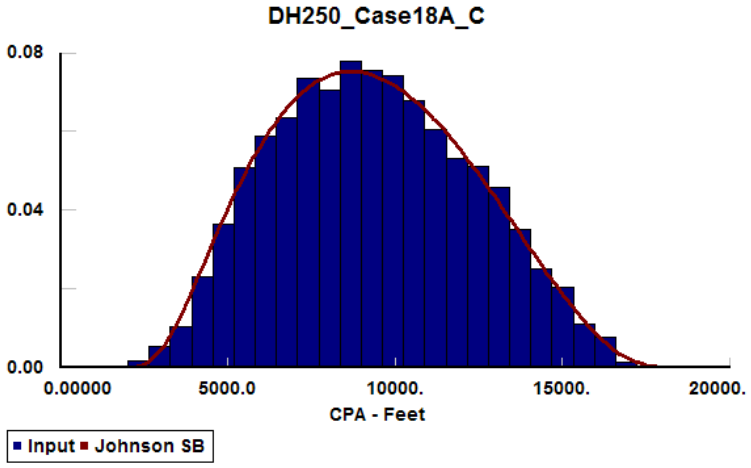
DH250_Case18A_C
0.08
0.04
0.00
0.00000 5000.0 10000. 15000. 20000.
CPA - Feet
Input Johnson SB

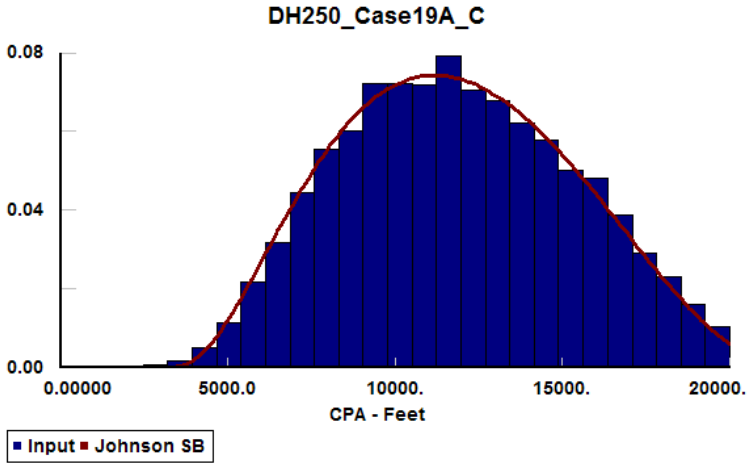
DH250_Case19A_C
0.08
0.04
0.00
0.00000
5000.0
10000.
15000.
20000.
CPA - Feet
Input
Johnson SB

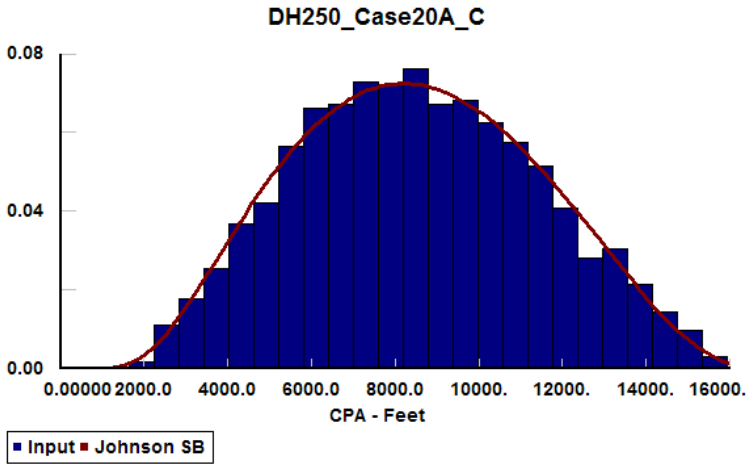
DH250_Case20A_C
0.08
0.04
0.00
0.00000
2000.0
4000.0
6000.0
8000.0
10000.
12000.
14000.
16000.
CPA - Feet
Input
Johnson SB

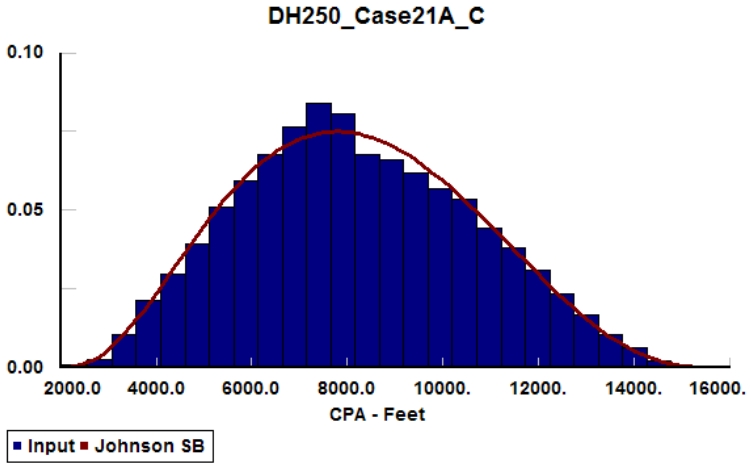
DH250_Case21A_C
0.10
0.05
0.00
2000.0
4000.0
6000.0
8000.0
10000.
12000.
14000.
16000.
CPA - Feet
Input
Johnson SB

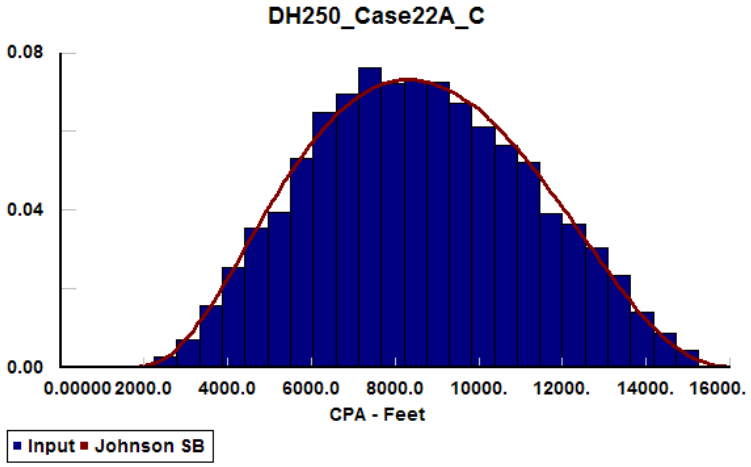
DH250_Case22A_C
0.08
0.04
0.00
0.00000 2000.0 4000.0 6000.0 8000.0 10000. 12000. 14000. 16000.
CPA - Feet
Input Johnson SB

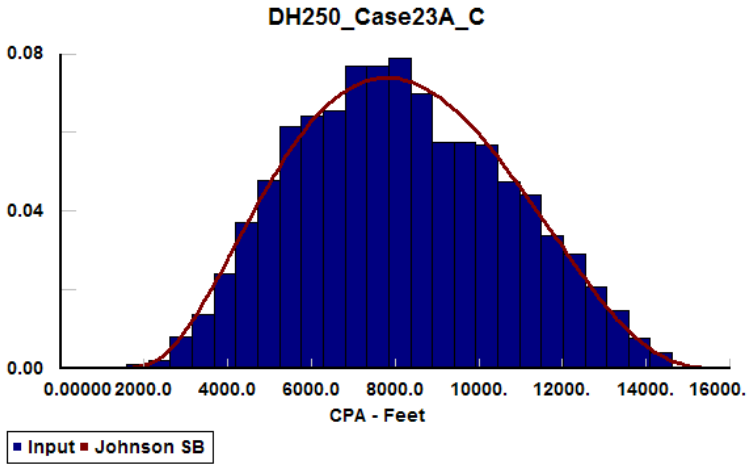
DH250_Case23A_C
0.08
0.04
0.00
0.00000 2000.0 4000.0 6000.0 8000.0 10000. 12000. 14000. 16000.
CPA - Feet
Input Johnson SB

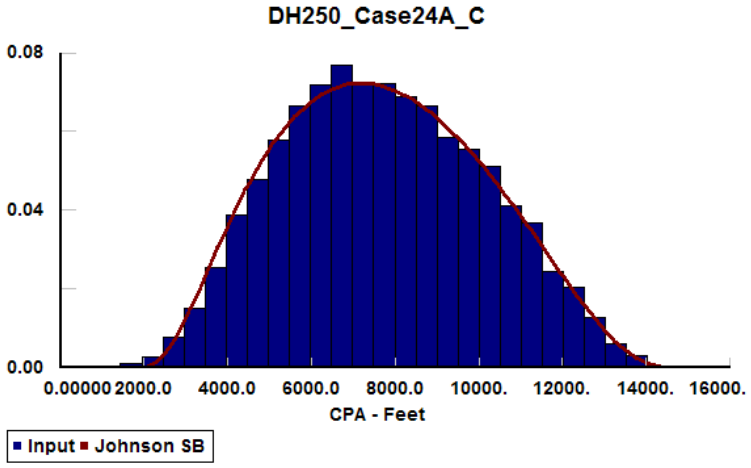
DH250_Case24A_C
0.08
0.04
0.00
0.00000 2000.0 4000.0 6000.0 8000.0 10000. 12000. 14000. 16000.
CPA - Feet
Input Johnson SB

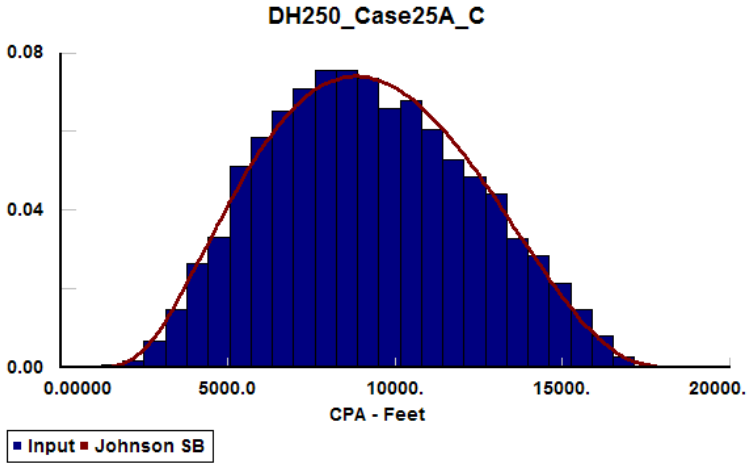
DH250_Case25A_C
0.08
0.04
0.00
0.00000
5000.0
10000.
15000.
20000.
CPA - Feet
Input
Johnson SB

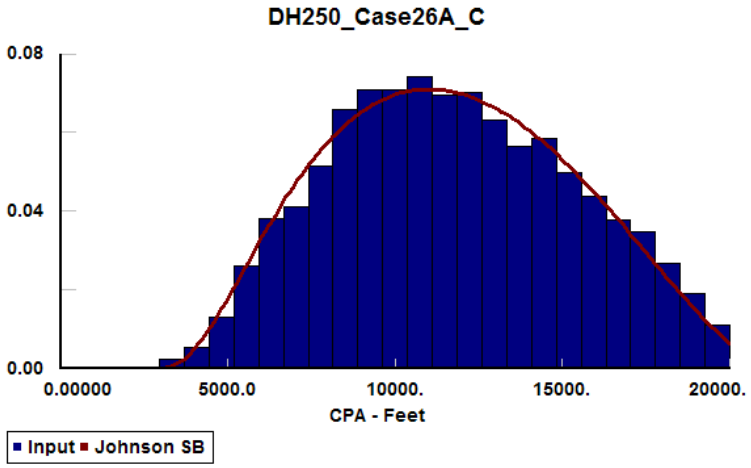
DH250_Case26A_C
0.08
0.04
0.00
0.00000
5000.0
10000.
15000.
20000.
CPA - Feet
Input
Johnson SB

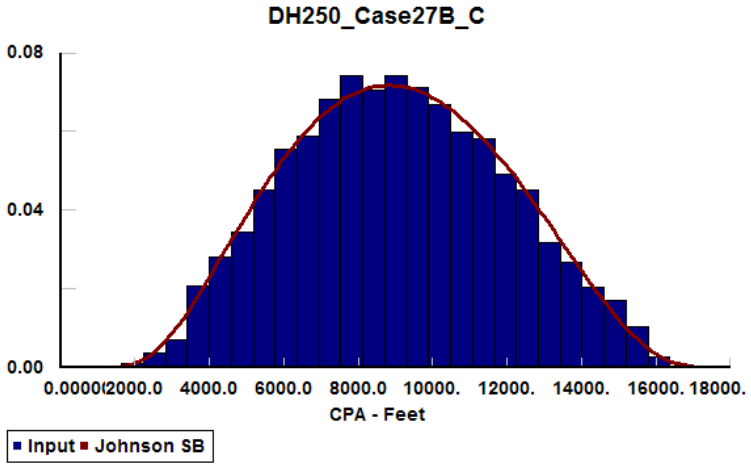
DH250_Case27B_C
0.08
0.04
0.00
0.00002000.0
4000.0
6000.0
8000.0
10000.
12000.
14000.
16000.
18000.
CPA - Feet
Input
Johnson SB

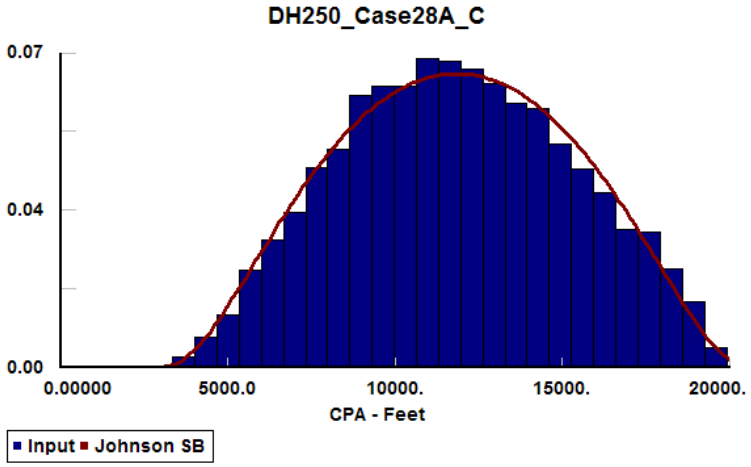
DH250_Case28A_C
0.07
0.04
0.00
0.00000
5000.0
10000.
15000.
20000.
CPA - Feet
Input
Johnson SB

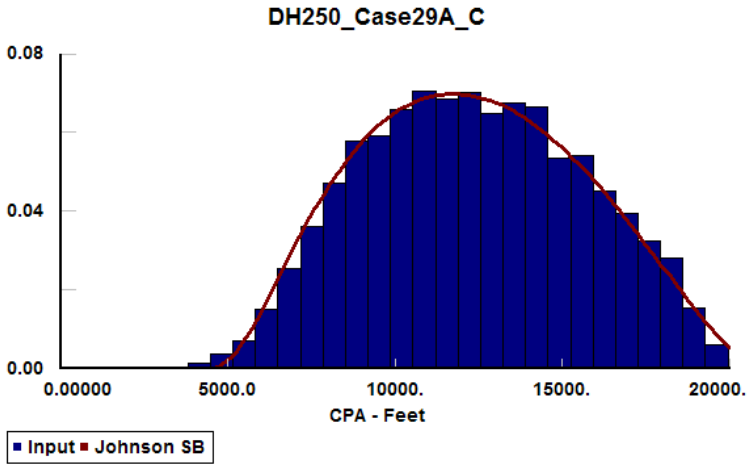
DH250_Case29A_C
0.08
0.04
0.00
0.00000
5000.0
10000.
15000.
20000.
CPA - Feet
Input
Johnson SB

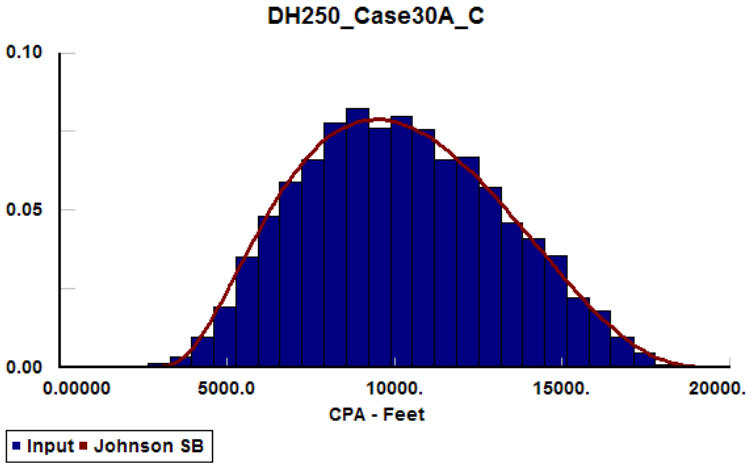
DH250_Case30A_C
0.10
0.05
0.00
0.00000
5000.0
10000.
15000.
20000.
CPA - Feet
Input
Johnson SB

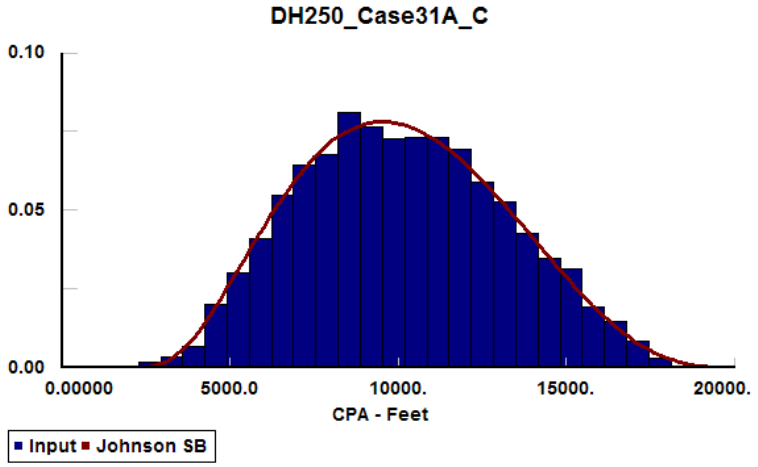
DH250_Case31A_C
0.10
0.05
0.00
0.00000
5000.0
10000.
15000.
20000.
CPA - Feet
Input
Johnson SB

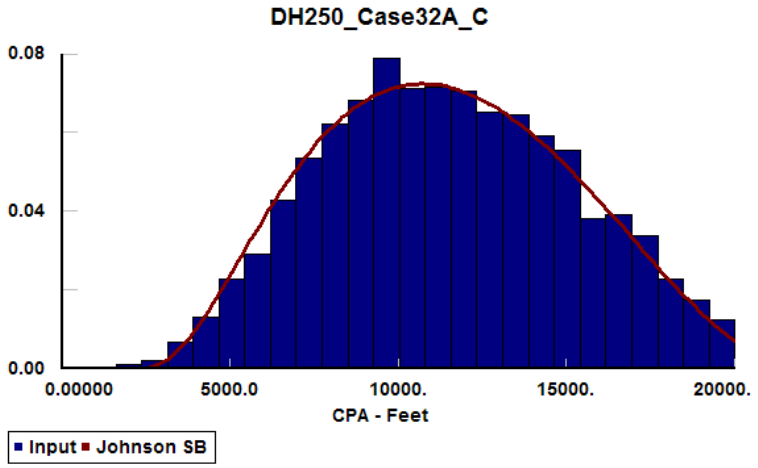
DH250_Case32A_C
0.08
0.04
0.00
0.00000
5000.0
10000.
15000.
20000.
CPA - Feet
Input
Johnson SB

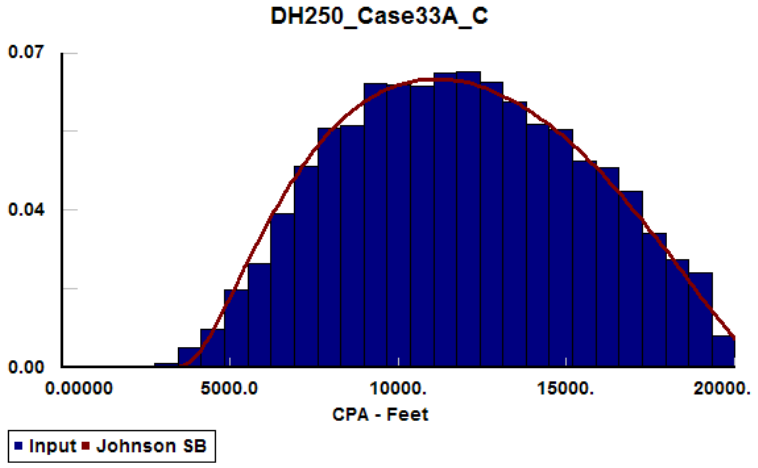
DH250_Case33A_C
0.07
0.04
0.00
0.00000
5000.0
10000.
15000.
20000.
CPA - Feet
Input
Johnson SB

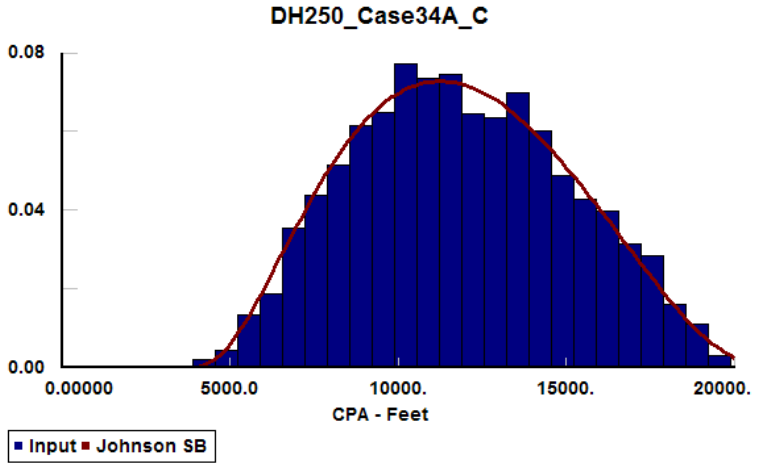
DH250_Case34A_C
0.08
0.04
0.00
0.00000
5000.0
10000.
15000.
20000.
CPA - Feet
Input
Johnson SB

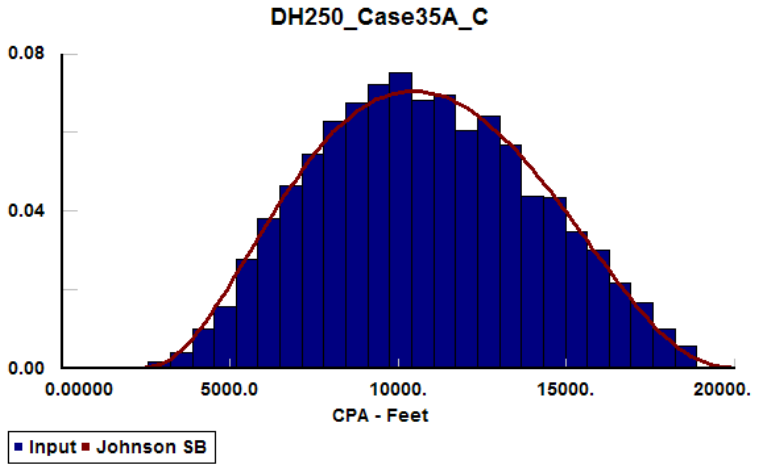
DH250_Case35A_C
0.08
0.04
0.00
0.00000
5000.0
10000.
15000.
20000.
CPA - Feet
Input
Johnson SB

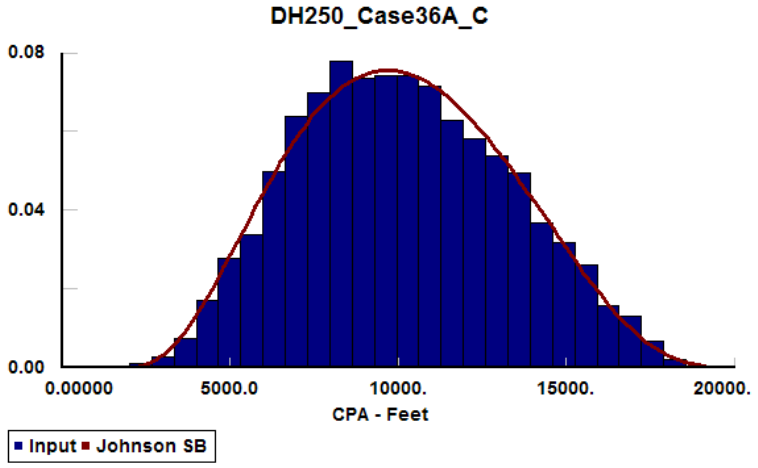
DH250_Case36A_C
0.08
0.04
0.00
0.00000
5000.0
10000.
15000.
20000.
CPA - Feet
Input
Johnson SB

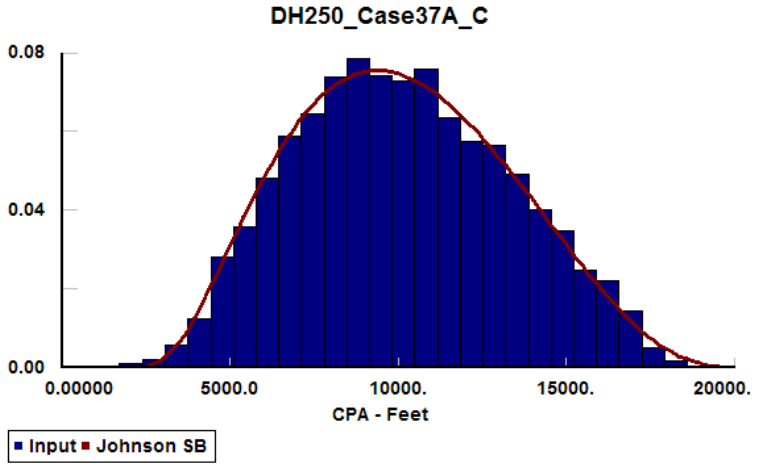
DH250_Case37A_C
0.08
0.04
0.00
0.00000
5000.0
10000.
15000.
20000.
CPA - Feet
Input
Johnson SB

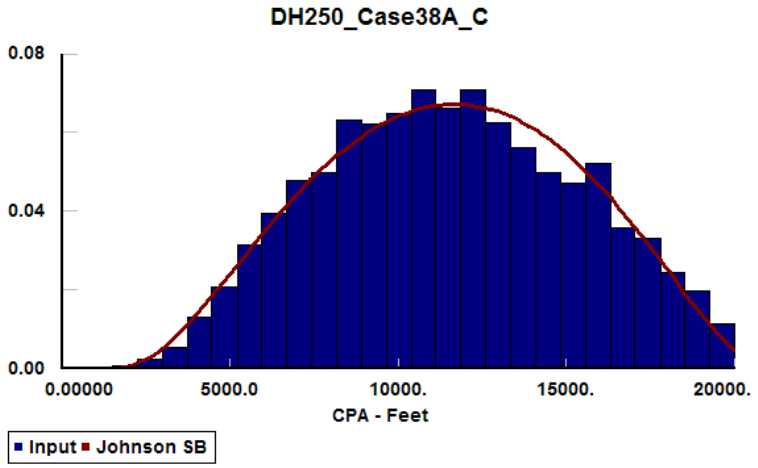
DH250_Case38A_C
0.08
0.04
0.00
0.00000
5000.0
10000.
15000.
20000.
CPA - Feet
Input
Johnson SB

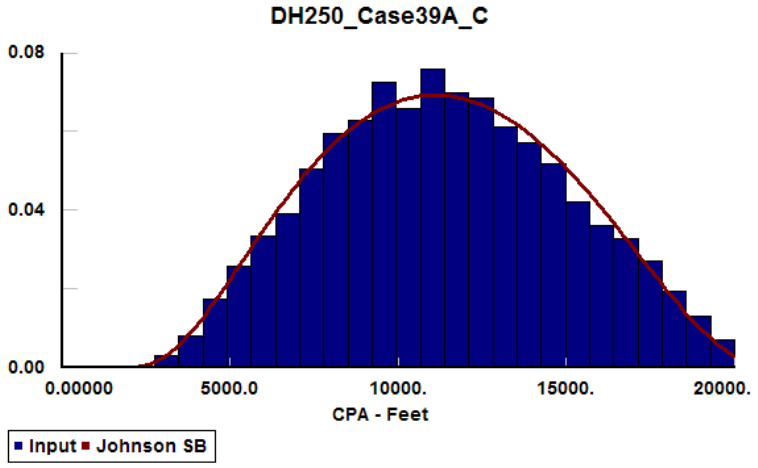
DH250_Case39A_C
0.08
0.04
0.00
0.00000
5000.0
10000.
15000.
20000.
CPA - Feet
Input
Johnson SB

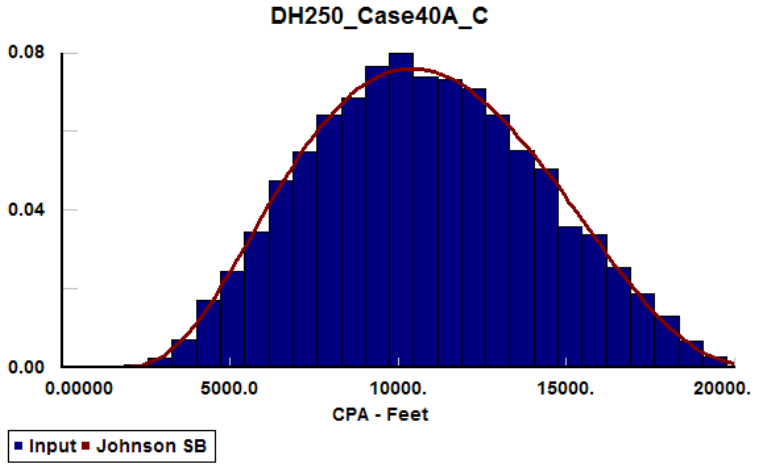
DH250_Case40A_C
0.08
0.04
0.00
0.00000
5000.0
10000.
15000.
20000.
CPA - Feet
Input
Johnson SB

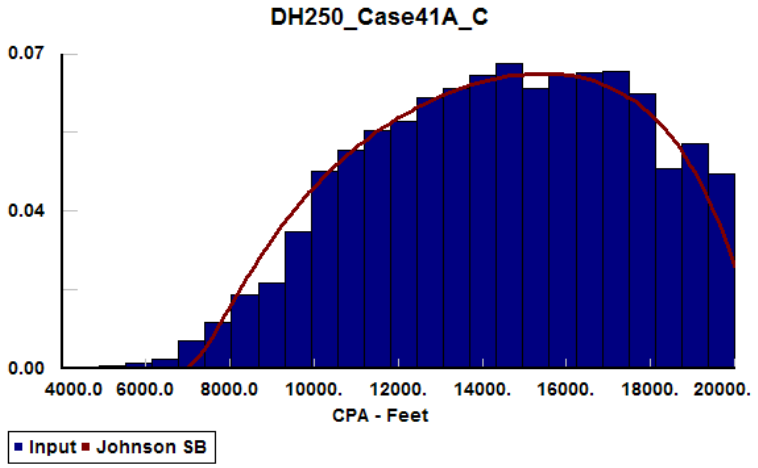
DH250_Case41A_C
0.07
0.04
0.00
4000.0
6000.0
8000.0
10000.
12000.
14000.
16000.
18000.
20000.
CPA - Feet
Input
Johnson SB

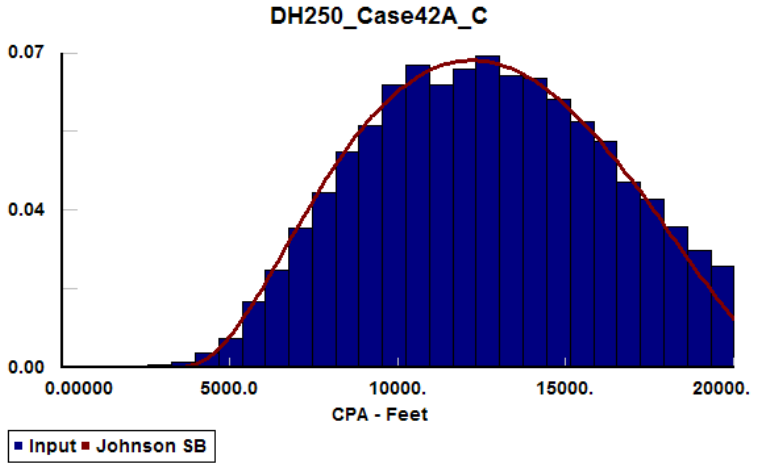
DH250_Case42A_C
0.07
0.04
0.00
0.00000
5000.0
10000.
15000.
20000.
CPA - Feet
Input
Johnson SB

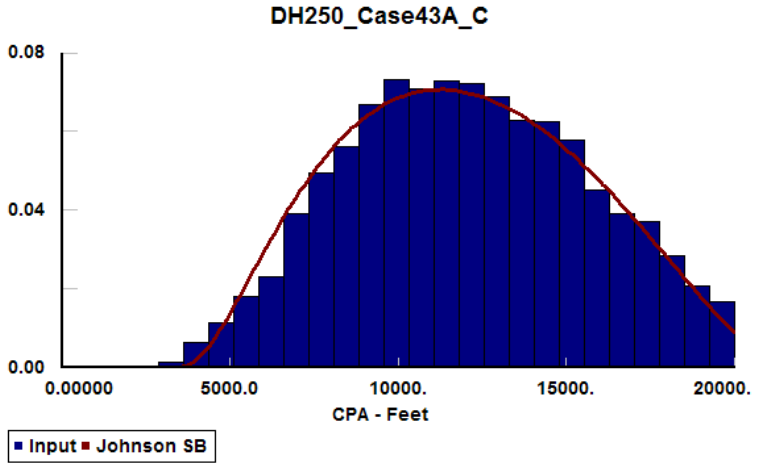
DH250_Case43A_C
0.08
0.04
0.00
0.00000
5000.0
10000.
15000.
20000.
CPA - Feet
Input
Johnson SB

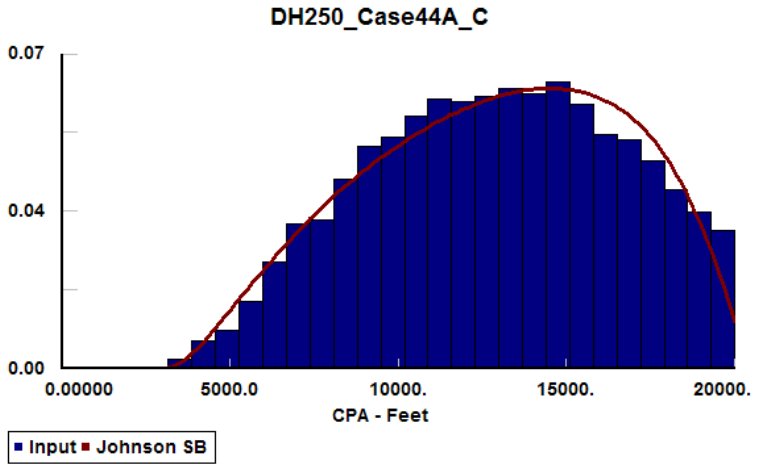
DH250_Case44A_C
0.07
0.04
0.00
0.00000
5000.0
10000.
15000.
20000.
CPA - Feet
Input
Johnson SB

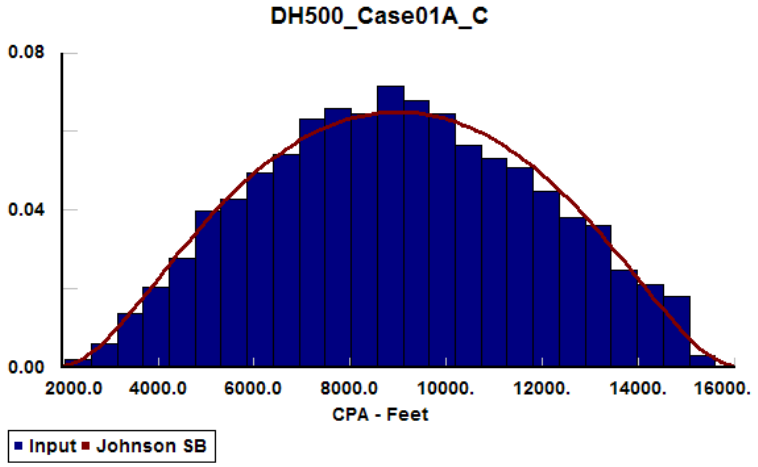
DH500_Case01A_C
0.08
0.04
0.00
2000.0
4000.0
6000.0
8000.0
10000.
12000.
14000.
16000.
CPA - Feet
Input
Johnson SB

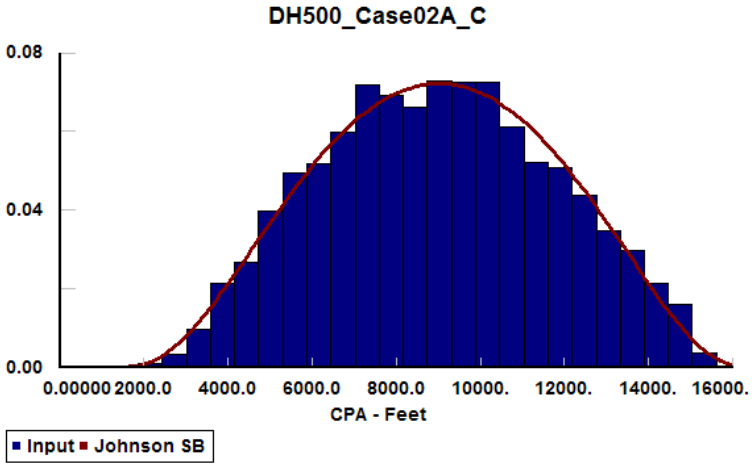
DH500_Case02A_C
0.08
0.04
0.00
0.00000 2000.0 4000.0 6000.0 8000.0 10000. 12000. 14000. 16000.
CPA - Feet
Input Johnson SB

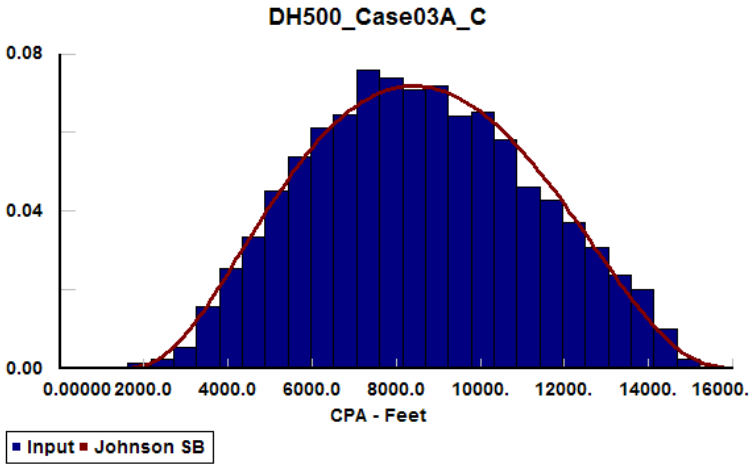
DH500_Case03A_C
0.08
0.04
0.00
0.00000 2000.0 4000.0 6000.0 8000.0 10000. 12000. 14000. 16000.
CPA - Feet
Input Johnson SB

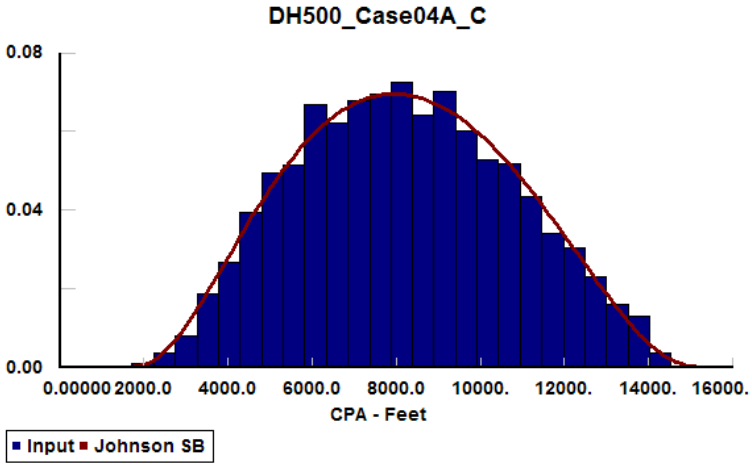
DH500_Case04A_C
0.08
0.04
0.00
0.00000 2000.0 4000.0 6000.0 8000.0 10000. 12000. 14000. 16000.
CPA - Feet
Input Johnson SB

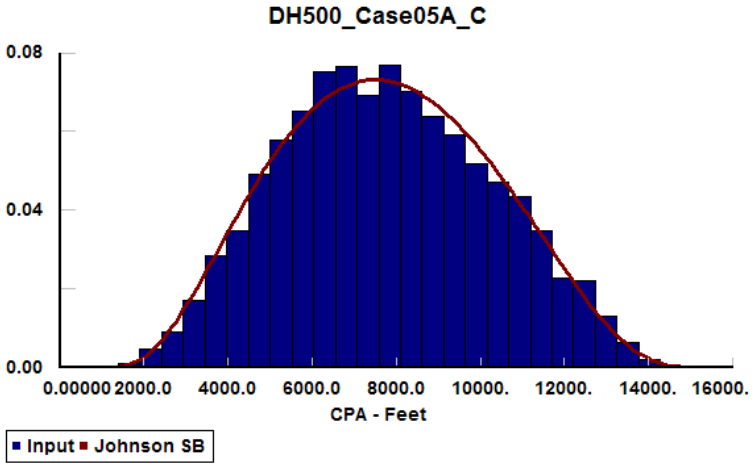
DH500_Case05A_C
0.08
0.04
0.00
0.00000 2000.0 4000.0 6000.0 8000.0 10000. 12000. 14000. 16000.
CPA - Feet
Input Johnson SB

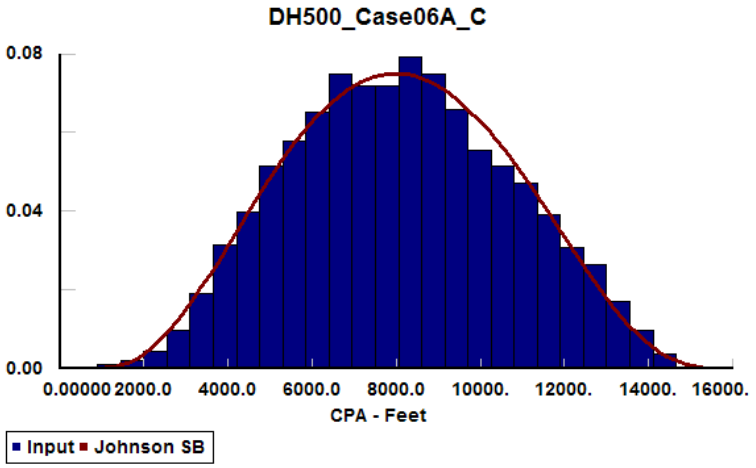
DH500_Case06A_C
0.08
0.04
0.00
0.00000 2000.0 4000.0 6000.0 8000.0 10000. 12000. 14000. 16000.
CPA - Feet
Input Johnson SB

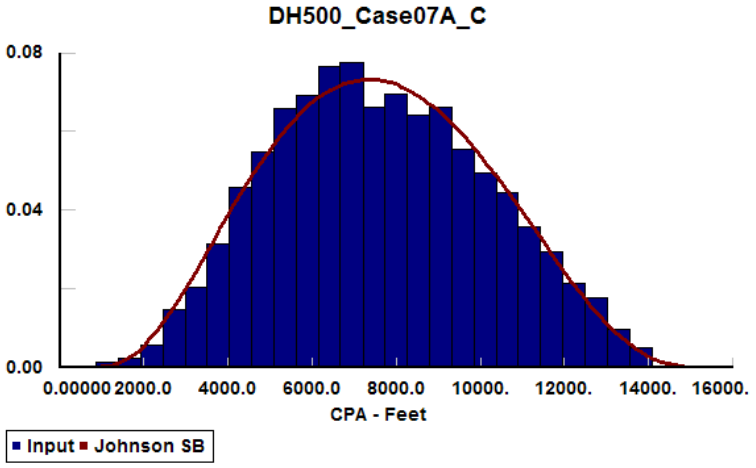
DH500_Case07A_C
0.08
0.04
0.00
0.00000 2000.0 4000.0 6000.0 8000.0 10000. 12000. 14000. 16000.
CPA - Feet
Input Johnson SB

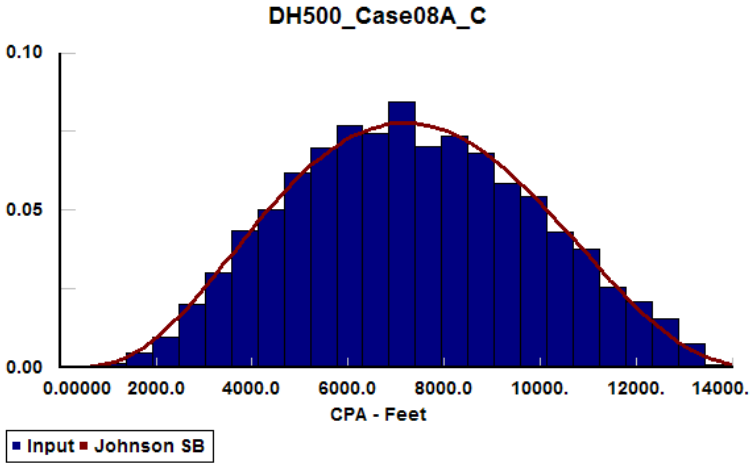
DH500_Case08A_C
0.10
0.05
0.00
0.00000
2000.0
4000.0
6000.0
8000.0
10000.
12000.
14000.
CPA - Feet
Input
Johnson SB

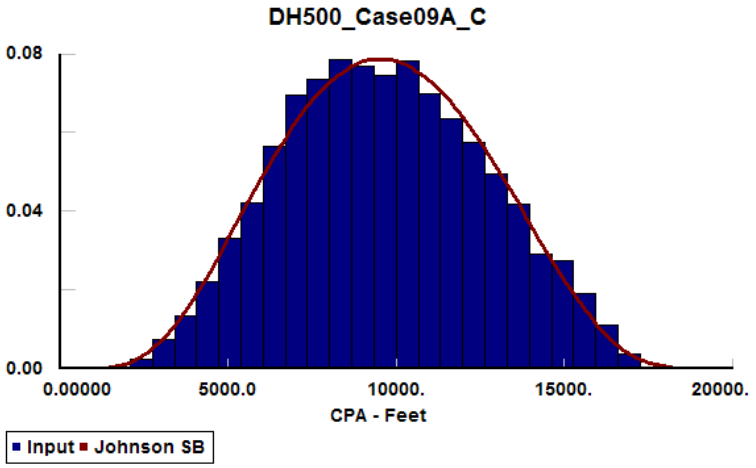
DH500_Case09A_C
0.08
0.04
0.00
0.00000
5000.0
10000.
15000.
20000.
CPA - Feet
Input
Johnson SB

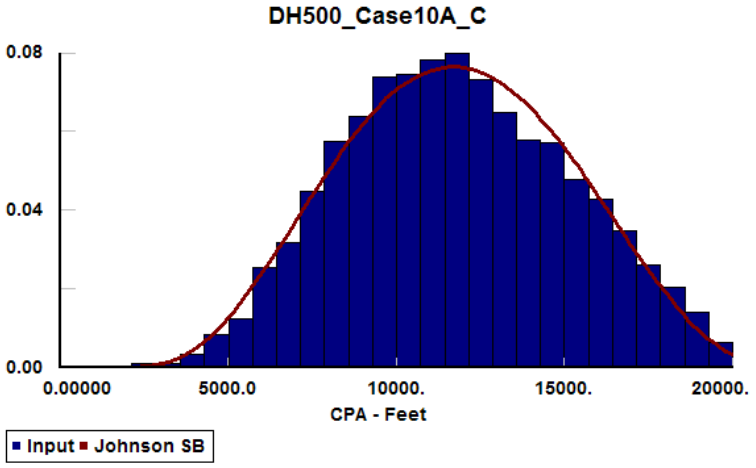
DH500_Case10A_C
0.08
0.04
0.00
0.00000
5000.0
10000.
15000.
20000.
CPA - Feet
Input
Johnson SB

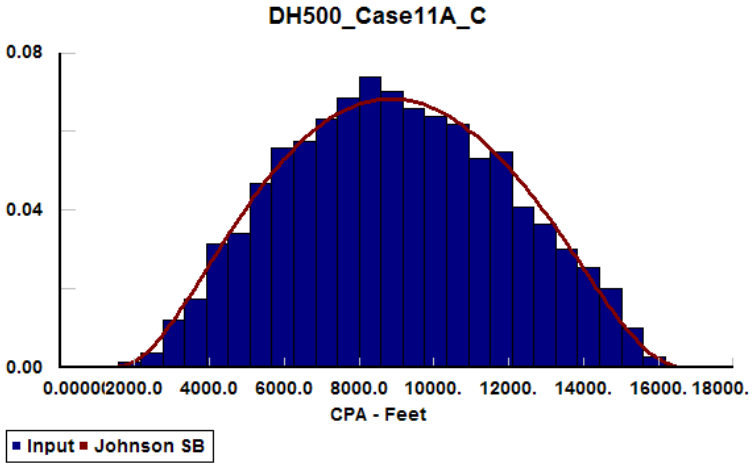
DH500_Case11A_C
0.08
0.04
0.00
0.00002000.0 4000.0 6000.0 8000.0 10000. 12000. 14000. 16000. 18000.
CPA - Feet
Input
Johnson SB

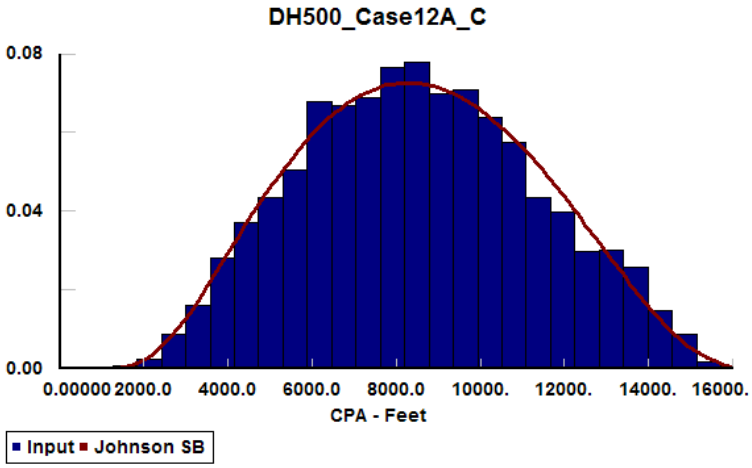
DH500_Case12A_C
0.08
0.04
0.00
0.00000 2000.0 4000.0 6000.0 8000.0 10000. 12000. 14000. 16000.
CPA - Feet
Input
Johnson SB

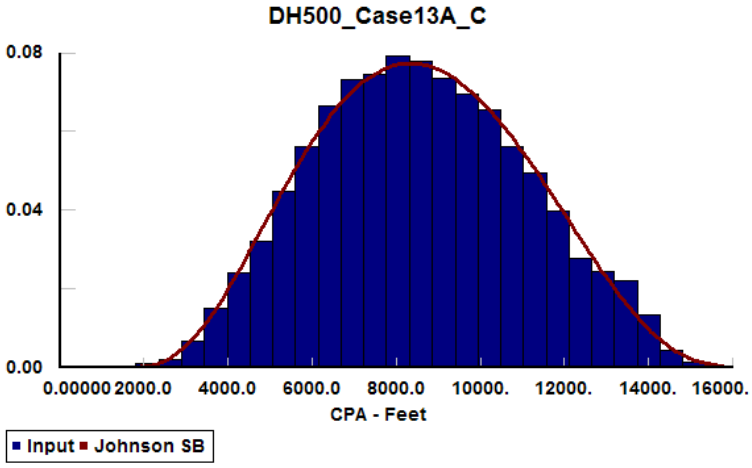
DH500_Case13A_C
0.08
0.04
0.00
0.00000 2000.0 4000.0 6000.0 8000.0 10000. 12000. 14000. 16000.
CPA - Feet
Input
Johnson SB

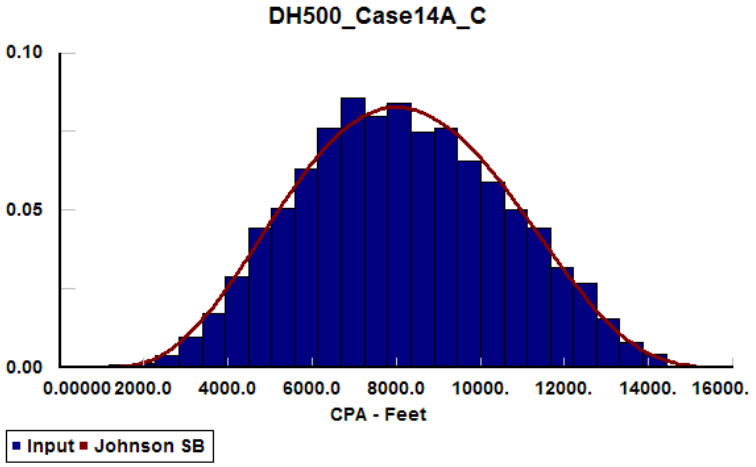
DH500_Case14A_C
0.10
0.05
0.00
0.00000 2000.0 4000.0 6000.0 8000.0 10000. 12000. 14000. 16000.
CPA - Feet
Input Johnson SB

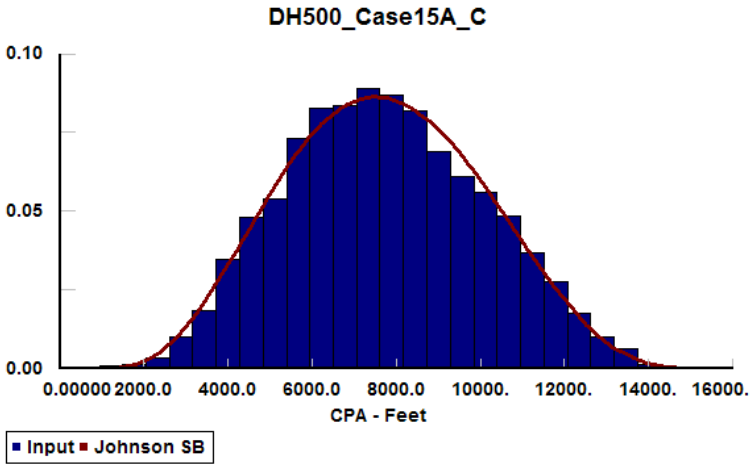
DH500_Case15A_C
0.10
0.05
0.00
0.00000 2000.0 4000.0 6000.0 8000.0 10000. 12000. 14000. 16000.
CPA - Feet
Input Johnson SB

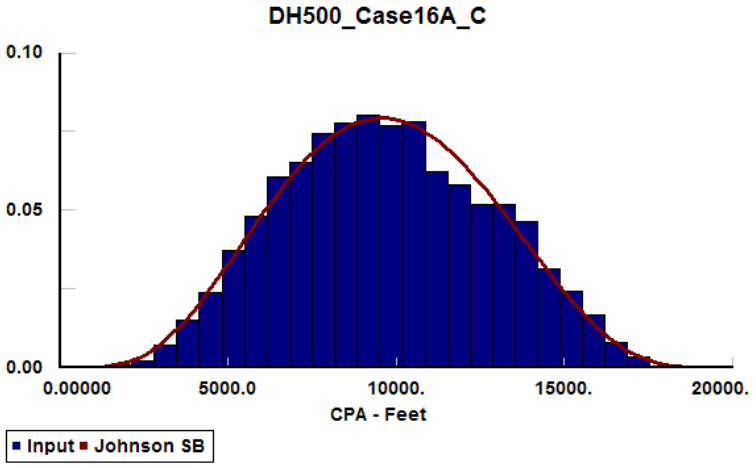
DH500_Case16A_C
0.10
0.05
0.00
0.00000 5000.0 10000. 15000. 20000.
CPA - Feet
Input Johnson SB

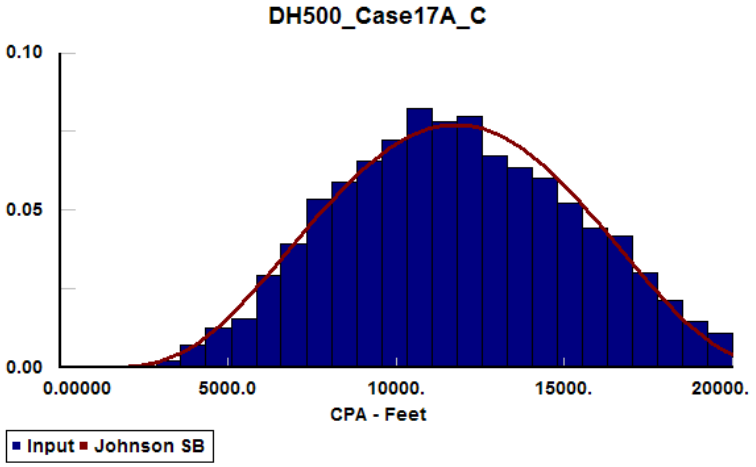
DH500_Case17A_C
0.10
0.05
0.00
0.00000
5000.0
10000.
15000.
20000.
CPA - Feet
Input
Johnson SB

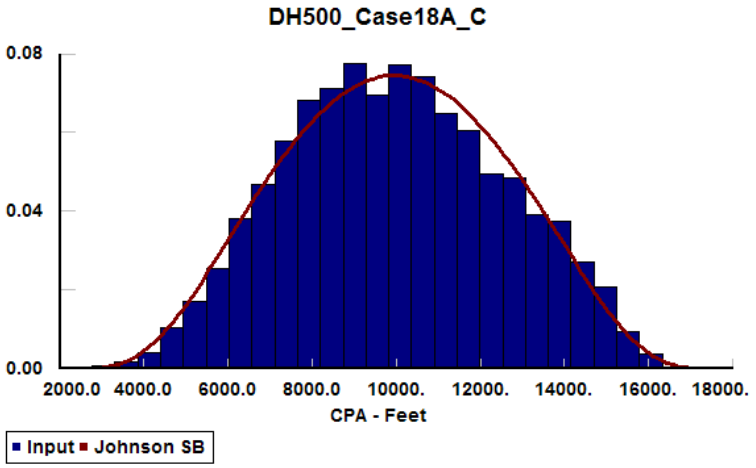
DH500_Case18A_C
0.08
0.04
0.00
2000.0
4000.0
6000.0
8000.0
10000.
12000.
14000.
16000.
18000.
CPA - Feet
Input
Johnson SB

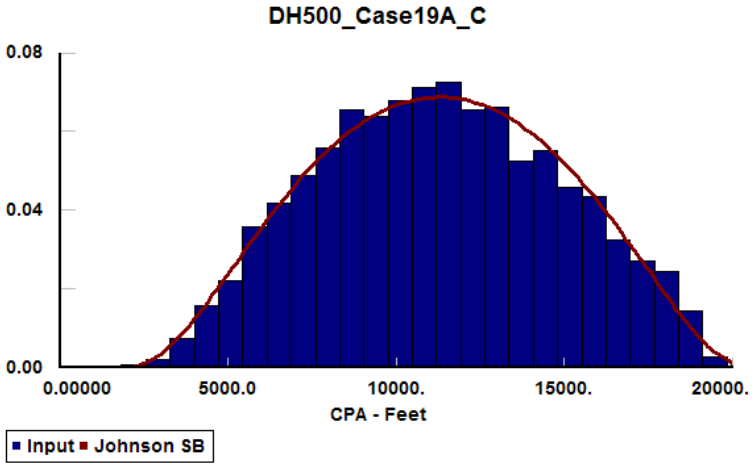
DH500_Case19A_C
0.08
0.04
0.00
0.00000
5000.0
10000.
15000.
20000.
CPA - Feet
Input
Johnson SB

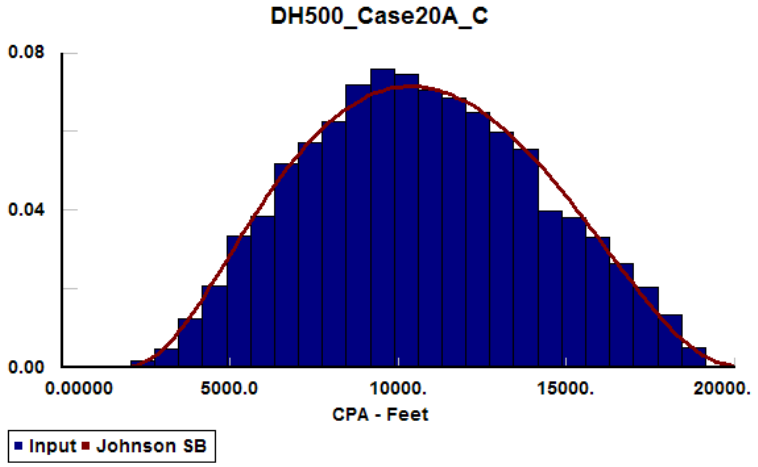
DH500_Case20A_C
0.08
0.04
0.00
0.00000
5000.0
10000.
15000.
20000.
CPA - Feet
Input
Johnson SB

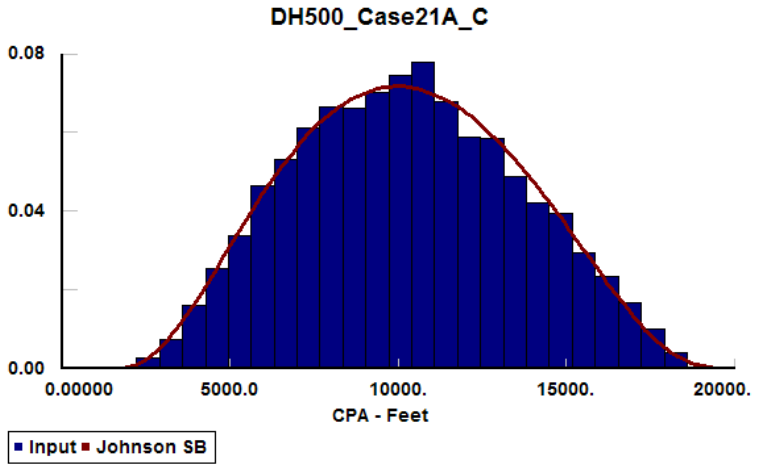
DH500_Case21A_C
0.08
0.04
0.00
0.00000
5000.0
10000.
15000.
20000.
CPA - Feet
Input
Johnson SB

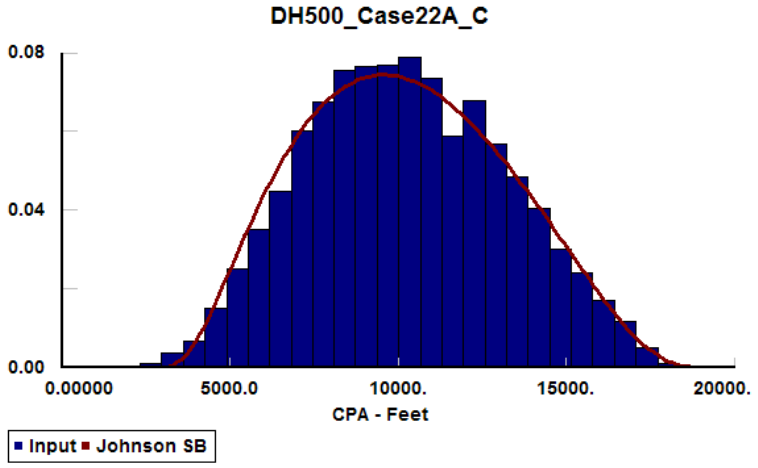
DH500_Case22A_C
0.08
0.04
0.00
0.00000
5000.0
10000.
15000.
20000.
CPA - Feet
Input
Johnson SB

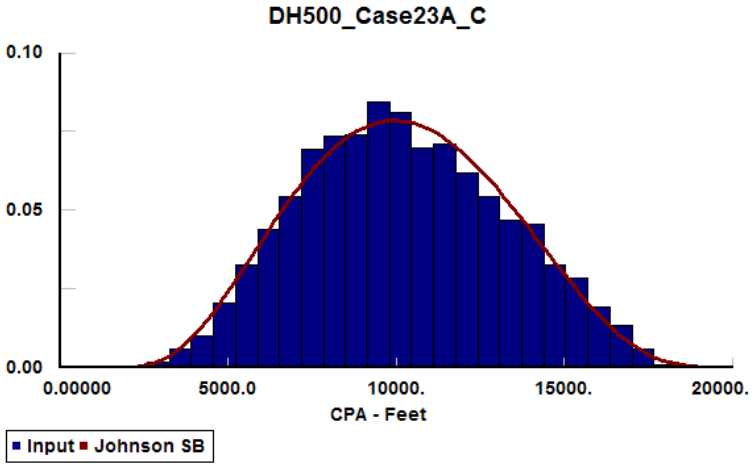
DH500_Case23A_C
0.10
0.05
0.00
0.00000
5000.0
10000.
15000.
20000.
CPA - Feet
Input
Johnson SB

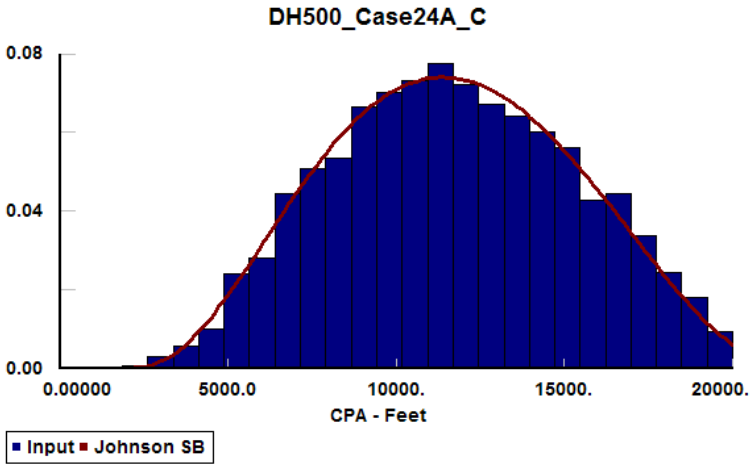
DH500_Case24A_C
0.08
0.04
0.00
0.00000
5000.0
10000.
15000.
20000.
CPA - Feet
Input
Johnson SB

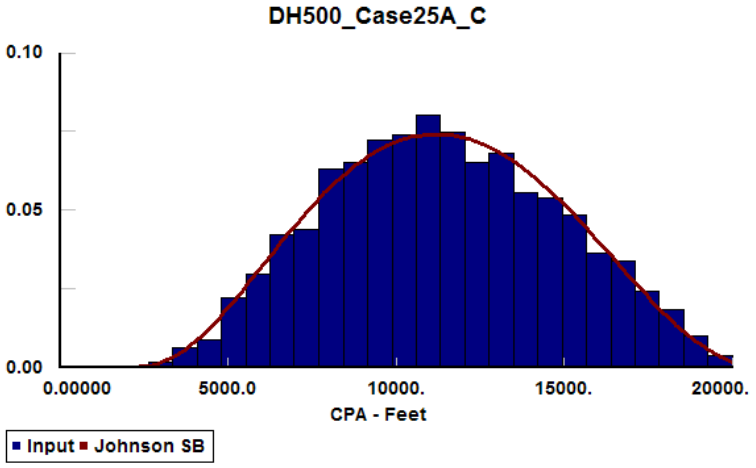
DH500_Case25A_C
0.10
0.05
0.00
0.00000
5000.0
10000.
15000.
20000.
CPA - Feet
Input
Johnson SB

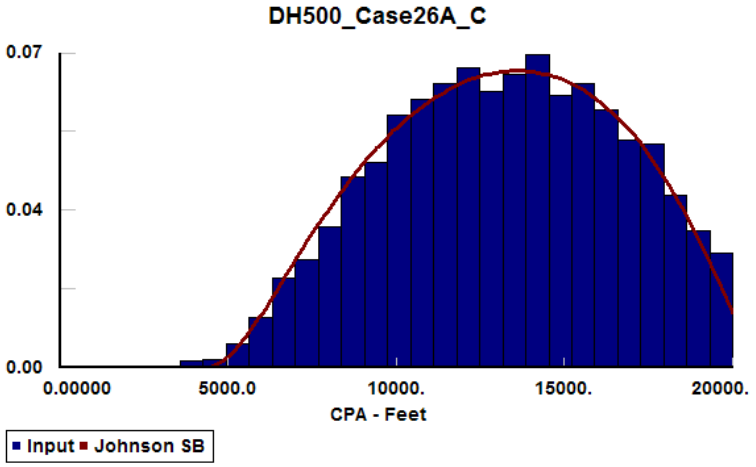
DH500_Case26A_C
0.07
0.04
0.00
0.00000
5000.0
10000.
15000.
20000.
CPA - Feet
Input
Johnson SB

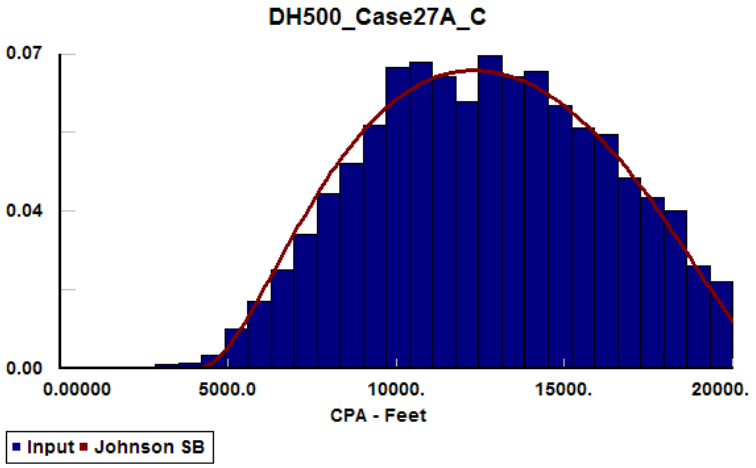
DH500_Case27A_C
0.07
0.04
0.00
0.00000
5000.0
10000.
15000.
20000.
CPA - Feet
Input
Johnson SB

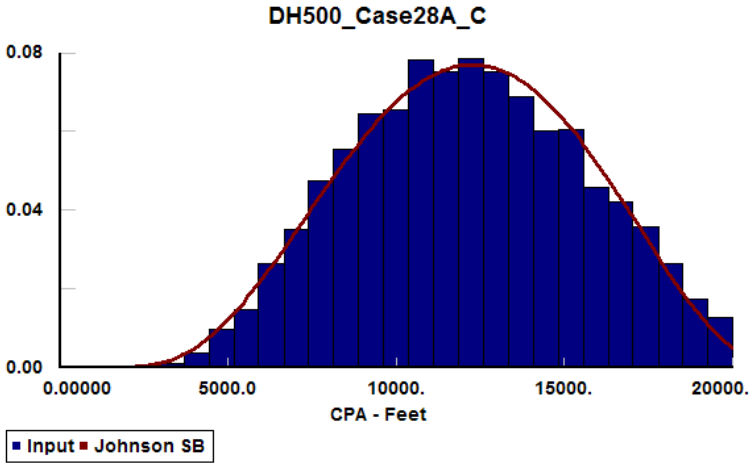
DH500_Case28A_C
0.08
0.04
0.00
0.00000
5000.0
10000.
15000.
20000.
CPA - Feet
Input
Johnson SB

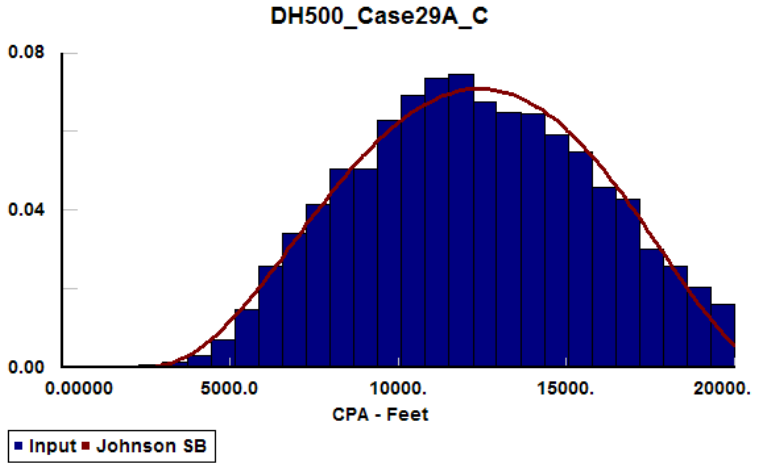
DH500_Case29A_C
0.08
0.04
0.00
0.00000
5000.0
10000.
15000.
20000.
CPA - Feet
Input
Johnson SB

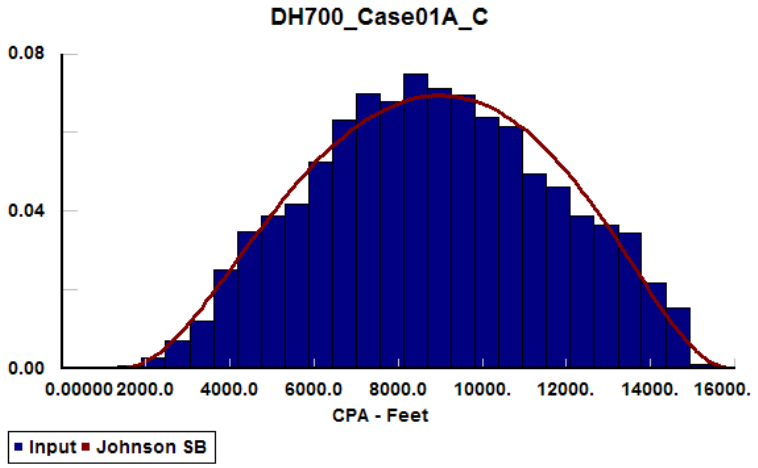
DH700_Case01A_C
0.08
0.04
0.00
0.00000
2000.0
4000.0
6000.0
8000.0
10000.
12000.
14000.
16000.
CPA - Feet
Input
Johnson SB

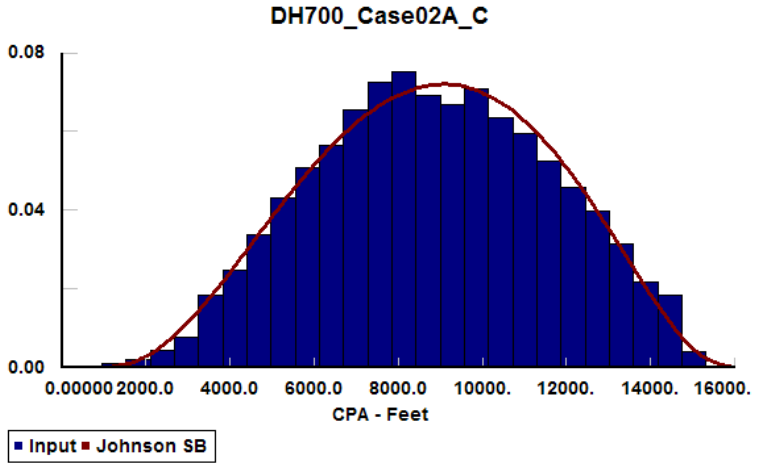
DH700_Case02A_C
0.08
0.04
0.00
0.00000
2000.0
4000.0
6000.0
8000.0
10000.
12000.
14000.
16000.
CPA - Feet
Input
Johnson SB

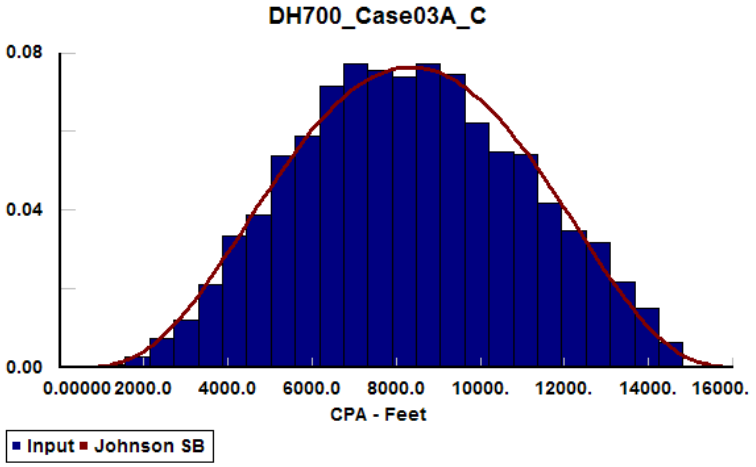
DH700_Case03A_C
0.08
0.04
0.00
0.00000 2000.0 4000.0 6000.0 8000.0 10000. 12000. 14000. 16000.
CPA - Feet
Input Johnson SB

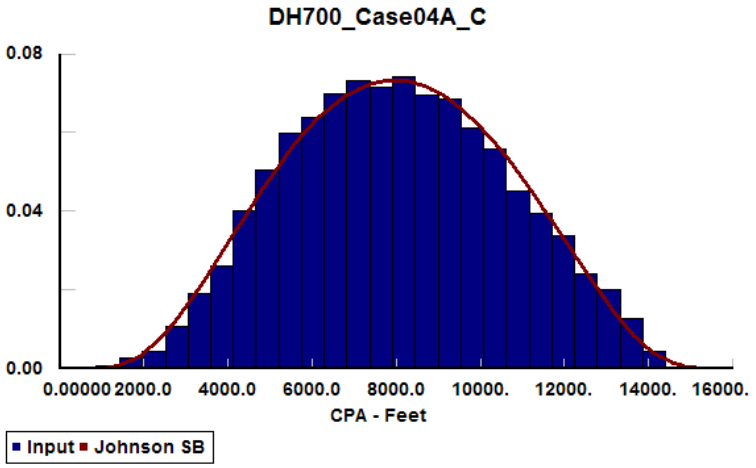
DH700_Case04A_C
0.08
0.04
0.00
0.00000 2000.0 4000.0 6000.0 8000.0 10000. 12000. 14000. 16000.
CPA - Feet
Input Johnson SB

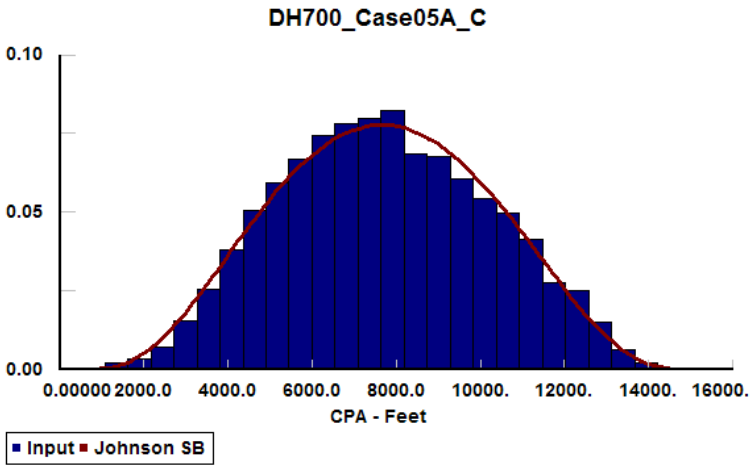
DH700_Case05A_C
0.10
0.05
0.00
0.00000 2000.0 4000.0 6000.0 8000.0 10000. 12000. 14000. 16000.
CPA - Feet
Input Johnson SB

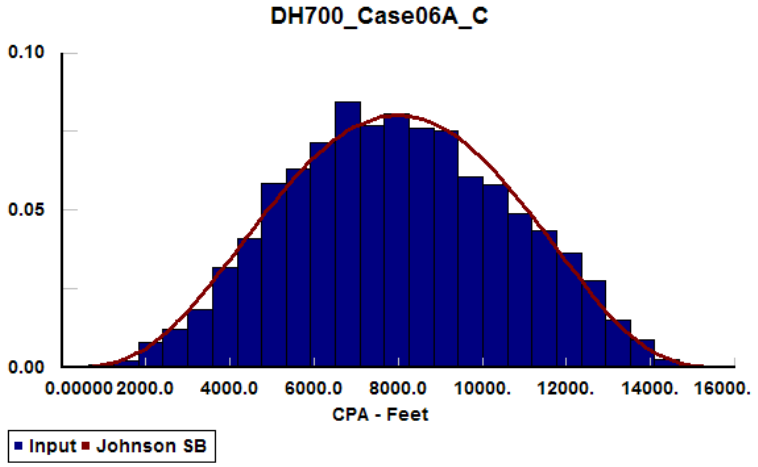
DH700_Case06A_C
0.10
0.05
0.00
0.00000 2000.0 4000.0 6000.0 8000.0 10000. 12000. 14000. 16000.
CPA - Feet
Input Johnson SB

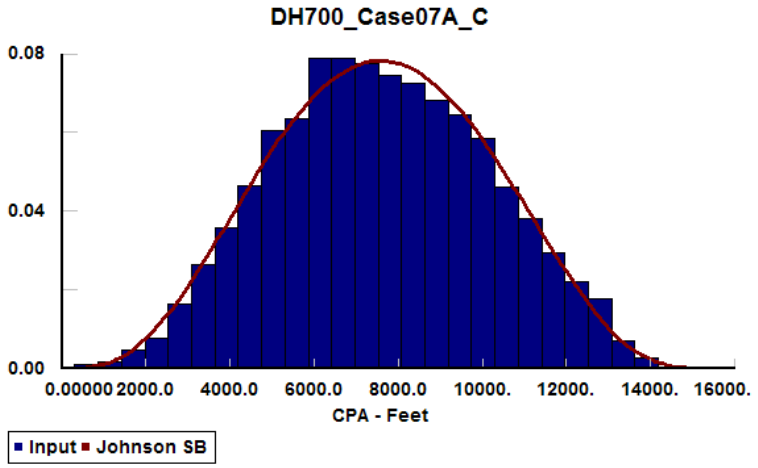
DH700_Case07A_C
0.08
0.04
0.00
0.00000 2000.0 4000.0 6000.0 8000.0 10000. 12000. 14000. 16000.
CPA - Feet
Input Johnson SB

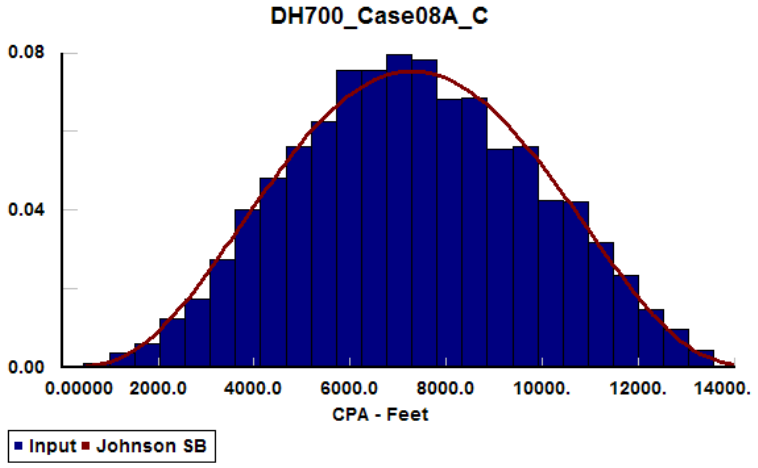
DH700_Case08A_C
0.08
0.04
0.00
0.00000 2000.0 4000.0 6000.0 8000.0 10000. 12000. 14000.
CPA - Feet
Input Johnson SB

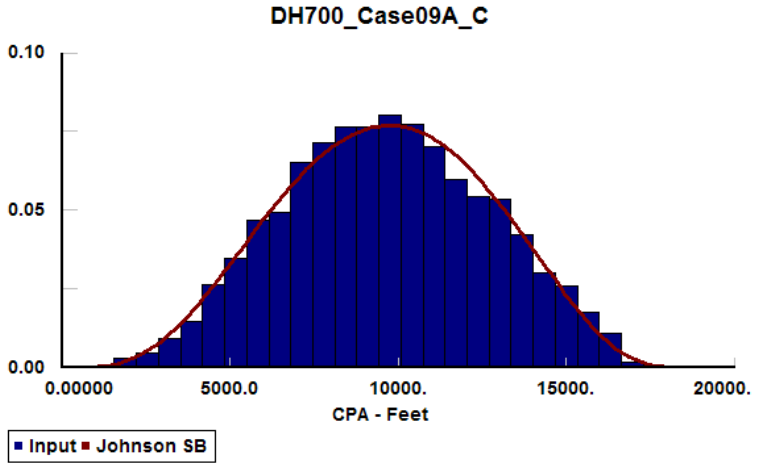
DH700_Case09A_C
0.10
0.05
0.00
0.00000
5000.0
10000.
15000.
20000.
CPA - Feet
Input
Johnson SB

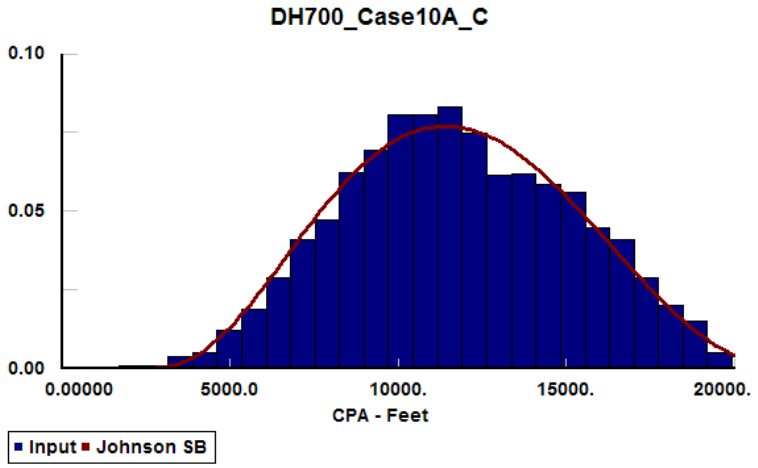
DH700_Case10A_C
0.10
0.05
0.00
0.00000
5000.0
10000.
15000.
20000.
CPA - Feet
Input
Johnson SB

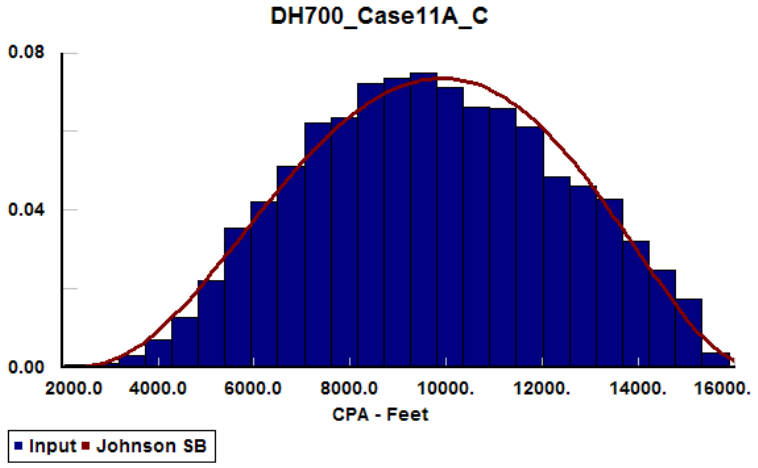
DH700_Case11A_C
0.08
0.04
0.00
2000.0
4000.0
6000.0
8000.0
10000.
12000.
14000.
16000.
CPA - Feet
Input
Johnson SB

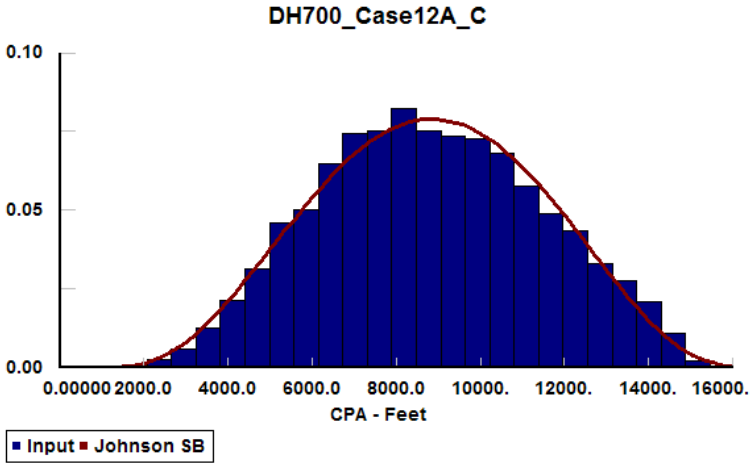
DH700_Case12A_C
0.10
0.05
0.00
0.00000 2000.0 4000.0 6000.0 8000.0 10000. 12000. 14000. 16000.
CPA - Feet
Input Johnson SB

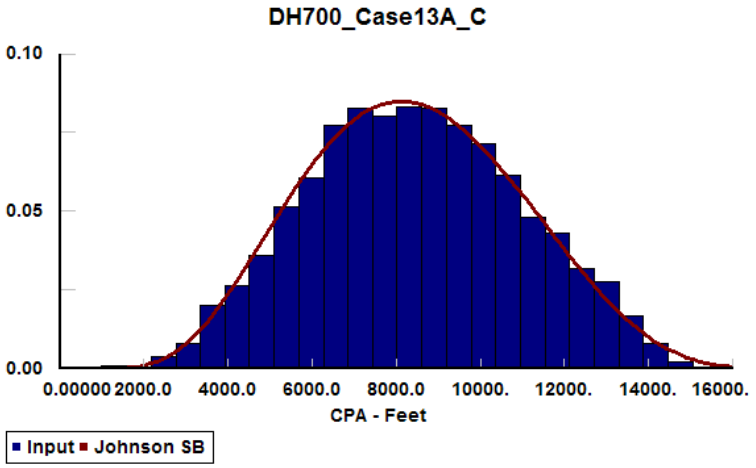
DH700_Case13A_C
0.10
0.05
0.00
0.00000 2000.0 4000.0 6000.0 8000.0 10000. 12000. 14000. 16000.
CPA - Feet
Input Johnson SB

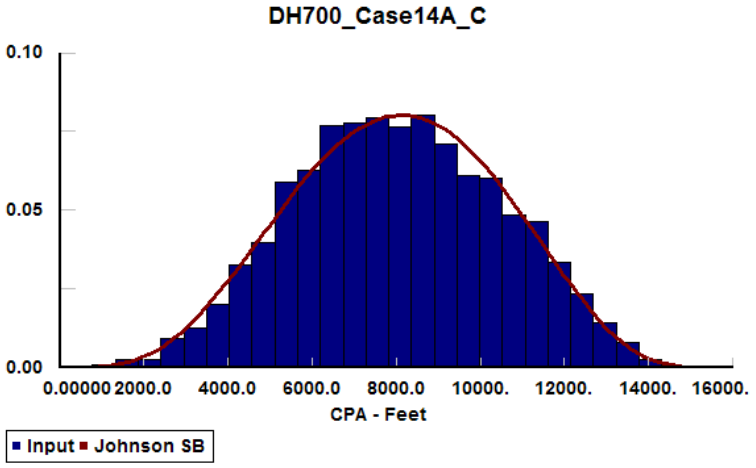
DH700_Case14A_C
0.10
0.05
0.00
0.00000 2000.0 4000.0 6000.0 8000.0 10000. 12000. 14000. 16000.
CPA - Feet
Input Johnson SB

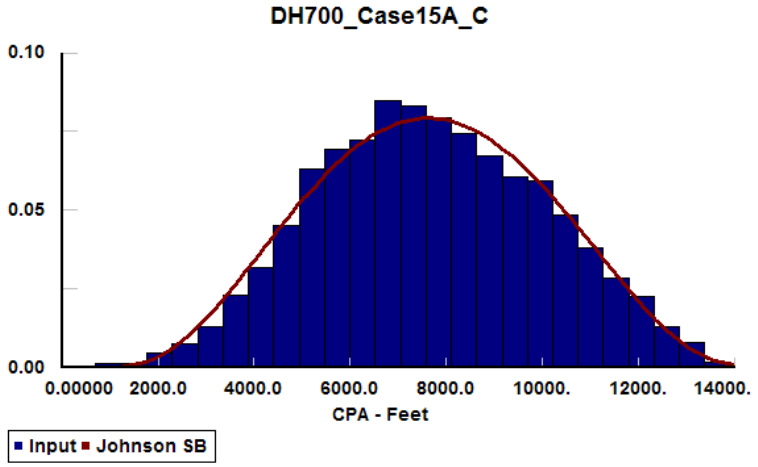
DH700_Case15A_C
0.10
0.05
0.00
0.00000
2000.0
4000.0
6000.0
8000.0
10000.
12000.
14000.
CPA - Feet
Input
Johnson SB

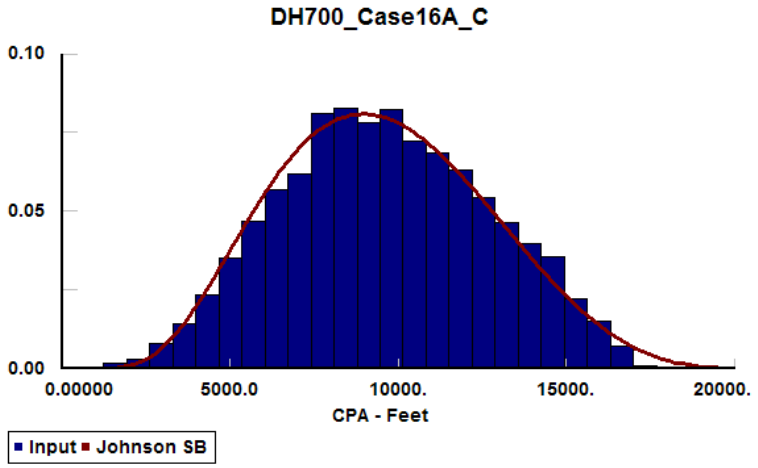
DH700_Case16A_C
0.10
0.05
0.00
0.00000
5000.0
10000.
15000.
20000.
CPA - Feet
Input
Johnson SB

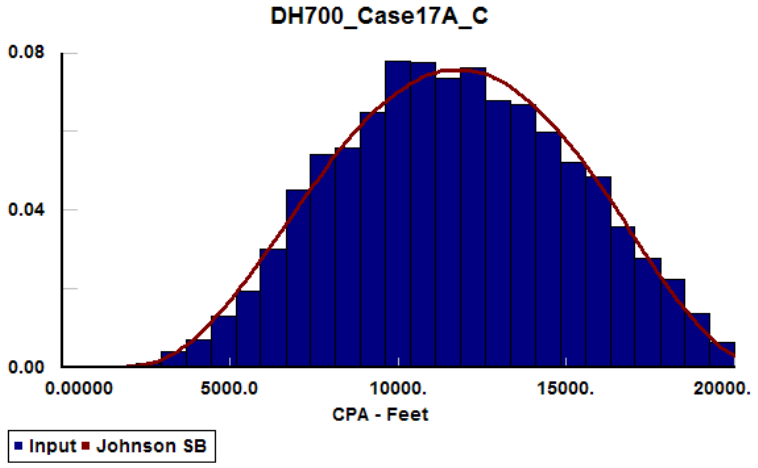
DH700_Case17A_C
0.08
0.04
0.00
0.00000
5000.0
10000.
15000.
20000.
CPA - Feet
Input
Johnson SB

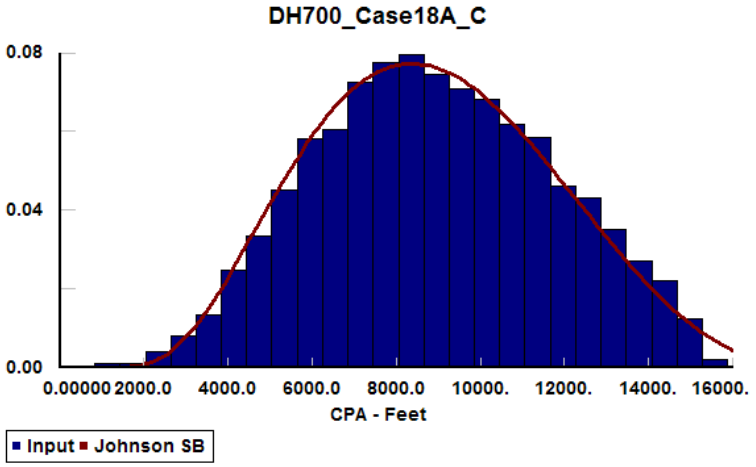
DH700_Case18A_C
0.08
0.04
0.00
0.00000 2000.0 4000.0 6000.0 8000.0 10000. 12000. 14000. 16000.
CPA - Feet
Input Johnson SB

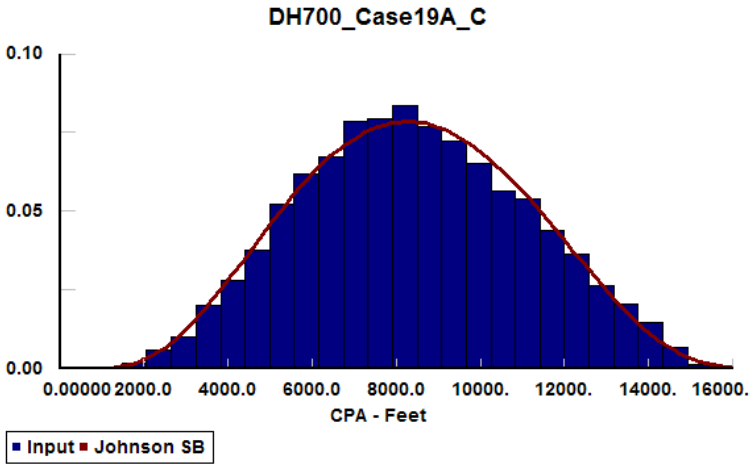
DH700_Case19A_C
0.10
0.05
0.00
0.00000 2000.0 4000.0 6000.0 8000.0 10000. 12000. 14000. 16000.
CPA - Feet
Input Johnson SB

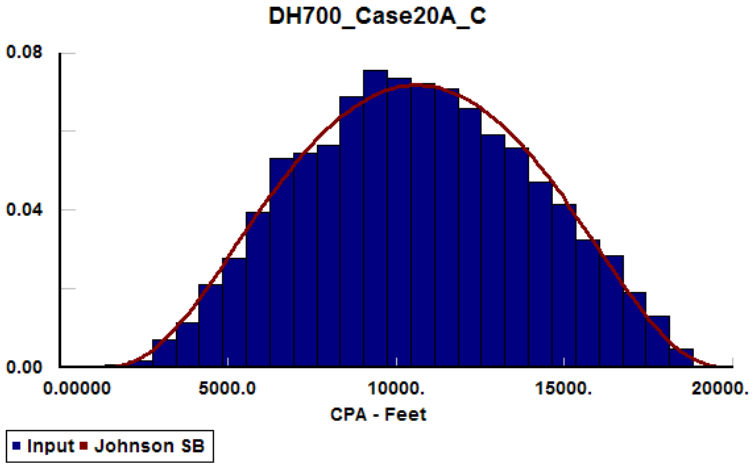
DH700_Case20A_C
0.08
0.04
0.00
0.00000 5000.0 10000. 15000. 20000.
CPA - Feet
Input Johnson SB

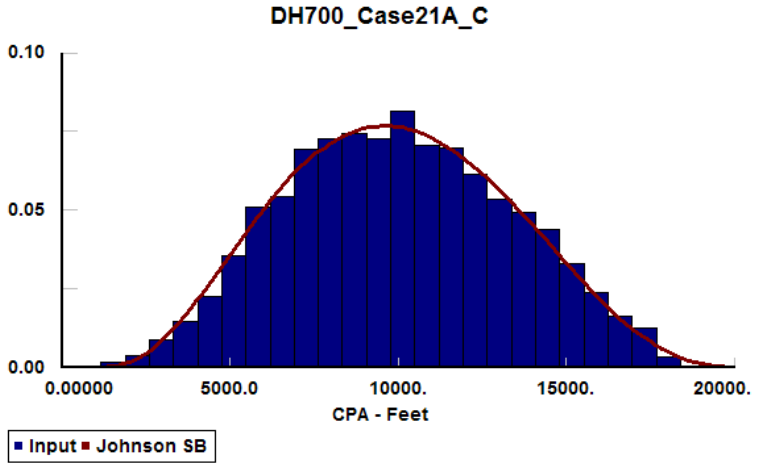
DH700_Case21A_C
0.10
0.05
0.00
0.00000
5000.0
10000.
15000.
20000.
CPA - Feet
Input
Johnson SB

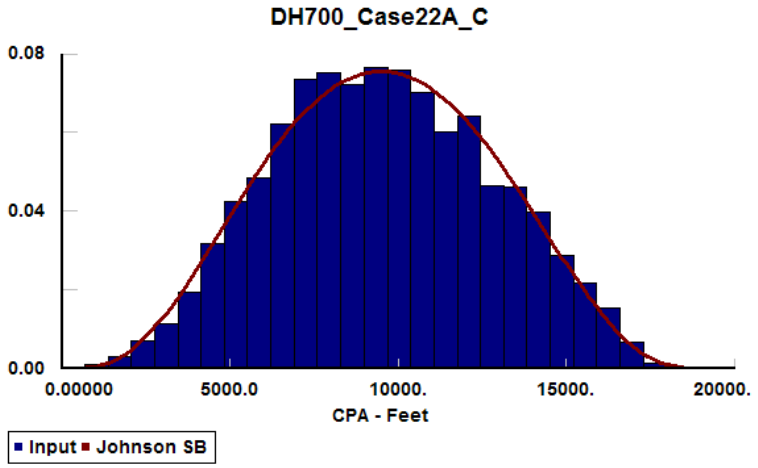
DH700_Case22A_C
0.08
0.04
0.00
0.00000
5000.0
10000.
15000.
20000.
CPA - Feet
Input
Johnson SB

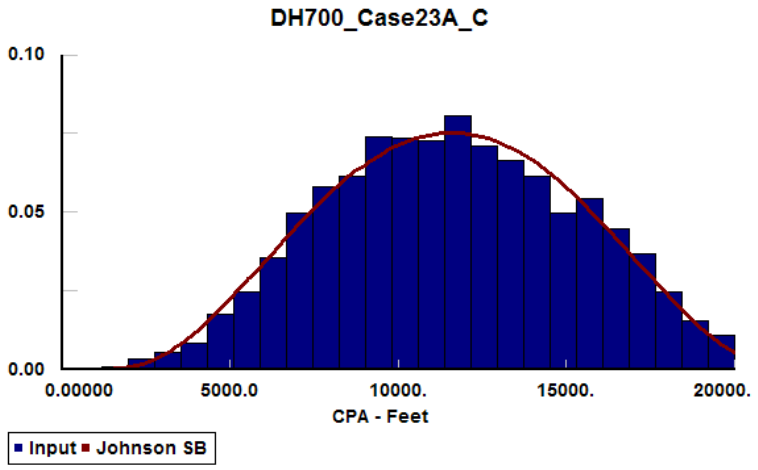
DH700_Case23A_C
0.10
0.05
0.00
0.00000
5000.0
10000.
15000.
20000.
CPA - Feet
Input
Johnson SB

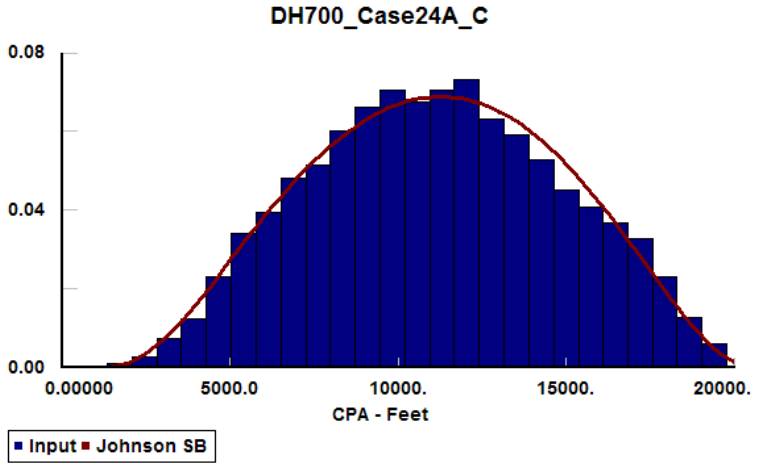
DH700_Case24A_C
0.08
0.04
0.00
0.00000
5000.0
10000.
15000.
20000.
CPA - Feet
Input
Johnson SB

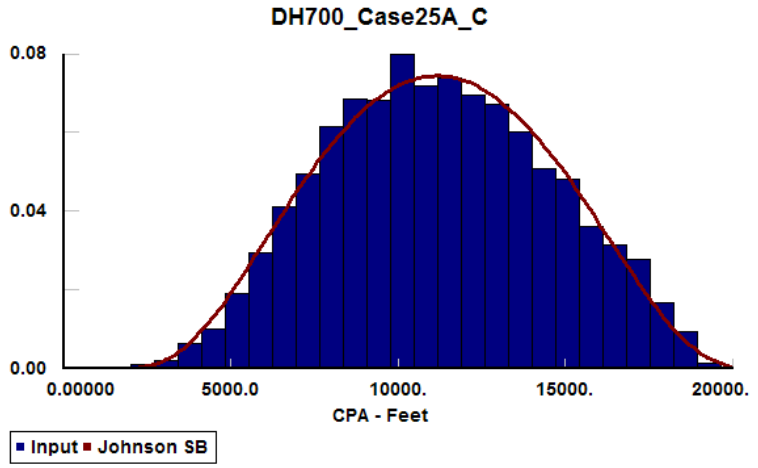
DH700_Case25A_C
0.08
0.04
0.00
0.00000
5000.0
10000.
15000.
20000.
CPA - Feet
Input
Johnson SB

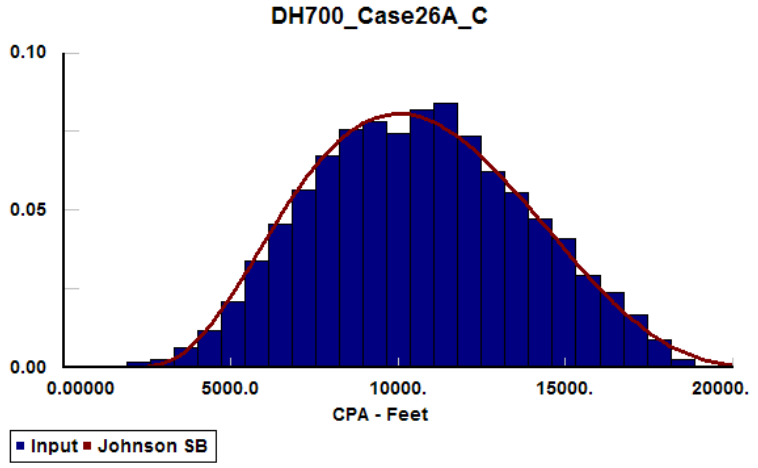
DH700_Case26A_C
0.10
0.05
0.00
0.00000
5000.0
10000.
15000.
20000.
CPA - Feet
Input
Johnson SB

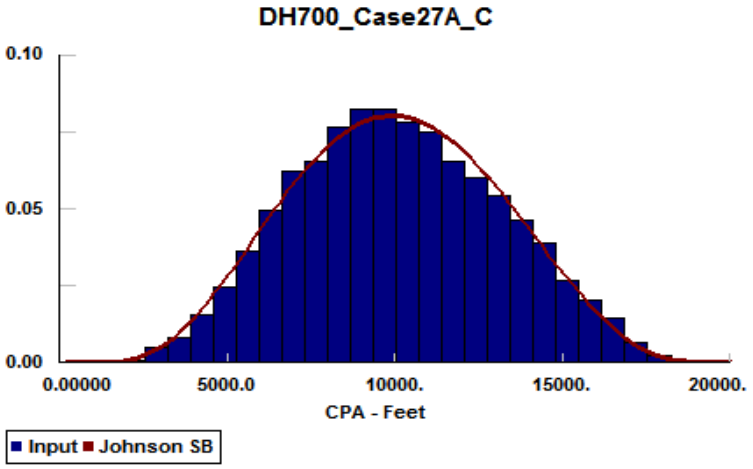
DH700_Case27A_C
0.10
0.05
0.00
0.00000
5000.0
10000.
15000.
20000.
CPA - Feet
Input
Johnson SB

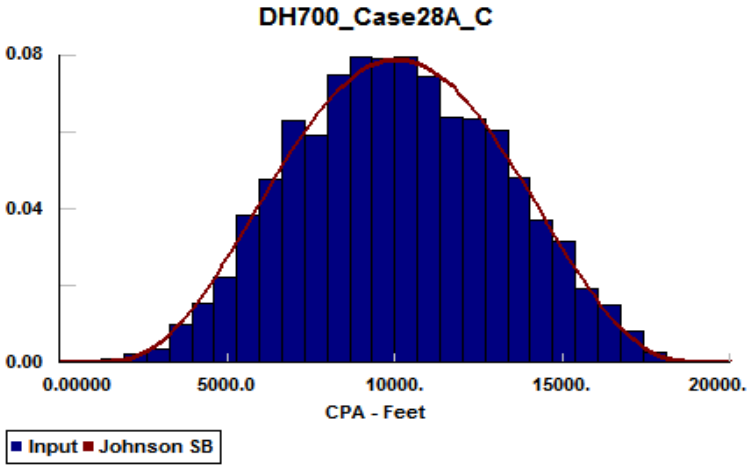
DH700_Case28A_C
0.08
0.04
0.00
0.00000
5000.0
10000.
15000.
20000.
CPA - Feet
Input
Johnson SB

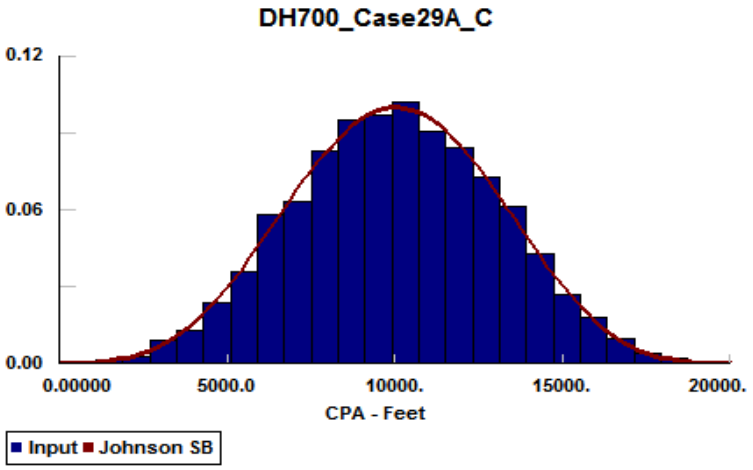
DH700_Case29A_C
0.12
0.06
0.00
0.00000
5000.0
10000.
15000.
20000.
CPA - Feet
Input
Johnson SB

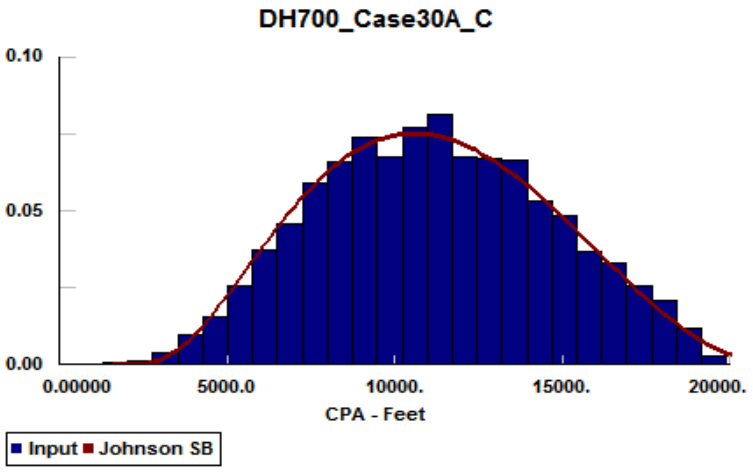
DH700_Case30A_C
0.10
0.05
0.00
0.00000
5000.0
10000.
15000.
20000.
CPA - Feet
Input
Johnson SB

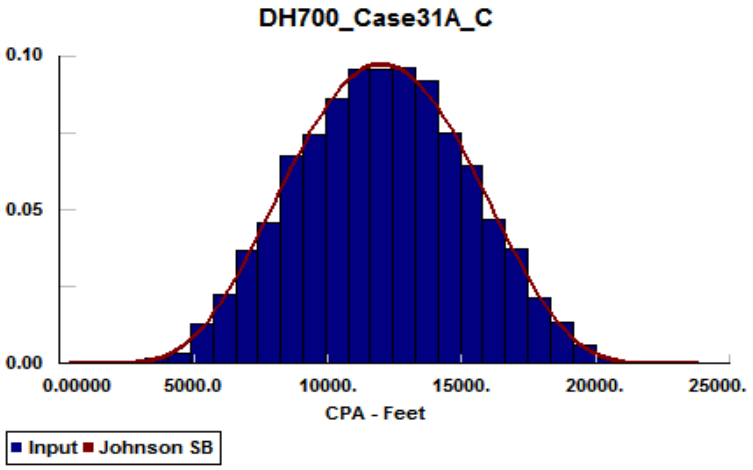
DH700_Case31A_C
0.10
0.05
0.00
0.00000
5000.0
10000.
15000.
20000.
25000.
CPA - Feet
Input
Johnson SB

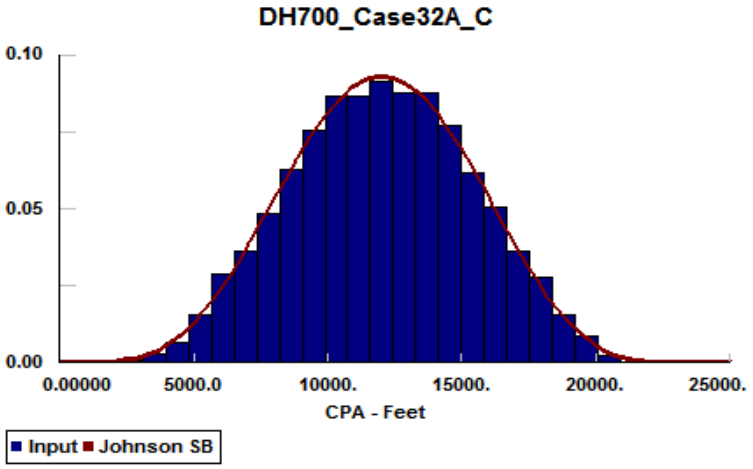
DH700_Case32A_C
0.10
0.05
0.00
0.00000
5000.0
10000.
15000.
20000.
25000.
CPA - Feet
Input
Johnson SB

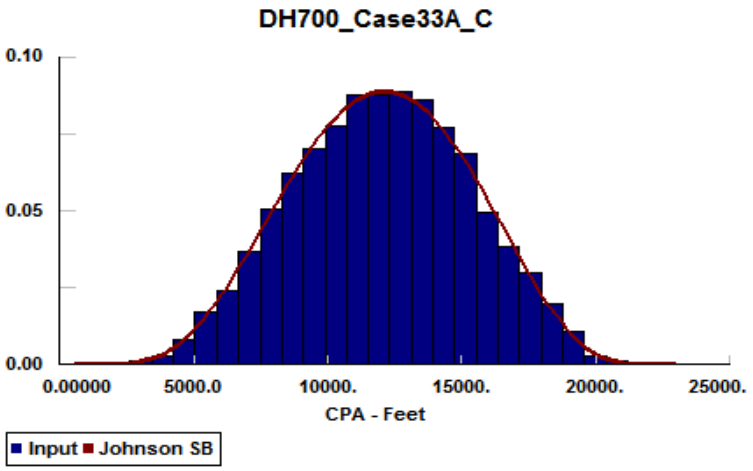
DH700_Case33A_C
0.10
0.05
0.00
0.00000
5000.0
10000.
15000.
20000.
25000.
CPA - Feet
Input
Johnson SB

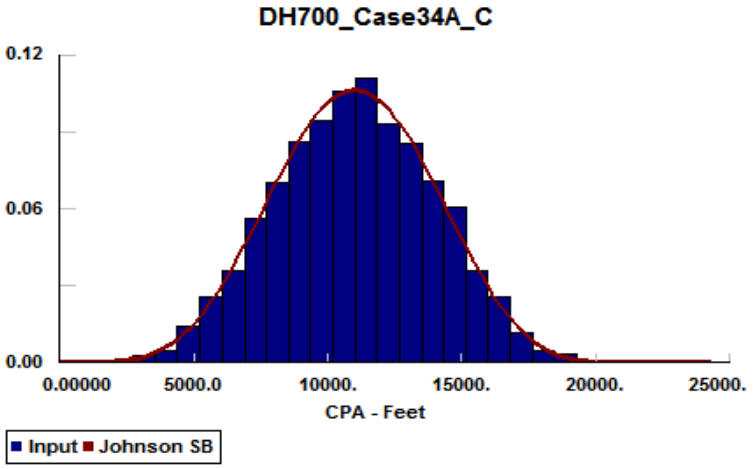
DH700_Case34A_C
0.12
0.06
0.00
0.00000
5000.0
10000.
15000.
20000.
25000.
CPA - Feet
Input
Johnson SB

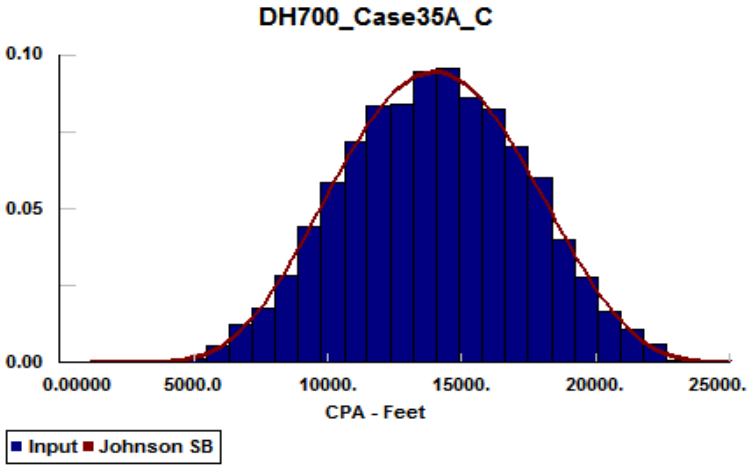
DH700_Case35A_C
0.10
0.05
0.00
0.00000
5000.0
10000.
15000.
20000.
25000.
CPA - Feet
Input
Johnson SB

Appendix C: Statistical Analysis of Higher Risk DCIA Cases

Purpose

The purpose of analyzing the higher risk DCIA cases was to determine the probability that the Closest Point of Approach (CPA) would be less than 500 feet. Data were generated and analyzed for the five cases (DH500 case 08, DH700 case 06, DH700 case 07, DH700 case 08, and DH700 case 29) that showed an increased probability of a Test Criteria Violation (TCV) of losing separation during the approach operations.

Method

For each case an attempt was made to find the best fit distribution that would match the given data set. The size of the data sets, 100,000 values in each, presented somewhat of a challenge. Because the data did not align perfectly with any known distribution, any best fit distribution was rejected when using more than about 5,000 values. In addition, the distribution-fitting software had a limit of 8,000 data values.

It was decided to take two samples of 5,000 values from each data set. Using the Kolmogorov-Smirnov and Anderson-Darling goodness of fit tests, it was determined that each of the samples match a Johnson S_B (bounded) distribution with appropriate parameters: ε (epsilon), λ (lambda), γ (gamma), and δ (delta). The best fit distributions for the samples from each data set were combined by taking the average value for each of the distribution parameters. Using both the combined, approximating distribution and the empirical data, the probability that the CPA would be less than 500 feet was determined.

As an example, consider the case DH700_Case08A_C.AFP_OUT_110_120. This example of DH700 case 08 examined only the runway convergence angles between 110° and 120°.

Two random samples of 5,000 values were taken, without replacement, from the original data set. For each sample, the best fit Johnson S_B distribution was determined with the following parameter values:

Table C1: Parameters for Best Fit Johnson S_B Distributions (DH700_Case08A_C.AFP_OUT_110_120)

	Sample 1	Sample 2	Average
ε (epsilon)	-2,148.39	-2,073.27	-2,110.83
λ (lambda)	13,631.5	13,311.4	13,471.45
γ (gamma)	-0.407823	-0.471928	-0.43988
δ (delta)	1.83682	1.81088	1.82385

For Sample 1, the Kolmogorov-Smirnov goodness of fit test gave a *p*-value of 0.0748. The Anderson-Darling goodness of fit test gave a *p*-value of 0.206. At a threshold of

0.05, both tests indicated that the null hypothesis, i.e., the sample was from the indicated Johnson S_B distribution, should not be rejected.

For Sample 2, the Kolmogorov-Smirnov goodness of fit test gave a *p*-value of 0.793. The Anderson-Darling goodness of fit test gave a *p*-value of 0.917. At a threshold of 0.05, both tests indicated that the null hypothesis, i.e., the sample was from the indicated Johnson S_B distribution, should not be rejected.

The following figures are the histograms and fitted distributions for the two samples. (Note that in the figures S_B is written as SB.)

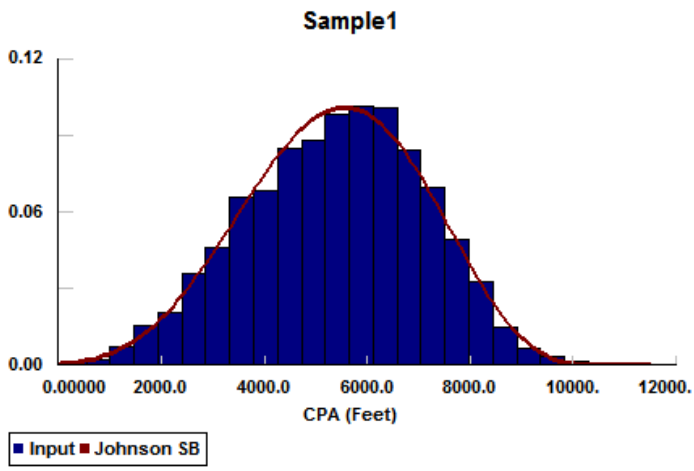

Figure C1: Histogram and Fitted Distribution for Sample 1 (DH700_Case08A_C.AFP_OUT_110_120)

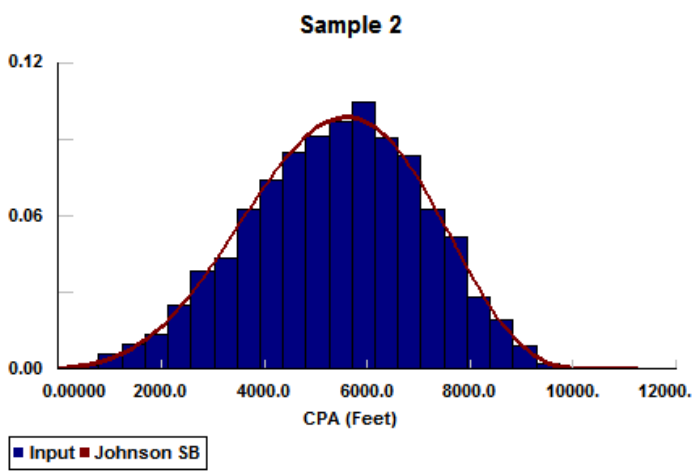

Figure C2: Histogram and Fitted Distribution for Sample 2 (DH700_Case08A_C.AFP_OUT_110_120)

The graph of the probability density function for the combined distribution is shown below.

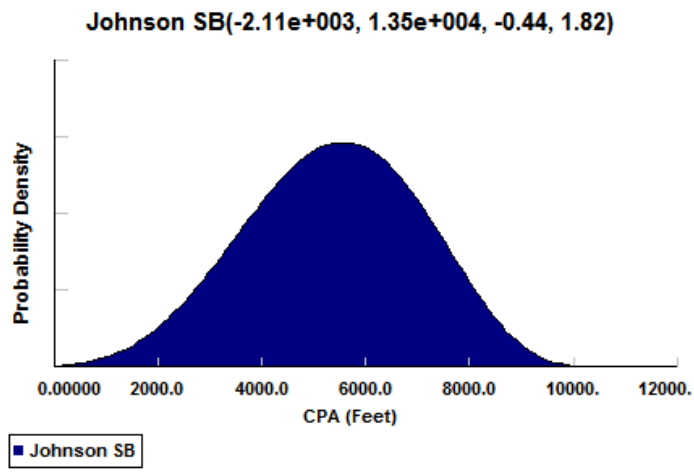

Figure C3: Probability Density for Sample Averages (DH700_Case08A_C.AFP_OUT_110_120)

The probability density function for this distribution is given by:

$$f(x) = \begin{cases} \dfrac{\delta\lambda}{\sqrt{2\pi}(x-\varepsilon)(\lambda - x + \varepsilon)} \exp\left(-\dfrac{1}{2}\left(\gamma + \delta \ln\left(\dfrac{x-\varepsilon}{\lambda - x + \varepsilon} \right) \right)^2 \right) & \varepsilon < x < \varepsilon + \lambda \\ 0 & \text{elsewhere} \end{cases}$$

where $\delta > 0, -\infty < \gamma < \infty, \lambda > 0, -\infty < \varepsilon < \infty.$

If X is a random variable from this distribution, the probability that X is less than α is given by the following:

$$P(X < \alpha) = \int_{-\infty}^{\alpha} f(x)dx .$$

So for DH700_Case08A_C.AFP_OUT_110_120,

$$P(CPA < 500) = \int_{-\infty}^{500} f(x)dx = 0.00118 .$$

In addition, the empirical probability that a CPA was less than 500 feet was calculated from the original data set. Of the 100,000 CPA values, 67 were less than 500 feet, so the empirical probability is given by

$$P(CPA < 500) = \frac{67}{100000} = .00067 .$$

Each of the other four test cases was analyzed in a similar way.

Case DH500_Case08A_C.AFP_OUT_110_120 Results:

Table C2: Parameters for Best Fit Johnson S_B distributions (Case DH500_Case08A_C.AFP_OUT_110_120)

	Sample 1	Sample 2	Average
ε (epsilon)	-2,148.39	-2,073.27	-2,110.83
λ (lambda)	13,631.5	13,311.4	13,471.45
γ (gamma)	-0.40782	-0.47193	-0.43988
δ (delta)	1.83682	1.81088	1.82385

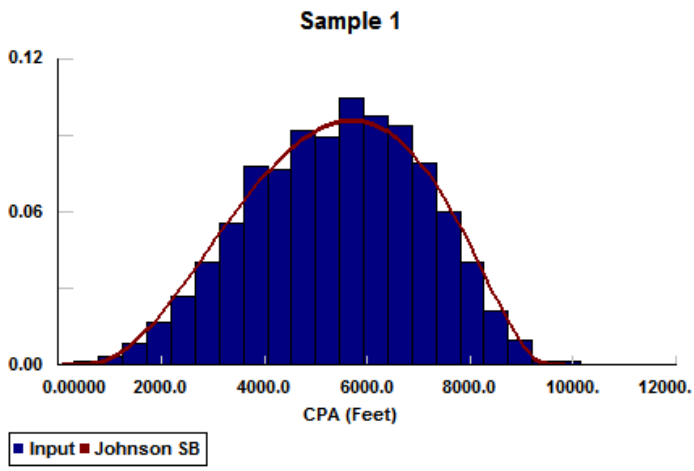

Figure C4: Histogram and Fitted Distribution for Sample 1 (Case DH500_Case08A_C.AFP_OUT_110_120)

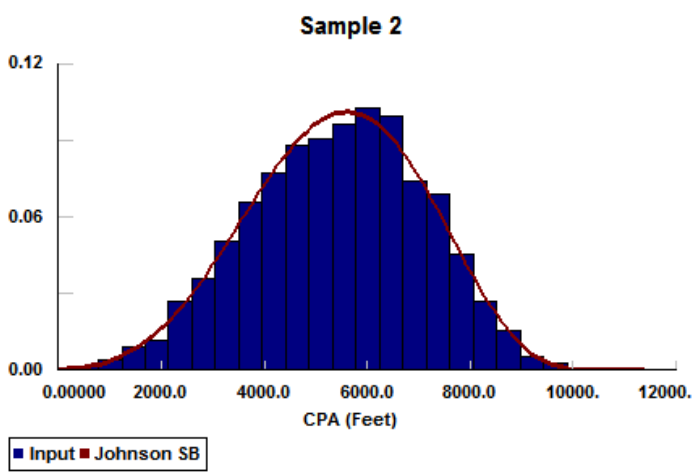

Figure C5: Histogram and Fitted Distribution for Sample 2 (Case DH500_Case08A_C.AFP_OUT_110_120)

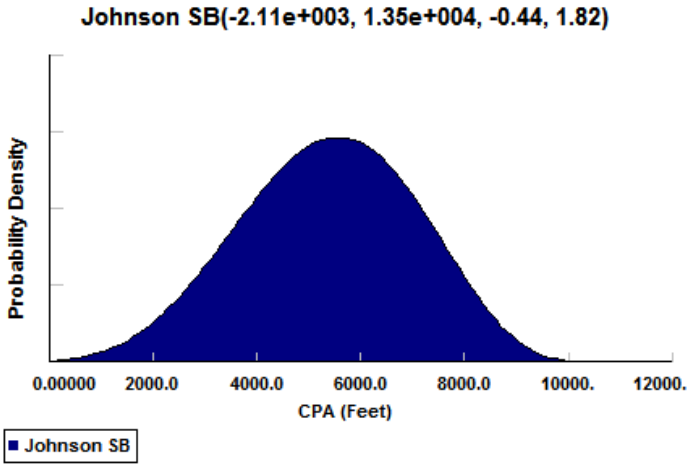

Figure C6: Probability Density for Sample Averages (Case DH500_Case08A_C.AFP_OUT_110_120)

Case DH700_Case07A_C.AFP_OUT_110_120 Results:

Table C3: Parameters for Best Fit Johnson S_B Distributions (Case DH700_Case07A_C.AFP_OUT_110_120)

	Sample 1	Sample 2	Average
ε (epsilon)	-3,533.41	-2,223.24	-2,878.33
λ (lambda)	16,154.2	14,311.8	15,233
γ (gamma)	-0.5994	-0.40461	-0.50201
δ (delta)	2.14069	1.88748	2.014085

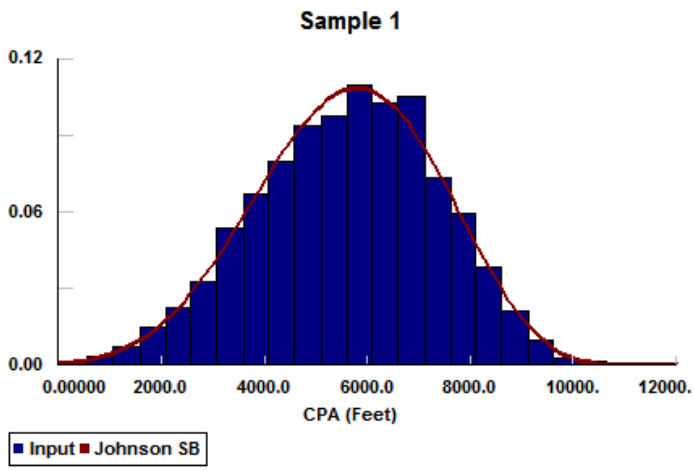

Figure C7: Histogram and Fitted Distribution for Sample 1 (Case DH700_Case07A_C.AFP_OUT_110_120)

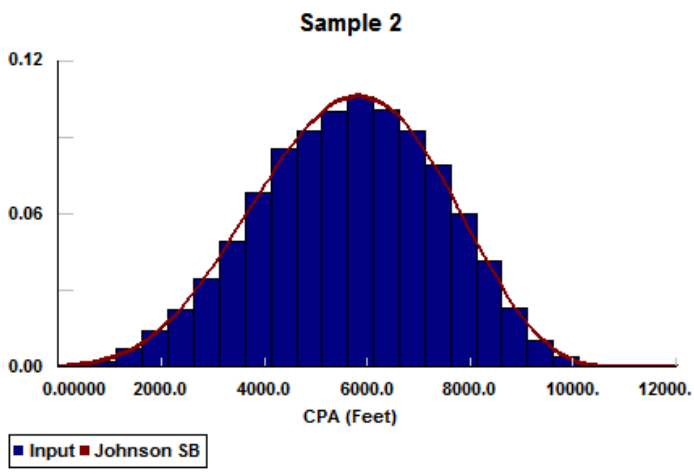

Figure C8: Histogram and Fitted Distribution for Sample 2 (Case DH700_Case07A_C.AFP_OUT_110_120)

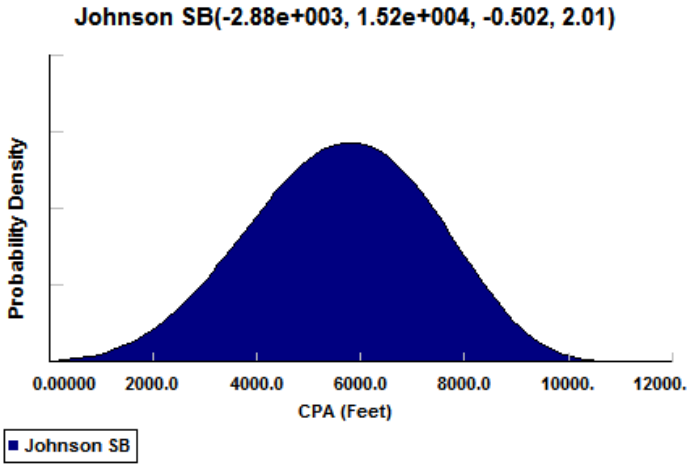

Figure C9: Probability Density for Sample Averages (Case DH700_Case07A_C.AFP_OUT_110_120)

Case DH700_Case06A_C.AFP_OUT_110_120 Results:

Table C4: Parameters for Best Fit Johnson S_B Distributions (Case DH700_Case06A_C.AFP_OUT_110_120)

	Sample 1	Sample 2	Average
ε (epsilon)	-3,793.34	-2,279.06	-3,036.2
λ (lambda)	17,397.9	14,909.8	16,153.85
γ (gamma)	-0.54125	-0.38748	-0.46436
δ (delta)	2.29286	1.88156	2.08721

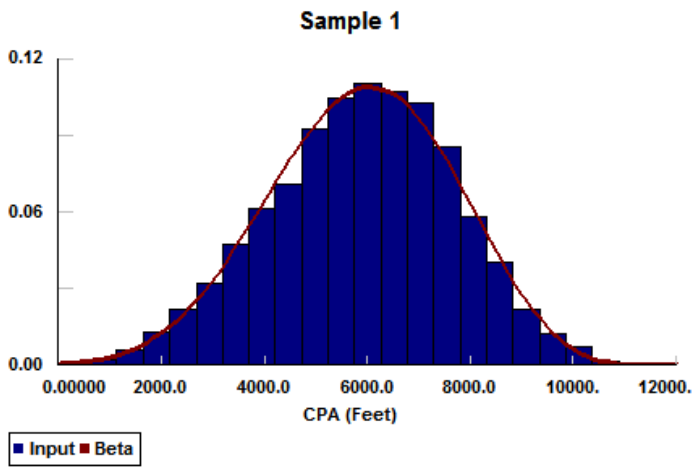

Figure C10: Histogram and Fitted Distribution for Sample 1 (Case DH700_Case06A_C.AFP_OUT_110_120)

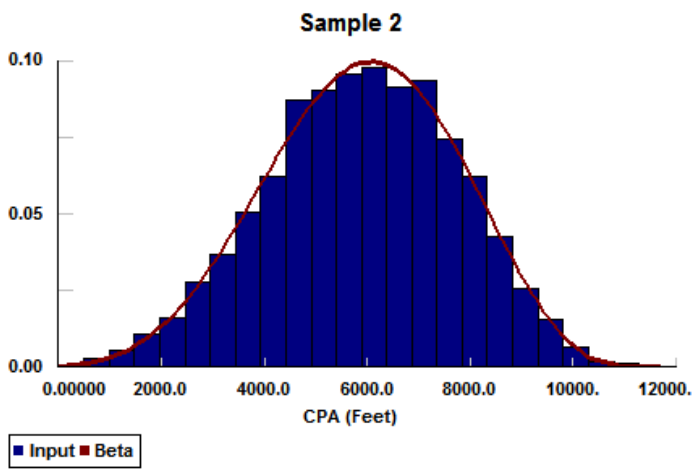

Figure C11: Histogram and Fitted Distribution for Sample 2 (Case DH700_Case06A_C.AFP_OUT_110_120)

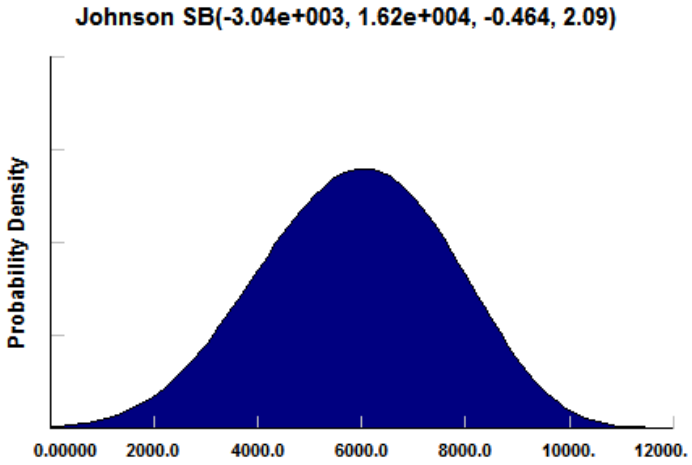

Figure C12: Probability Density for Sample Averages (Case DH700_Case06A_C.AFP_OUT_110_120)

Case DH700_Case08A_C.AFP_OUT_110_120 Results:

Table C5: Parameters for Best Fit Johnson S_B Distributions (Case DH700_Case08A_C.AFP_OUT_110_120)

	Sample 1	Sample 2	Average
ε (epsilon)	-2,148.39	-2,073.27	-2,110.83
λ (lambda)	13,631.5	13,311.4	13,471.45
γ (gamma)	-0.40782	-0.47193	-0.43988
δ (delta)	1.83682	1.81088	1.82385

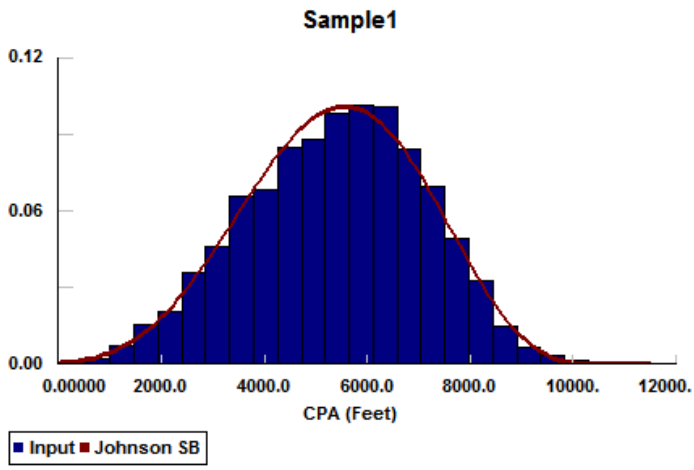

Figure C13: Histogram and Fitted Distribution for Sample 1 (Case DH700_Case08A_C.AFP_OUT_110_120)

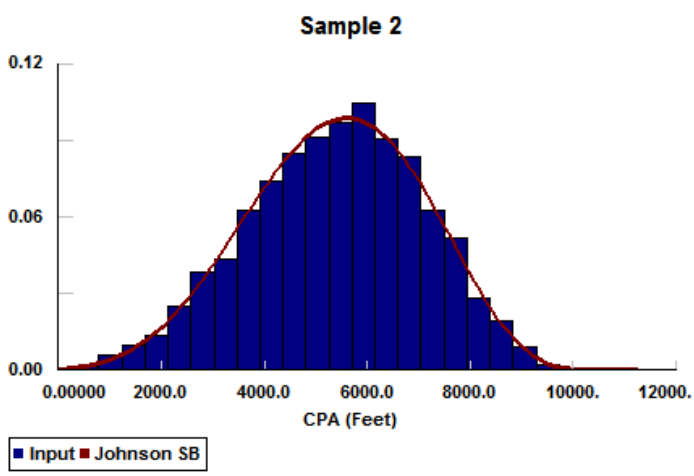

Figure C14: Histogram and Fitted Distribution for Sample 2 (Case DH700_Case08A_C.AFP_OUT_110_120)

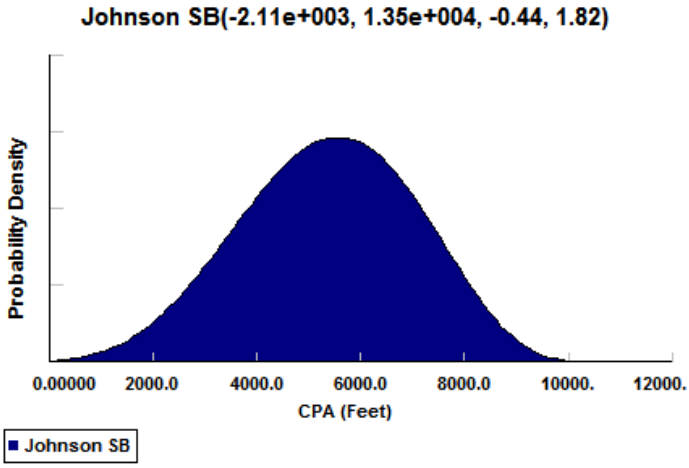

Figure C15: Probability Density for Sample Averages (Case DH700_Case08A_C.AFP_OUT_110_120)

Case DH700_Case29A_C.AFP_OUT_110_120 Results:

Table C6: Parameters for Best Fit Johnson S_B Distributions (Case DH700_Case29A_C.AFP_OUT_110_120)

	Sample 1	Sample 2	Average
ε (epsilon)	-3,419.74	-2,736.01	-3,077.88
λ (lambda)	21,591.9	20,800.1	21,196
γ (gamma)	-0.46638	-0.33886	-0.40262
δ (delta)	1.96309	1.86311	1.9131

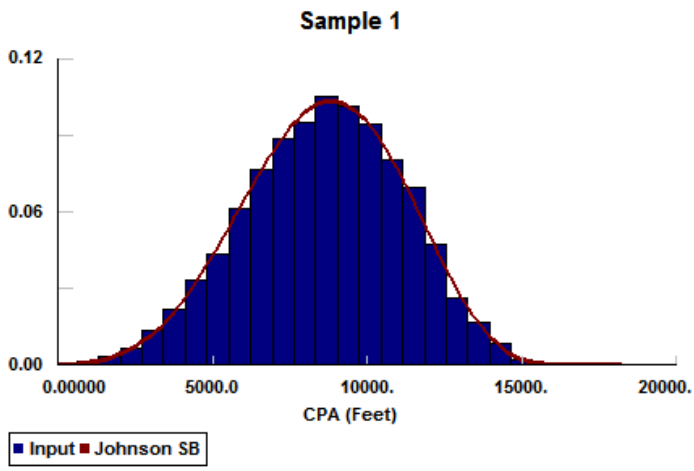

Figure C16: Histogram and Fitted Distribution for Sample 1 (Case DH700_Case29A_C.AFP_OUT_110_120)

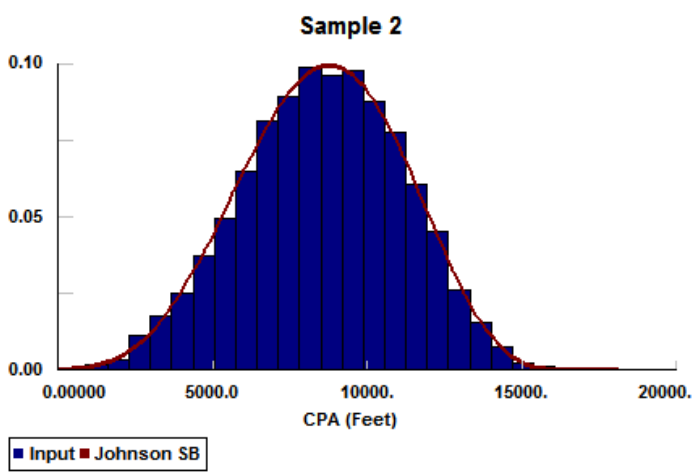

Figure C17: Histogram and Fitted Distribution for Sample 2 (Case DH700_Case29A_C.AFP_OUT_110_120)

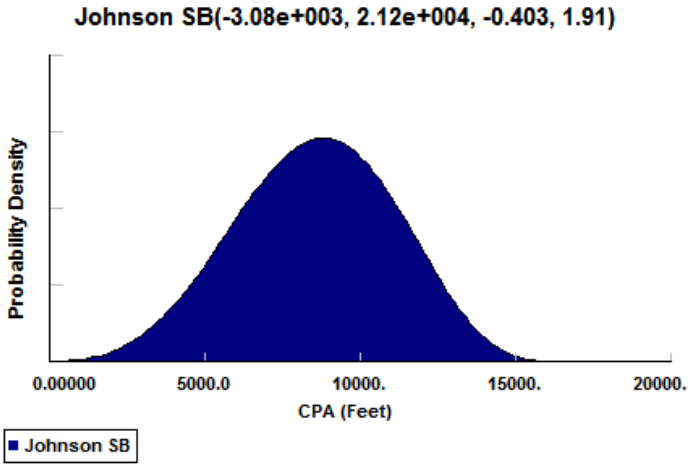

Figure C18: Probability Density for Sample Averages (Case DH700_Case29A_C.AFP_OUT_110_120)

References

[1] FAA Order 7110.110A**,** *Dependent Converging Instrument Approaches (DCIA) with Converging Runway Display Aid (CRDA)*. 7/20/95.

[2] Hinton, D.A. "An Aircraft Vortex Spacing System (AVOSS) for Dynamical Wake Vortex Spacing Criteria." AGARD 78th Fluid Dynamics Panel Meeting and Symposium on the Characterisation & Modification of Wakes from Lifting Vehicles in Fluids. Trondheim, Norway. 20-23 May 1996. AGARD CP-584, Paper 23.

[3] FAA Order 7110.65T, *Air Traffic Control*, 2/11/2010.

[4] Greenhaw, Richard (2008) *Safety Study Report on Simultaneous Parallel Instrument Landing System (ILS) and Area Navigation (RNAV)/Required Navigation Performance (RNP) Approaches–Phases 1B and 2B* (DOT-FAA-AFS-450-41). FAA/AFS-450, Oklahoma City, OK.